



**KLIMA- OG  
FORURENSNINGS-  
DIREKTORATET**

Statlig program for forurensningsovervåking  
Rapportnr. 1102/2011

Monitoring of greenhouse gases and aerosols at Svalbard and  
Birkenes: Annual report 2009

TA  
2805  
2011

Utført av NILU – Norsk institutt for luftforskning







KLIMA- OG  
FORURENSNINGS-  
DIREKTORATET

**Statlig program for forurensningsovervåking:**

Monitoring of greenhouse gases and aerosols at the Zeppelin Observatory, Svalbard, and Birkenes Observatory, Aust-Agder, Norway

SPFO-rapport: 1102/2011

TA-2805/2011

ISBN 978-82-425-2403-4

ISBN 978-82-425-2404-1

Oppdragsgiver: Klima- og forurensningsdirektoratet (Klif)

Utførende institusjon: NILU – Norsk institutt for luftforskning

**Monitoring of greenhouse gases  
and aerosols at Svalbard and  
Birkenes**

Rapport  
1102/2011

Annual report 2009



Authors: C. Lund Myhre, O. Hermansen, A.M. Fjæraa, C. Lunder, M. Fiebig, N. Schmidbauer, T. Krognnes, K. Stebel (all NILU), C. Toledano, (GOA), C. Wehrli (WORCC)

NILU project no.: O-99093

NILU report no.: 33/2011

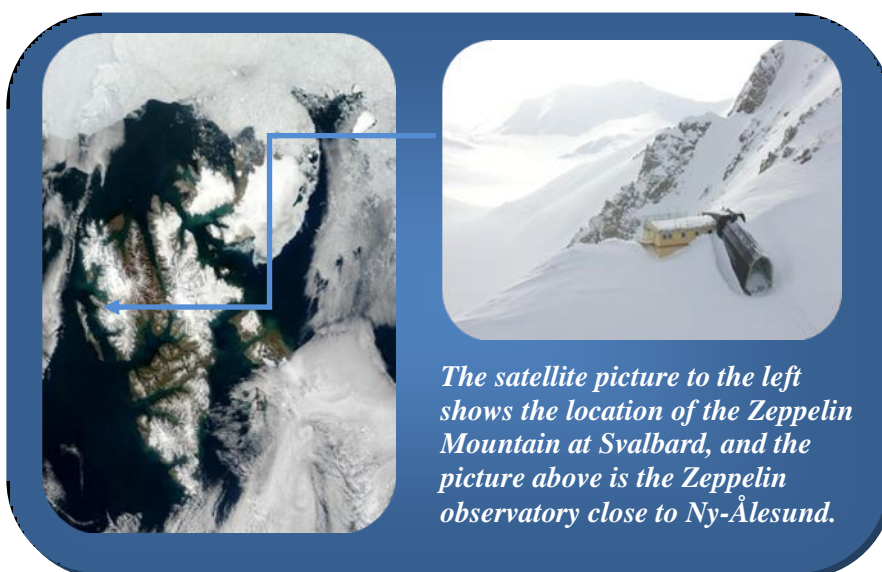


## Preface

In 1999 The Climate and Pollution Agency (Klif, the former SFT) and Norwegian Institute for Air research (NILU) signed a contract commissioning NILU to run a programme for monitoring greenhouse gases at the Zeppelin station, close to Ny-Ålesund at Svalbard. This collaborative Klif/NILU programme includes monitoring of 23 greenhouse gases at the Zeppelin observatory in the Arctic. In 2009 NILU upgraded and extended the observational activity at the Birkenes Observatory in Aust-Agder. In 2010 the Klif/NILU monitoring programme was extended to also include the new observations from Birkenes of the greenhouse gases CO<sub>2</sub> and CH<sub>4</sub> and selected aerosol observations relevant for the understanding of climate change. The first results from the start period in 2009 are presented in this report.

The following are regulated through the Montreal protocol and measured at the Zeppelin Observatory: chlorofluorocarbons (CFC), hydrochlorofluorocarbons (HCFC), and halones as well as other halogenated organic gases. Further the following gases included in the Kyoto protocol are monitored; methane (CH<sub>4</sub>), nitrous oxide (N<sub>2</sub>O) from 2010, hydrofluorocarbons (HFC), sulphurhexafluoride (SF<sub>6</sub>). Additionally carbon monoxide (CO) and tropospheric ozone (O<sub>3</sub>) are a part of the programme. The amount of particles in the air above the stations is also measured. The station is hosting measurements of carbon dioxide (CO<sub>2</sub>) performed by ITM, University of Stockholm as well, but the availability of data is limited. This activity is funded by the Swedish Environmental Protection Agency.

The unique location of the Zeppelin observatory at Svalbard together with the infrastructure of the scientific research community at Ny-Ålesund makes it ideal for monitoring the global changes of the atmosphere. There are few local sources of emissions, and the Arctic location is also important as the Arctic is a particularly vulnerable region. The observations at the Birkenes Observatory complement the Arctic site. Birkenes Observatory is located in a forest area with few local sources. However, the observatory often receives long range transported pollution from Europe and the site is ideal to analyse the contribution of long range transported greenhouse gases and aerosol properties.



In 1987 the Montreal Protocol was signed and entered into force in 1989 in order to reduce the production and use of the ozone-depleting substances (ODS). The amount of most ODS in the troposphere is now declining slowly and one expects to be back to pre-1980 levels around year 2050. It is crucial to follow the development of the concentration of these ozone depleting gases in order to verify that the Montreal Protocol and its amendments work as expected. Further these gases and their replacement gases are strong greenhouse gases making it even more important to follow the development of their concentrations. In December 1997 the Kyoto protocol was adopted. The target set by the Kyoto protocol is to reduce the total emissions of greenhouse gases from the industrialized countries during the period 2008 to 2012. The six most important groups of greenhouse gases included are: CO<sub>2</sub>, CH<sub>4</sub>, N<sub>2</sub>O, fluorinated hydrocarbons (HFKs and PFKs) and sulphurhexafluoride (SF<sub>6</sub>).

The Norwegian Institute for Air Research (NILU) is responsible for the operation and maintenance of the monitoring programme. The purpose of the programme is to:

- Provide continuous measurements of greenhouse gases in the Arctic region resulting in high quality data that can be used in trend analysis
- Provide continuous measurements of the greenhouse gases CO<sub>2</sub> and CH<sub>4</sub> at the Birkenes Observatory resulting in high quality data that can be used in trend analysis
- Provide trend analysis and interpretations of the observations from Zeppelin assess the influence regional anthropogenic emissions of greenhouse gases has on the radiative balance
- Provide information on the status and the development of the greenhouse gases with a particular focus on the gases included in the international conventions the Montreal and Kyoto protocol.
- Provide results of aerosol observations of relevance to the understanding of climate change
- Indicate sources regions with high influence on the measurements.

Observations and results from the monitoring programme are processed and used to assess the progress towards compliance with international agreements like the Kyoto and the Montreal Protocols. This report summarises the activities and results of the greenhouse gas and aerosol monitoring programme for the year 2009, and comprises a trend analysis for the period 2001-2009 including interpretation of the results.

Kjeller, June 2011

Cathrine Lund Myhre  
Senior scientist and project manager

## Table of Contents

<b>Preface</b> .....	<b>3</b>
<b>1. Executive summary</b> .....	<b>7</b>
<b>2. Introduction</b> .....	<b>12</b>
<b>3. The Norwegian Observatories measuring long lived greenhouse gases</b> .....	<b>15</b>
3.1 The Zeppelin observatory .....	15
3.2 The Birkenes observatory .....	17
<b>4. Observations and trends of greenhouse gases at the Zeppelin Observatory in the Norwegian Arctic</b> .....	<b>19</b>
4.1 Greenhouse gases with natural and anthropogenic sources .....	20
4.1.1 Observations of methane in the period 2001-2009.....	20
4.1.2 First observations of Nitrous Oxide at the Zeppelin Observatory.....	24
4.1.3 Observations of Carbon Dioxide (CO <sub>2</sub> ) in the period 1988-2009.....	25
4.1.4 Observations of Methyl Chloride in the period 2001-2009.....	27
4.1.5 Observations of Methyl Bromide in the period 2001-2009.....	28
4.1.6 Observations of tropospheric ozone in the period 1990-2009.....	30
4.1.7 Observations of CO in the period 2001-2009.....	31
4.2 Greenhouse gases with solely anthropogenic sources.....	32
4.2.1 Observations of Chlorofluorocarbons (CFCs) in the period 2001-2009.....	33
4.2.2 Observations of Hydrochlorofluorocarbons (HCFCs) in the period 2001-2009.....	34
4.2.3 Observations of hydrofluorocarbons (HFCs) in the period 2001-2009.....	36
4.2.4 Observations of halons in the period 2001-2009.....	39
4.2.5 Observations of other chlorinated hydrocarbons in the period 2001-2009.....	40
4.2.6 Perfluorinated compounds.....	41
<b>5. Observations of greenhouse gases observed at the Birkenes Observatory in Aust-Agder</b> .....	<b>43</b>
<b>6. Aerosols and climate: Observations from Zeppelin and Birkenes Observatory</b> .....	<b>45</b>
6.1 Observations of aerosol properties in Norway in a global context .....	45
6.2 Aerosol properties measured at Birkenes in 2009 .....	47
6.3 Observations of the total aerosol load above Zeppelin and Birkenes observatories ....	52
6.3.1 Measurements of the total aerosol load above the Birkenes observatory .....	54
6.3.2 Measurements of the total aerosol load above Ny-Ålesund.....	57
<b>7. Transport of pollution to the Zeppelin Observatory and the influence on the observations</b> .....	<b>61</b>
7.1 Regional emissions and the influence on methane levels .....	62
<b>8. References</b> .....	<b>65</b>
<b>Appendix I: Description of instruments, methods and trend analysis</b> .....	<b>69</b>
<b>Appendix II: Acknowledgments and affiliations of external authors</b> .....	<b>79</b>



## 1. Executive summary

This annual report describes the activities and main results of the programme “*Monitoring of greenhouse gases and aerosols at the Zeppelin Observatory, Svalbard, and Birkenes Observatory, Aust-Agder, Norway*” for 2009. This is a part of the Governmental programme for monitoring pollution in Norway. The report comprises all natural well mixed greenhouse gases, the most important anthropogenic greenhouse gases as well as various particles properties with relevance to climate change. Many of the gases also have strong ozone depleting effect.

*Table 1: Key findings; Greenhouse gases measured at Ny-Ålesund; lifetimes in years, global warming potential (GWP), absolute change in concentrations since 2008, concentrations in 2009, their trends per year over the period 2001-2009, and relevance to the Montreal and Kyoto Protocols. All concentrations are mixing ratios in ppt<sub>v</sub>, except for methane and carbon monoxide (ppb<sub>v</sub>) and carbon dioxide (ppm<sub>v</sub>).*

Compound	Formula	Life-time	GWP <sup>1</sup>	Change last year	2009	Trend / Year	Montreal or Kyoto Prot.	Comments on use for the halocarbons
Methane	CH <sub>4</sub>	12.0 <sup>2</sup>	25	4.0	1892	<b>+4.5</b>	<b>K</b>	
Carbon monoxide	CO	Months		-0.4	117.9	<b>-2.5</b>		
Carbondioxide <sup>3</sup>	CO <sub>2</sub>		1		387.0	<b>+1.7</b>	<b>K</b>	
<b>Chlorofluorocarbons</b>								
CFC-11*	CCl <sub>3</sub> F	45	4750	-1.6	245	<b>-2.6</b>	<b>M</b> phased out	foam blowing, aerosol propellant
CFC-12*	CF <sub>2</sub> Cl <sub>2</sub>	100	10900		544	<b>-1.8</b>	<b>M</b> phased out	temperature control
CFC-113*	CF <sub>2</sub> ClCFCl <sub>2</sub>	640	6130	0.3	78	<b>-0.7</b>	<b>M</b> phased out	solvent, electronics industry
CFC-115*	CF <sub>3</sub> CF <sub>2</sub> Cl	1700	7370	0.0	8.4	<b>+0.01</b>	<b>M</b> phased out	temperature control, aerosol propellant
<b>Hydrochlorofluorocarbons</b>								
HCFC-22	CHClF <sub>2</sub>	12	1810	9.1	212.7	<b>+6.5</b>	<b>M</b> freeze	temperature control, foam blowing
HCFC-141b	C <sub>2</sub> H <sub>3</sub> FCl <sub>2</sub>	9.3	725	0.7	21.5	<b>+0.5</b>	<b>M</b> freeze	foam blowing, solvent
HCFC-142b*	CH <sub>3</sub> CF <sub>2</sub> Cl	17.9	2310		21.4	<b>+0.80</b>	<b>M</b> freeze	foam blowing
<b>Hydrofluorocarbons</b>								
HFC-125	CHF <sub>2</sub> CF <sub>3</sub>	29	3500	1.0	7.9	<b>+0.7</b>	<b>K</b>	temperature control
HFC-134a	CH <sub>2</sub> FCF <sub>3</sub>	14	1430	4.4	57.7	<b>+4.5</b>	<b>K</b>	temperature control, foam blowing, solvent, aerosol propellant
HFC-152a	CH <sub>3</sub> CHF <sub>2</sub>	1.4	124	0.3	9.0	<b>+0.8</b>	<b>K</b>	foam blowing
<b>Halons</b>								
H-1211*	CBrClF <sub>2</sub>	16	1890	-0.1	4.3	<b>-0.01</b>	<b>M</b> phased out	fire extinguishing
H-1301	CBrF <sub>3</sub>	65	7140	0.0	3.3	<b>+0.03</b>	<b>M</b> phased out	fire extinguishing
<b>Halogenated compounds</b>								
Methylchloride	CH <sub>3</sub> Cl	1.0	13	3.7	527.9	<b>+1.38</b>		natural emissions (algae)
Methylbromide	CH <sub>3</sub> Br	0.7	5	-0.5	7.7	<b>-0.14</b>	<b>M</b> freeze	agriculture, natural emissions (algae)
Dichloromethane	CH <sub>2</sub> Cl <sub>2</sub>	0.38	8.7	1.0	38.4	<b>+0.91</b>		solvent
Chloroform	CHCl <sub>3</sub>	0.5	30	0.5	10.8	<b>-0.04</b>		Solvent, natural emissions
Methylchloroform	CH <sub>3</sub> CCl <sub>3</sub>	5	146	-1.7	9.3	<b>-3.56</b>	<b>M</b> phased out	solvent
Trichloromethane	CHClCCl <sub>2</sub>			0.1	0.4	<b>-0.04</b>		solvent
Perchloroethylene	CCl <sub>2</sub> CCl <sub>2</sub>			0.3	2.9	<b>-0.24</b>		solvent
Sulphurhexafluoride* SF <sub>6</sub>		3200	22800	0.3	6.9	<b>+0.25</b>	<b>K</b>	Mg-production, electronics

\*The measurements of these components have higher uncertainty and are not within the required precision of AGAGE. See Appendix I for more details.

<sup>1</sup>GWP (Global warming potential) 100 years time period, CO<sub>2</sub> = 1

<sup>2</sup>The lifetimes for CH<sub>4</sub> are adjustment times including feedbacks of indirect effects on the lifetime.

<sup>3</sup>Measurements of CO<sub>2</sub> is performed by Stockholm University. This is preliminary data and the trend calculation is for the period 1988-2009.

The lifetimes and GWPs in Table 1 are updated in accordance with the 4<sup>th</sup> Assessment Report of the IPCC. Trends are calculated for the period 2001–2009 and are given in mixing ratio (concentration) per year. Further details and interpretations are presented in section 3 of the report.

### **Greenhouse gases regulated through the Kyoto protocol – Key findings from the Zeppelin observatory**

---

The report includes the 6 greenhouse gases or groups of gases regulated through the Kyoto protocol. The key findings are:

- **Methane – CH<sub>4</sub>:** In 2009 the **mixing ratios of methane reached new record levels** with an annual mean value of 1892 ppb. This is an increase of 4 ppb or 0.21% since 2008, and continues the observed increase the last years, but at a slower rate. Also the global mean methane level reached a new record level in 2009. On average there was a global increase of 5 ppb from 2008 (WMO, 2010).

The methane increase at the Zeppelin observatory since 2005 is around 1.6%. We consider this as a relatively large change compared to the evolution of the methane levels in the period from 1998-2005; the change was close to zero for this period both at our observatory and globally, according to IPCC (Forster et al., 2007).

There is yet no clear explanation for the increase in methane that started in 2005, but a possible explanation could be increased methane emissions from wetlands, both in the tropics as well as in the Arctic region. Melting permafrost, both in terrestrial regions and permafrost at the sea floor, might introduce new possible methane emission sources initiated by the temperature increase the last years. If this should be the case, it would be an alarming development.

To improve our understanding of the ongoing processes an immediate extension of the monitoring of methane, focusing in particular on identification of possible sources in the Arctic is needed. Methane from various sources have different isotopic ratios of <sup>13</sup>C/<sup>12</sup>C. Isotopic measurements of methane at Zeppelin combined with transport modeling would be a very powerful tool to distinguish between methane from various sources as wetlands, oceans and exploitation of gas fields included gas transportation.

- **Nitrous Oxide –N<sub>2</sub>O:** The global mean level of N<sub>2</sub>O has increased from around 270 ppb prior to industrialization and up to an average global mean of 322.5 ppb in 2009 (WMO, 2010) which is new record level. In 2009 NILU installed a new instrument at Zeppelin to measure N<sub>2</sub>O to follow the evolution of this compound in the future in the Arctic. The instrument was in full operation in April 2010 and the first observations are presented in this report.

- **CO<sub>2</sub> reached new record level in 2009 both globally and at the Zeppelin Observatory in the Arctic.** The global abundance was 386.8 according to WMO (2010) and the preliminary analysis of the Zeppelin observations was 387 ppm. The growth rates are comparable to the last years, slightly below 2 ppm per year both globally and at Zeppelin.

- **Hydrofluorocarbons:** These gases have replaced ozone depleting substances, and are relatively new gases emitted to the atmosphere. They are all of solely anthropogenic origin. The mixing ratios of HFC-125, HFC-134a, HFC-152a have **increased by as much as 300%, 178% and 216% respectively since 2001** at the Zeppelin observatory. However, their concentrations are still very low, thus the total radiative forcing of these gases since the start of their emissions and up to 2009 is only about  $0.011 \text{ W m}^{-2}$ . This is less than 1 % of the radiative forcing from the change in  $\text{CO}_2$  since pre-industrial time (which is  $1.66 \text{ W m}^{-2}$ ). Thus the contribution from these manmade gases to the global warming is small today, but given the observed extremely rapid increase in the use and atmospheric concentrations, it is crucial to follow the development of these gases in the future.
- **The perfluorinated compound –  $\text{SF}_6$ :** The only perfluorinated compound measured at Zeppelin is Sulphurhexafluoride,  $\text{SF}_6$ . This is an **extremely potent greenhouse gas**, but the concentration is still very low. However, measurements show that the concentration has increased by almost 40% since 2001.

### Greenhouse gases regulated through the Montreal protocol – Key findings

---

All gases regulated through the Montreal protocol are substances depleting the ozone layer. In addition they are all greenhouse gases. The amount of most of the ozone-depleting substances (ODS) in the troposphere is now declining slowly globally and is expected to be back to pre-1980 levels around the year 2050. The gases included in the monitoring programme at Zeppelin are the man-made greenhouse gases called chlorofluorocarbons (CFCs), the hydrogen chlorofluorocarbons (HCFCs), which are CFC substitutes, and halons.

- **CFCs:** In total the development of the CFC gases measured at the global background site Zeppelin give reason for optimism. The concentrations of the observed CFCs, **CFC-11, CFC-12, CFC-113 and CFC-115 are all declining or at the same level as in 2001**. The mixing ratios of all four gases are now at a lower level than in 2001 when measurements started at Zeppelin.
- **HCFCs:** The CFC substitutes **HCFC-22, HCFC-141b and HCFC-142b all had a relatively strong increase in the levels measured at Zeppelin from 2001-2009**. HCFC-22 used for temperature control and foam blowing had the largest growth rate. This is the most abundant substance of the HCFCs and is currently increasing at a rate of 6.5 ppt/year which is more than 4% per year. HCFC-142b had the strongest relative increase with more than 21% since 2007 and more than 40% since 2001.
- **Halons:** The levels of the two gases monitored have been quite stable over the observation period at Zeppelin. However, based on the recent results it seems like there was a maximum in 2004 for halon-1211 at Zeppelin, and a small decline after that. According to the Ozone Assessment (WMO, 2007) it is currently unclear whether the atmospheric mixing ratios of halon-1301 is increasing, and our last observations now indicate that the growth has stopped. However, this is uncertain, and longer time series and improved measurements are necessary for both these components.

## Greenhouse gases not regulated through the protocols – Key findings

---

The monitoring programme also includes five greenhouse gases not regulated through any of the two protocols.

- **Chlorinated greenhouse gases:** These are the following chlorinated gases: methylchloride ( $\text{CH}_3\text{Cl}$ ), dichloromethane ( $\text{CH}_2\text{Cl}_2$ ), chloroform ( $\text{CHCl}_3$ ), trichloromethane ( $\text{CHCl}_2\text{CCl}_3$ ), perchloroethylene ( $\text{CCl}_2\text{CCl}_2$ ). The concentrations of all these gases show small variations from year to year and most of them have decreased the last years. Exceptions are dichloromethane, trichloromethane, methylchloride, and chloroform showing recent increases. **Dichloromethane shows an increase of almost 25% since 2001**, and as much as 2.5% the last year. The main use of this compound is as an active ingredient in paint removers.

## Long range transport of pollutions; aerosols and reactive gases – Key findings

---

- **Aerosols:** Aerosols are small particles suspended in the atmosphere. Major sources of anthropogenic aerosols are burning of fossil fuel, coal, biomass burning, both from agriculture and forests. Aerosols can have a cooling or warming effect depending on the chemical compositing. Globally the cooling effect dominates and offsets the warming of the greenhouse gases since the year 1750 by around 1/3. However, this is connected with uncertainty and the effects of aerosols on the radiative balance and climate is one of the reasons for the large uncertainty in IPCC's projected range of the increase in global temperature. Monitoring of aerosols is therefore crucial for improved understanding of global warming and its mitigation.

Observations of the total amount of aerosol particles above Ny-Ålesund show increased concentration levels during spring time compared to the rest of the year. This is called Arctic haze which is due to transport of pollution from lower latitudes (mainly Europe and Russia) during winter/spring. In 2009 this aerosol pollution was at approximate the same level as previous years. There were also shorter episodes with elevated levels of particles later. Aerosol particles are short-lived climate forcing agents, and an extension of the aerosol observations at Zeppelin by including measurements of the aerosol absorption properties will be very useful to improve the knowledge of the aerosol type and their effects in the Arctic atmosphere.

New aerosol observations from the Birkenes observatory are included in the program for the first time. The aerosols observed at Birkenes are characterized by long-range transport from Great Britain, Central Europe, and the Arctic, with occasional long-range transport episodes also from North America including forest fire aerosol. In addition to the transported aerosols, local or regional emissions, either natural or anthropogenic are visible. For local or regional influence on the aerosol particle phase, it seems like natural emissions dominate in summer, whereas anthropogenic emissions dominate in winter at Birkenes.

- **Reactive gases:** Tropospheric ozone and CO have elevated levels in polluted regions like central Europe. They are suitable indicators for long range transport of pollution from the continents to Svalbard, and CO is also a proper tracer for transport of emissions from biomass burning and other fire events. There are several episodes with elevated levels of ozone and CO in 2009 at Zeppelin indicating long range transport. No episode is as extreme as the one in

2006. In general there has been **a reduction in the CO concentration the last years at Zeppelin from 2003**. The explanation to this is not yet understood. The annual mean value for 2009 was 118 ppb which is the same as for 2008.

- ***Episodes of long range transport:*** Also in 2009 there were several episodes with polluted air transported to Zeppelin resulting in elevated levels of CH<sub>4</sub>, CO, CO<sub>2</sub> and aerosols. In 2009 the Zeppelin observatory experienced air categorised as clean Arctic and Atlantic air masses around 60% of the time. This is lower than the previous years. In particular the observatory received air masses from the Russian area and Central Europe. This means that the observations at Zeppelin might seem to be more influenced by long range transport of pollution from Russia and central Europe in 2009 than in 2007 and 2008. However, **it is important to remember that air masses representative for the Arctic region is high also in 2009** and observations at Zeppelin represent Arctic background air.

## 2. Introduction

The greenhouse effect is a naturally occurring process in the atmosphere caused by trace gases, especially water vapour (H<sub>2</sub>O), carbon dioxide (CO<sub>2</sub>), methane (CH<sub>4</sub>) and nitrous oxide (N<sub>2</sub>O) that naturally occur in the atmosphere. The content of the last three gases in the atmosphere are closely related to emissions from main sources, whilst the water content varies mainly with temperature. Without these gases the global mean temperature would have been much lower. These gases absorb infrared radiation and thereby trap energy emitted by the Earth. Due to this energy trapping the global mean temperature is approximately 13.7°C, more than 30 degrees higher than it would have been without these gases present (IPCC, 2007). This is the natural greenhouse effect. The enhanced greenhouse effect refers to the additional effect of the greenhouse gases from human activities. In the industrial era, after 1750, the concentration of greenhouse gases in the atmosphere has increased significantly. The global atmospheric mean mixing ratios of CO<sub>2</sub> has increased by 38% (from 280 ppm as a pre-industrial concentration to 386.8 ppm in 2009) and methane has increased by as much as 157% from 700 ppb to 1803 ppb in 2009) according to WMO (WMO, 2010). 2009 showed new record levels of both these gases. The overall changes in the concentrations of the greenhouse gases are the main cause of the global mean temperature rise of 0.74°C over the last century reported by IPCC (2007). Depending on the various emission scenarios used and natural feed-back mechanisms the temperature is predicted to increase with 1.1-6.4°C approaching the year 2100, according to IPCC (2007).

Radiative forcing<sup>1</sup> is a useful tool to estimate the relative climate impacts of various components inducing atmospheric radiative changes. The influence of external factors on the climate can be broadly compared using this concept. Revised global-average radiative forcing estimates from the 4<sup>th</sup> IPCC assessment report are shown in Figure 1 (IPCC, 2007). The estimates represent radiative forcing caused by changes in anthropogenic factors since pre-industrial time and up to the year 2005.

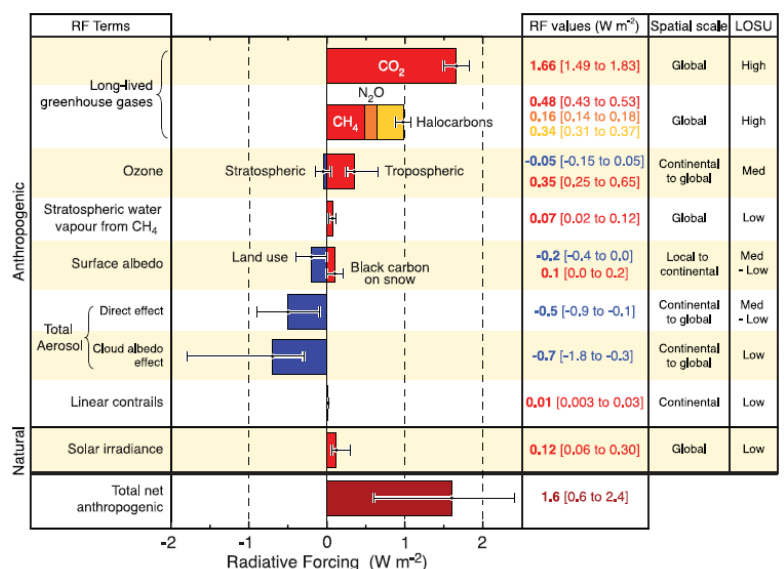


Figure 1: Global-average radiative forcing (RF) estimates for important anthropogenic agents and mechanisms together with the typical spatial scale of the forcing and the assessed level of scientific understanding (LOSU).

<sup>1</sup> Radiative forcing is a measure of the influence a factor has in altering the balance of incoming and outgoing energy in the Earth-atmosphere. It is an index of the importance of the factor as a potential climate change mechanism. It is expressed in Wm<sup>-2</sup> and positive radiative forcing tends to warm the surface. A negative forcing tends to cool the surface.

The most important greenhouse gas emitted from anthropogenic activities is CO<sub>2</sub> with a radiative forcing of 1.66 W m<sup>-2</sup> given in the 4<sup>th</sup> IPCC report (IPCC, 2007). This is an increase of 0.2 W m<sup>-2</sup> since the IPCC report from 2001. CH<sub>4</sub> and N<sub>2</sub>O are other components with strong forcings of 0.48 W m<sup>-2</sup> and 0.16 W m<sup>-2</sup> respectively. It is worth noting that even the change in CO<sub>2</sub> radiative forcing since 2001 is stronger than the forcing of e.g. N<sub>2</sub>O, emphasising the importance of CO<sub>2</sub>.

The joint group of halocarbons is also a significant contributor to the radiative forcing. Halocarbons include a wide range of components. The most important ones are the ozone depleting gases regulated through the Montreal protocol. This includes the CFCs, the HCFCs, chlorocarbons, bromocarbons and halons. Other gases are the HFC (fluorinated halocarbons), PFCs (per fluorinated halocarbons), and SF<sub>6</sub>. These fluorinated gases are regulated through the Kyoto protocol. The total forcing of the halocarbons is 0.337 Wm<sup>-2</sup>, and the single component CFC-12 is presently stronger than N<sub>2</sub>O, but the concentration of CFC-12 seems to have reached its peak value. The trend for CFC-12, seemingly to lower concentrations, gives reason for optimism for this substance. Observations of the halocarbons and methane are central activities at the Zeppelin observatory. Most of the halocarbons have now a negative trend in the development of the atmospheric mixing ratios.

The diagram below shows the relative contribution (in percent) of the long-lived greenhouse gases and ozone to the anthropogenic greenhouse warming since pre-industrial times (1750). The numbers are based on the radiative forcing estimates in the last IPCC report. The diagram shows that CO<sub>2</sub> has contributed to 55% of the changes in the radiative balance while methane has contributed 16% since pre-industrial times. The halocarbons have contributed 11% to the direct radiative forcing of all long-lived greenhouse gases.

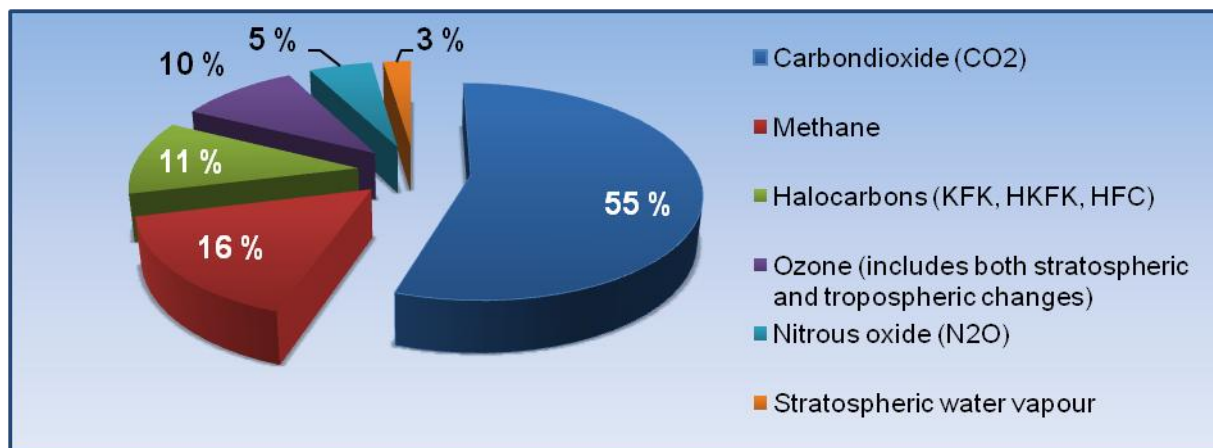


Figure 2: The relative contribution in percent of the long-lived greenhouse gases and ozone to the anthropogenic warming since pre-industrial times (1750). The numbers are based on the radiative forcing estimates in the last IPCC report.

According to the last IPCC report (IPCC, 2007), a large source of uncertainty in climate predictions is caused by insufficient understanding of the atmospheric aerosol processes and historic evolution.

There are two dominant pathways for atmospheric aerosols to influence climate, both exerting a cooling effect in most cases. On one hand, aerosol scatter incoming solar radiation back into

space, preventing it from reaching the ground and warm the surface. This is the so-called direct aerosol climate effect. Additionally, aerosols are activated to cloud particles. Increasing the number of aerosols will in turn increase the cloud particles and also the reflectivity and lifetime of the cloud, again with a cooling effect. This is called indirect aerosol climate effect. Both effects are quantified by negative aerosol radiative forcing in Figure 1 leading to cooling of the surface. The negative aerosol radiative forcing partially offsets the positive, warming radiative forcing by greenhouse gases. In this way the aerosols mask the warming of the greenhouse gases, the magnitude is still uncertain.

***The main objective of NILU's monitoring programme*** is to observe, analyse and interpret the changes in the atmospheric concentrations of the gases included in the Montreal protocol and the Kyoto protocol. An overview of all gases observed together with their trends, lifetime and GWP is given in Table 1 in the Summary. Furthermore the programme shall provide relevant information about aerosols observations important for increased understanding of climate change.

The international collaboration regarding the protection of the ozone layer leading to the Montreal protocol started with the Vienna convention in 1985. Two years later the Montreal protocol was signed and for the first time there was an international agreement forcing the participating countries to reduce and phase out anthropogenic substances. Halocarbons and their relation to the Montreal protocol are indicated in Table 1. Today more than 190 countries have ratified the protocol and many countries have also ratified the later additions to the protocol. The Montreal protocol has goals and strategies for all of the ozone reducing substances and the protocol is a part of the UN environmental program UNEP. According to the last ozone assessment report from WMO (WMO, 2007) the total combined abundance of anthropogenic ozone-depleting gases in the troposphere had decreased by 8-9% from the peak value observed in the 1992-1994 time period. This was related to 2005 levels, and the gases have continued to decrease since.

The target set by the Kyoto protocol is to reduce the total emissions of greenhouse gases from the industrialized countries during the period 2008 to 2012. The four most important greenhouse gases and two groups of gases are included: CO<sub>2</sub>, CH<sub>4</sub>, N<sub>2</sub>O, SF<sub>6</sub> (sulphur-hexafluoride), hydrofluorocarbons (HFCs) and perfluorocarbons (PFCs). The emissions are calculated as annual mean values during the period 2008-2012. The gases are considered jointly and weighted in accordance with their global warming potentials as given by IPCC (2007) and shown in Table 1.

A Norwegian introduction to the Montreal and Kyoto protocol can be found at "Miljøstatus Norge" (<http://www.miljostatus.no>). The English link to the Montreal protocol is [http://ozone.unep.org/Ratification\\_status/montreal\\_protocol.shtml](http://ozone.unep.org/Ratification_status/montreal_protocol.shtml) whereas the Kyoto protocol can be found at [http://unfccc.int/essential\\_background/kyoto\\_protocol/items/1678.php](http://unfccc.int/essential_background/kyoto_protocol/items/1678.php).

### 3. The Norwegian Observatories measuring long lived greenhouse gases



Figure 3: Location of NILU's the atmospheric sites measuring long lived greenhouse gases.

Trough different monitoring programmes, NILU operates many measurements sites, and three of these are comprehensive observatories measuring various long lived greenhouse gases illustrated in Figure 3. The national monitoring programme of greenhouse gases has only included measurements from Zeppelin from 2001, but in 2009 measurements of CO<sub>2</sub> and CH<sub>4</sub> at Birkenes was also included. Additionally, NILU performs measurements of CO and CO<sub>2</sub> at Andøya from 2010 through the [Marine Pollution Monitoring Programme](#).

Norway has a national interest and particular responsibility to develop harmonized and high quality GHG observation infrastructures in the northern region including the Sub-arctic and Arctic areas. Long range transport of air pollution from the central-European continent is occurring, and of high relevance. There is also transport from the North-American continent, China and other Asian regions (Stohl, 2006) detected at Zeppelin. Furthermore, the industrial development in the Arctic regions, particularly the increase in oil, gas, and ship activities, will influence the GHG levels in this vulnerable region. Moreover, possible emission from the

huge reservoirs of methane in the Arctic region is crucial to follow over long time. These are typical emissions from regions with thawing of permafrost, changes in wetlands and thaw lakes, and methane hydrates at the sea floor. All are sensitive to global warming, with strong positive feedbacks.

The measurement activities at the Zeppelin and Birkenes Observatories contribute to a number of global, regional and national monitoring networks:

- EMEP (European Monitoring and Evaluation Programme under "UN Economic Commission for Europe")
- AGAGE (Advanced Global Atmospheric Gases Experiment)
- Global Atmospheric Watch (GAW under WMO)
- Network for detection of atmospheric change (NDAC under UNEP and WMO)
- Arctic Monitoring and Assessment Programme (AMAP)

Most data are public available through the international data base hosted at NILU: <http://ebas.nilu.no>.

#### 3.1 The Zeppelin observatory

The monitoring observatory is located in the Arctic on the Zeppelin Mountain, close to Ny-Ålesund at Svalbard. At 79° north the station is placed in an undisturbed arctic environment, away from major pollution sources. Situated 474 meters a.s.l and most of the time above the inversion layer, there is minimal influence from local pollution sources in the nearby small community of Ny-Ålesund.

The unique location of the station makes it an ideal platform for the monitoring of global atmospheric change and long-range transport of pollution. The main goals of NILU's research activities at the Zeppelin station are:

- Studies of climate related matters and stratospheric ozone
- Exploration of atmospheric long-range transport of pollutants. This includes greenhouse gases, ozone, persistent organic pollutants, aerosols and others.
- Characterization of the arctic atmosphere and studies of atmospheric processes and changes

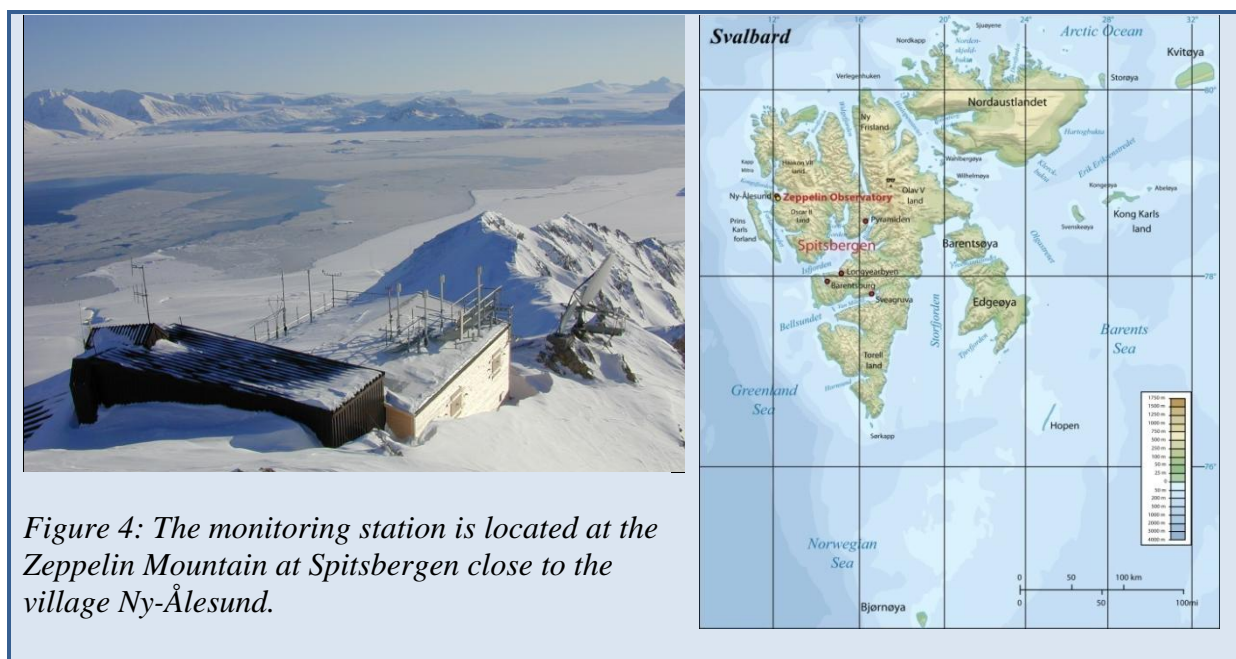


Figure 4: The monitoring station is located at the Zeppelin Mountain at Spitsbergen close to the village Ny-Ålesund.

The Zeppelin station is owned and maintained by the Norwegian Polar Institute. NILU is co-ordinating the scientific activities at the station. The station was built in 1989-1990. After 10 years of use, the old building was removed to give place to a new modern station that was opened in May 2000. The building contains several separate laboratories, some for permanent use by NILU and Stockholm University, others intended for short-term use like measurement campaigns and visiting scientists. A permanent data communication line permits on-line contact with the station for data reading and instrument control.

NILU performs measurements of more than 20 greenhouse gases including halogenated greenhouse gases, methane and carbon monoxide. In Appendix I there are more details about sampling techniques and frequency of observations. Methane and CO are sampled 3 times per hour. This high sampling frequency gives valuable data for the examination of episodes caused by long-range transport of pollutants as well as a good basis for the study of trends and global atmospheric change. Close cooperation with AGAGE-partners on the halocarbon instrument and audits on the methane and CO-instruments (performed by EMPA on the behalf of GAW/WMO) results in show data of high quality.

The amount of particles in the air is monitored by a Precision-Filter-Radiometer (PFR) sun photometer. This instrument gives the aerosol optical depth (AOD). AOD is a measure of the aerosols attenuation of solar radiation in the total atmospheric column.

The station at Zeppelin Mountain is also used for a wide range of other measurements, which are not directly related to climate gas monitoring, including daily measurements of sulphur and nitrogen compounds ( $\text{SO}_2$ ,  $\text{SO}_4^{2-}$ ,  $(\text{NO}_3^- + \text{HNO}_3)$  and  $(\text{NH}_4^+ + \text{NH}_3)$ , main compounds in precipitation (performed in Ny-Ålesund), total gaseous mercury, particulate heavy metals, persistent organic pollutants (HCB, HCH, PCB, DDT, PAH etc.) in air, as well as tropospheric ozone. Zeppelin observatory is also widely used in campaigns as during the International Polar Year.

At the Zeppelin station carbon dioxide ( $\text{CO}_2$ ) is measured by Stockholm University (SU) (Institute of Applied Environmental Research, ITM). SU maintain an infrared  $\text{CO}_2$  instrument measuring  $\text{CO}_2$  continuously. The instrument has been in operations since 1989. The continuous data are enhanced by the weekly flask sampling programme in co-operation with NOAA CMDL. Analysis of the flask samples provide  $\text{CH}_4$ ,  $\text{CO}$ ,  $\text{H}_2$ ,  $\text{N}_2\text{O}$  and  $\text{SF}_6$  data for the Zeppelin station in addition to  $\text{CO}_2$ .

### 3.2 The Birkenes observatory

Birkenes is located in Southern-Norway at 58° 23'N, 8° 15'E, 190 m a.s.l. The observatory has been in operation since 1971 and is one of the longest-running sites in Europe. In 2009, the aerosol observation programme at Birkenes Atmospheric Observatory received a major upgrade along with the upgrade of the general station infrastructure. The observatory was moved a few hundred meters and considerably upgraded in 2009 now measuring  $\text{CO}_2$  and  $\text{CH}_4$  with a Picarro instrument and a comprehensive aerosol program. The old station was situated in a hollow with limited line of sight to the oncoming flow. Since summer 2009, the observations are housed in a container assembly on the top of a hill a, with free line of sight to the oncoming flow in all directions (see Figure 5). The land use in the close vicinity of the site is characterized by 65% forest, 10% meadow, 15% freshwater lakes, and 10% agricultural areas (low intensity). This relocation improved the regional representativeness of the station significantly. The observation programme concerning atmospheric aerosol parameters was augmented by measurements of coarse mode particle size distribution, spectral particle scattering coefficient, and aerosol optical depth. It meets now EUSAAR<sup>2</sup> and GAW standards, and comprises now almost all observations considered by the GAW aerosol scientific advisory group as relevant for aerosol climate effect assessments. This upgrade is also an important improvement of the Norwegian observation programme of climate forcing agents, which so far was more focussed on the polar regions. While there is agreement that climate changes will become visible first in Arctic and Antarctic, it is Central and Southern Norway where the largest fraction of the Norwegian population resides. Accurate observations of climate relevant aerosol properties are a prerequisite for better climate predictions for this region.

All electrical and data infrastructure is new and upgrade with Near-Real-Time measurements controlled at NILU. Data from Birkenes (e.g. daily measurements  $\text{SO}_2$ ,  $\text{SO}_4^{2-}$ ,  $\text{NO}_3^- + \text{HNO}_3$  and  $\text{NH}_4^+ + \text{NH}_3$ , main compounds in precipitation, mercury and other heavy metals, persistent organic pollutants, tropospheric ozone) have been essential for the study of long-range transport and deposition of air pollution to Scandinavia. The monitoring at this site, together with other central European regional sites, has provided the necessary background for establishing international binding agreements for targeting emission reductions, c.f. the convention for long-range transboundary air pollutions (CLTRAP) and the protocols

---

<sup>2</sup> EUSAAR: European Supersites for Atmospheric Aerosol Research <http://www.eusaar.net>

hereunder. Personnel is visiting the observatory on a daily basis, and engineers from NILU are present at the station regularly (approximately once per month).

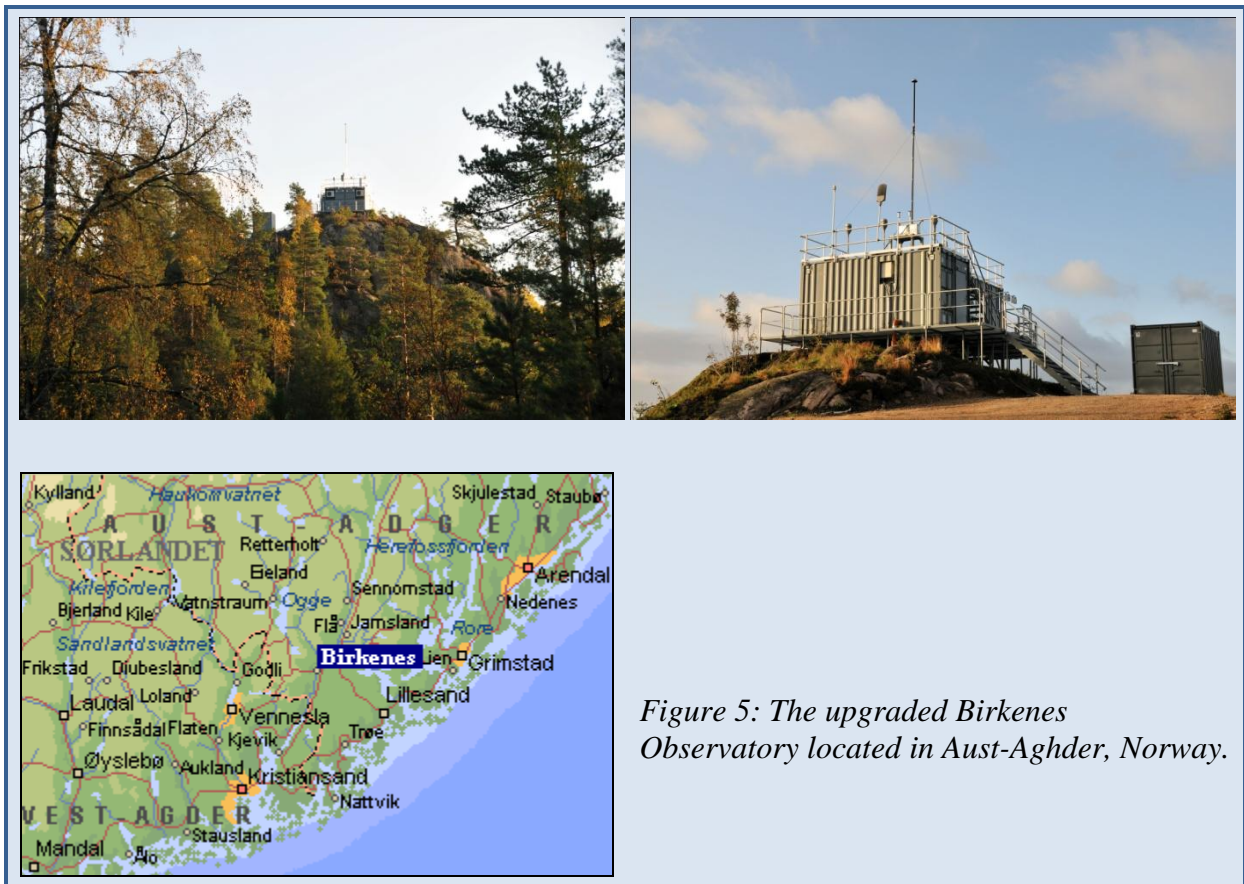


*Figure 5: The upgraded Birkenes Observatory located in Aust-Agder, Norway.*

#### 4. Observations and trends of greenhouse gases at the Zeppelin Observatory in the Norwegian Arctic

NILU measures 23 greenhouse gases at the Zeppelin observatory at Svalbard. The results from the measurements, analysis and interpretations are presented in this chapter. Also observations of CO<sub>2</sub>, which are performed by the Stockholm University - Department of Applied Environmental Science (ITM), are included in the report.

Table 2 presents the main results with annual mean values since the beginning of the observation period in 2001. Also trend per year and change (acceleration) in the trend for each component is given. The acceleration in the trend show how the growth rate has changed the last few years, and indicates the expected change in the coming years<sup>3</sup>, assuming the same development in the emissions.

Table 2: Yearly average concentration levels of greenhouse gases measured at the Zeppelin station for the years 2001-2009. All concentrations are in ppt<sub>v</sub>, except for methane and carbon monoxide (ppb<sub>v</sub>) and CO<sub>2</sub> (ppm<sub>v</sub>). The trends are calculated from observations for the period 2001-2009.

Compound	Formula	2001	2002	2003	2004	2005	2006	2007	2008	2009	Trend / year	Change in trend
<b>Methane</b>	CH <sub>4</sub>	1858	1852	1870	1859	1863	1865	1878	1888	1892	+4.5	+1.40
<b>Carbon monoxide</b>	CO		125.9	141.5	132.9	132.6	125.6	120.9	122.9	112.9	-2.5	-0.98
<b>Carbon dioxide**</b>	CO <sub>2</sub>	371	373	376	378	381	382	384	386	387	+1.7**	-0.41**
<b>Chlorofluorocarbons</b>												
CFC-11*	CFCl <sub>3</sub>	262	264	264	260	259	256	249	247	245	-2.6	-0.6
CFC-12*	CF <sub>2</sub> Cl <sub>2</sub>	548	561	563	562	559	558	547	544	544	-1.8	-1.7
CFC-113*	CF <sub>2</sub> ClCFCl <sub>2</sub>	81.5	82.7	82.5	81.8	80.9	79.6	78.2	77.9	78.1	-0.7	-0.1
CFC-115*	CF <sub>3</sub> CF <sub>2</sub> Cl	8.3	8.5	8.5	8.6	8.6	8.5	8.5	8.5	8.4	+0.01	-0.03
<b>Hydrochlorofluorocarbons</b>												
HCFC-22	CHF <sub>2</sub> Cl	159	165	171	177	181	188	196	204	213	+ 6.48	-0.50
HCFC-141b	CH <sub>3</sub> CFCl <sub>2</sub>	16.6	18.1	19.0	19.5	19.6	19.9	20.3	20.8	21.5	+ 0.52	-0.09
HCFC-142b*	CH <sub>3</sub> CF <sub>2</sub> Cl	14.9	15.6	16.4	17.0	17.7	18.8	19.4	20.4	21.4	+ 0.80	+0.04
<b>Hydrofluorocarbons</b>												
HFC-125	CHF <sub>2</sub> CF <sub>3</sub>	2.0	2.6	3.1	3.8	4.4	5.1	5.9	6.9	7.9	+0.72	+0.06
HFC-134a	CH <sub>2</sub> FCF <sub>3</sub>	20.7	26.1	31.0	35.7	40.1	44.3	48.5	53.3	57.7	+4.55	-0.10
HFC-152a	CH <sub>3</sub> CHF <sub>2</sub>	2.9	3.4	4.1	4.9	5.6	6.8	7.8	8.7	9.0	+0.83	+0.02
<b>Halons</b>												
H-1301	CF <sub>3</sub> Br	3.0	3.1	3.2	3.2	3.3	3.2	3.2	3.3	3.3	+ 0.03	-0.02
H-1211*	CF <sub>2</sub> ClBr	4.4	4.5	4.6	4.7	4.6	4.6	4.5	4.4	4.3	- 0.01	-0.04
<b>Halogenated compounds</b>												
Methyl Chloride	CH <sub>3</sub> Cl	505	525	529	524	521	521	522	524	528	+1.38	-0.86
Methyl Bromide	CH <sub>3</sub> Br	9.3	9.1	8.8	8.9	8.7	8.9	8.9	8.2	7.7	-0.14	-0.04
Dichloromethane	CH <sub>2</sub> Cl <sub>2</sub>	30.9	31.4	32.9	32.7	32.1	33.6	35.5	37.4	38.4	+0.91	+ 0.21
Chloroform	CHCl <sub>3</sub>	10.9	10.6	10.9	10.5	10.5	10.5	10.6	10.3	10.8	-0.04	+0.01
Trichloromethane	CH <sub>3</sub> CCl <sub>3</sub>	37.6	32.4	27.6	23.0	19.2	16.0	13.3	10.9	9.3	-3.56	+0.52
Trichloroethylene	CHClCCl <sub>2</sub>	0.7	0.6	0.5	0.5	0.4	0.4	0.3	0.3	0.4	-0.04	0.02
Perchloroethylene	CCl <sub>2</sub> CCl <sub>2</sub>	4.4	4.1	4.0	3.7	3.1	2.7	3.0	2.6	2.9	-0.24	+0.08
Sulphurhexafluoride*	SF <sub>6</sub>	5.0	5.1	5.3	5.5	5.7	6.1	6.3	6.6	6.9	+0.25	+0.02

<sup>\*</sup>The measurements of these components are not within the required precision of AGAGE. See Appendix I for more details.

<sup>\*\*</sup>Measurements of Carbon dioxide are performed by Stockholm University, Department of Applied Environmental Science (ITM).

<sup>3</sup> As the time series still are short and the seasonal and annual variations are large for many of the components, there are considerable uncertainties connected with the results.

Greenhouse gases have numerous sources both anthropogenic and natural. Trends and future changes in concentrations are determined by their sources and the sinks, and in section 4.1 are observations and trends of the monitored greenhouse gases with both natural and anthropogenic sources presented in more detail. In section 4.2 are the detailed results of the gases with purely anthropogenic sources presented. These gases are not only greenhouse gases but also a considerable source of chlorine and bromine in the stratosphere, and are thus responsible for the ozone depletion and the ozone hole discovered in 1984. The ozone depleting gases are controlled and regulated through the successful Montreal protocol. Section 3 describes the Zeppelin observatory at Svalbard where the measurements take place and the importance of the unique location. Zeppelin observatory is a unique site for observations of changes in the background level of atmospheric components. All peak concentrations of the measured gases are significantly lower at Ny-Ålesund than at other sites, due to the stations remote location. A description of the instrumental and theoretical methods applied is included in Appendix I.

## **4.1 Greenhouse gases with natural and anthropogenic sources**

All gases presented in this section (methane, carbon dioxide, methyl chloride, methyl bromide, carbon monoxide and tropospheric ozone) have both natural and anthropogenic sources. This makes it complex to interpret the observed changes as the sources and sinks are numerous. Moreover, several of these gases are produced in the atmosphere from chemical precursor gases and often also dependant on the solar intensity.

### **4.1.1 Observations of methane in the period 2001-2009**

Methane (CH<sub>4</sub>) is the second most important greenhouse gas after CO<sub>2</sub> with a radiative forcing of 0.48 W m<sup>-2</sup> since 1750 and up to 2005. The average CH<sub>4</sub> concentration in the atmosphere is determined by a balance between emission from the various sources at the earth's surface and reaction and removal by free hydroxyl radicals (OH) in the troposphere. The atmospheric lifetime of methane is 12 years (Forster et al., 2007). In addition to be a dominating greenhouse gas, methane also plays a significant role in the atmospheric chemistry.

The atmospheric mixing ratio of methane has, after a strong increase during the 20. century, been relatively stable over the period 1998-2005. The global average change was close to zero for this period according to IPCC (Forster et al, 2007), and also at our site for the short observation period 2001-2004. 2003 was an exception globally and at Zeppelin; a maximum annual mean of 1870 ppb at Zeppelin was obtained, considerable higher than the other years. This was probably caused by increased precipitation in the tropical regions leading to increased methane emissions from wetland areas and a global rise in the concentration. Recently an increase in the methane levels is evident from both our observations, and observations at other sites (Rigby et al., 2008; WMO, 2009). The year 2009 showed new record levels at Zeppelin and globally. Figure 6 presents the observations of methane at Zeppelin since the start in 2001.

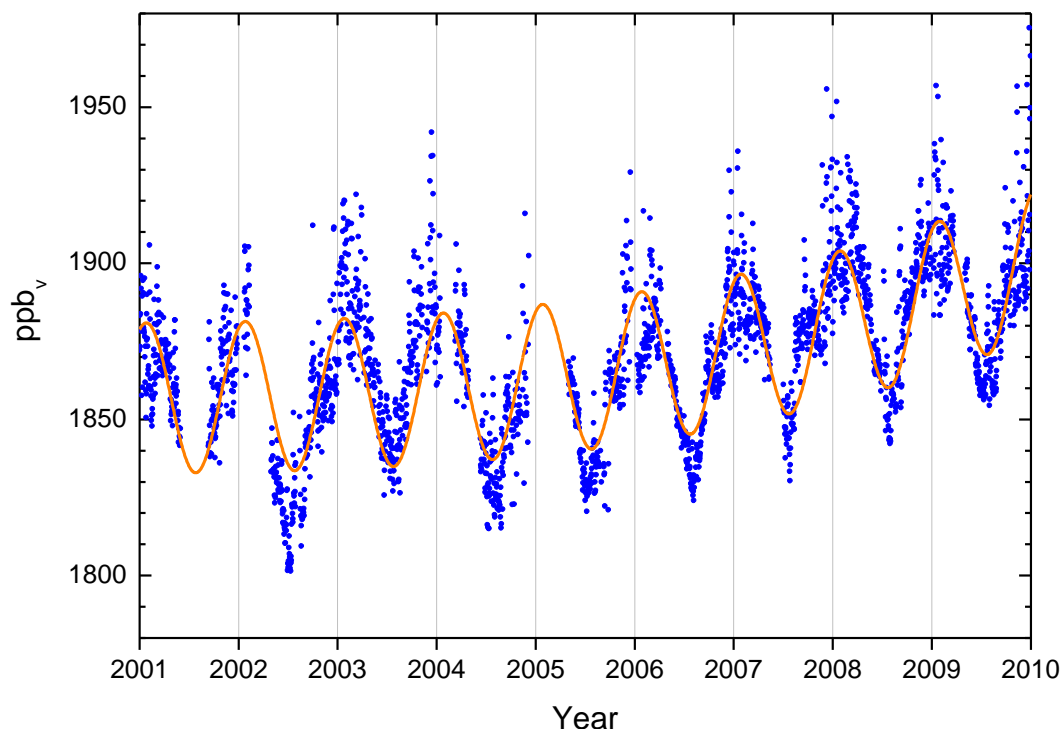


Figure 6: Observations of daily averaged methane concentrations for the period 2001-2009 at the Zeppelin observatory. Blue dots: observations, orange solid line: modelled background methane mixing ratio.

As can be seen from Figure 6 there has been an increase in the concentrations of methane observed at Zeppelin in the last years. The pronounced increase started in November/December 2006 and continues throughout the years 2007 - 2009, and is particularly evident in the late summer-winter 2007, and late autumn 2009. A maximum methane mixing ratio as high as 1975 ppb<sub>v</sub> was observed 26<sup>th</sup> December 2009. This was 2.9% above the modelled background value, and the highest value ever recorded at Zeppelin. There were no values nearly as high as this in 2008. Other periods with very high values have occurred in during the year. More detailed analyses of possible source regions for emissions resulting in elevated levels at Zeppelin are included in section 7.

To retrieve the annual trends in the methane levels for the entire period the observations have been fitted by an empirical equation as described in Appendix I. The modelled methane values are included as the orange solid line in Figure 6. Only the observations during periods with clean air arriving at Zeppelin are used in the model, thus the model represents the background level of methane at the site.

During 1980s when the methane concentration showed a large increase, the annual change was around 15 ppb<sub>v</sub> per year. At Zeppelin the average annual growth rate was +4.5 ppb<sub>v</sub> per year for the period 2001-2009. This corresponds to an increase of 0.17% per year. Comparably the annual trend for the period 2001-2007 was +2.7 ppb<sub>v</sub> thus the increased growth during the last years has changed the trend substantially. In 2009 there has been an acceleration of 1.4 in the trend (see Table 2). The development in the future is connected with large uncertainty as the reason for the observed increase since 2005 is not clear, and additionally, the seasonal and annual variations are large and the time series still short.

The increase in the methane levels the last years is visualized in Figure 7 showing the CH<sub>4</sub> annual mean mixing ratio for the period 2001-2009. The annual means are based on a combination of the observed methane values and the modelled background values; during periods with lacking observations we have used the modelled background mixing ratios in the calculation of the annual mean.

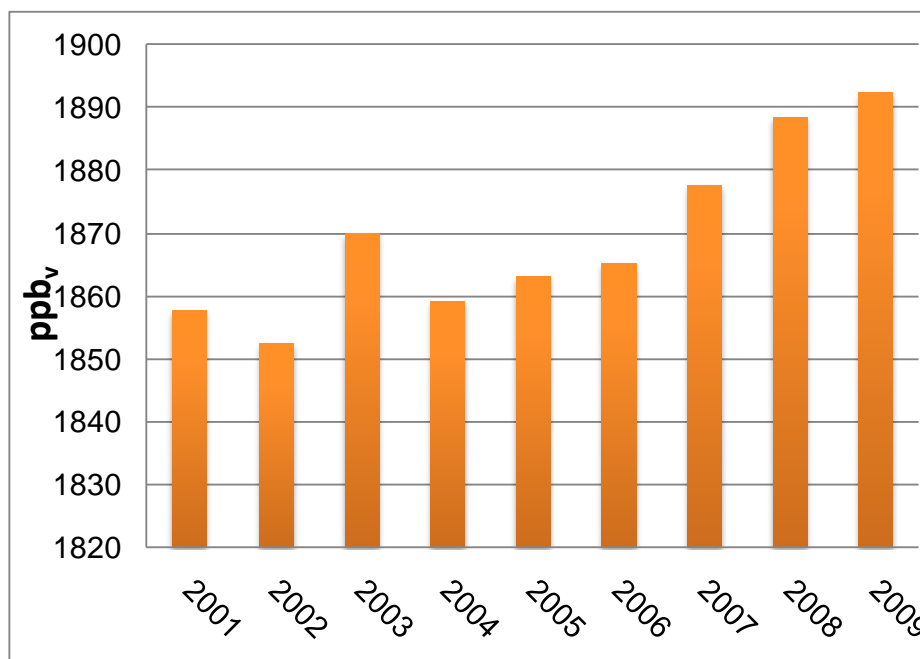


Figure 7: Development of the annual mean mixing ratio of methane measured at the Zeppelin Observatory for the period 2001-2009.

This diagram clearly illustrates the increase in the concentrations of methane the last years, with 2009 as a new record year. The annual mean mixing ratio for 2009 was 1892 ppb<sub>v</sub> while the level was 1888 ppb<sub>v</sub> in 2008. The increase of 5 ppb (0.21%) in 2009 was weaker than from 2007-2008 when the increase was as high as 11 ppb. The increase since 2005 is 29 ppb (ca. 1.6 %) which is considered as relatively large compared to the development of the global methane mixing ratio in the period from 1999-2005. It is also larger than the global mean increase since 2005 which is 20 ppb (1.1%) (WMO, 2009; 2010).

Also stations at other locations show a significant increase in methane for the year 2007, 2008, and 2009 at both hemispheres. According to WMO (WMO, 2009) there has been a global increase in the methane concentration by 0.34% from 2006 to 2007 and a continuation of the increase up to a new record level in 2009, and absolute increase of 5 ppb (0.28%) above the 2008 level. Thus the global increase is slightly higher than what we observed at Zeppelin for 2009. For 2007, Rigby and his co-workers report a global increase of methane (Rigby et al., 2008). They have analyzed methane observations from 12 sites worldwide, and found an increase of around 10 ppb<sub>v</sub> at all sites since 2006. The largest increase was observed at Mace Head in Ireland and Alert. Alert is a site north in Canada (82°N), and the site closest to the Zeppelin observatory at Svalbard, but interestingly they also found a large increase at sites at low latitudes e.g. in California and Ragged Point, Barbados.

The main sources of methane today include boreal and tropical wetlands, rice paddies, emissions from ruminant animals, biomass burning, and fossil fuels combustion. Further, methane is the principal component of natural gas and e.g. leakage from pipelines, off-shore and on-shore installations are known source of atmospheric methane. The distribution between natural and anthropogenic sources is approximately 40% natural sources, and 60% of the sources are direct a result of anthropogenic emissions. Of natural sources there is a large unknown potential methane source at the ocean floor, so called methane hydrates. Other sources include mud volcanoes which are connected with deep geological faults, and also emissions from plants are suggested (Keppler et al., 2006). Further a large unknown amount of methane is bounded in the permafrost layer in Siberia and North America and this might be released if the permafrost layer melts as a feedback to climate change. According to the last IPCC report (Alley et al. 2007) the temperature of the top of the permafrost layer has generally increased by up to 3°C since 1980s.

In the atmosphere methane is destroyed by the reaction with the hydroxyl radical (OH) giving water vapour and CO<sub>2</sub>. A small fraction is also removed by surface deposition. The stratospheric impact of CH<sub>4</sub> is due to the fact that CH<sub>4</sub> contributes to water vapor buildup in this region of the atmosphere influencing the ozone layer. Since the reaction with OH also represents a significant loss path for the oxidant OH, additional CH<sub>4</sub> emission will suppress OH and thereby increase the CH<sub>4</sub> lifetime, implying further increases in atmospheric CH<sub>4</sub> concentrations (Isaksen and Hov, 1987; Prather et al., 2001). This positive chemical feedback is estimated to be significant in the current atmosphere with a feedback factor of about 1.4<sup>4</sup> (Prather et al., 2001). The OH radical has a crucial role in the tropospheric chemistry by reactions with many emitted components and is responsible for the cleaning of the atmosphere (like removal of CO, hydrocarbons, HFCs, and others).

Currently the observed increase the last years is not explained or understood. According to Rigby et al. (2008) there might be signs of a reduction in the hydroxyl radical OH, which is essential in the destruction of methane, which is not in agreement with other observations. Furthermore the OH concentration is low in the Arctic particularly during autumn and winter. There might also be new methane sources. The high level observed in 2003 was a global feature, and is still not fully understood. It is essential to find out if the increase since 2005 is due to large point emissions or if it is caused by newly initiated processes releasing methane to the atmosphere like e.g. the melting of the permafrost layer. Recent and ongoing scientific discussions point in the direction of increased emissions from wetlands located both in the tropical region and in the Arctic region. High effort should be put on the issue to understand the increase in the CH<sub>4</sub> concentrations as the consequence might be severe. NILU will coordinate a research project, *GAME: Causes and effects of Global and Arctic changes in the MEthane budget*, under the Norwegian research Council program NORKLIMA from 2001-2014. The main goal of the project is to increase the understanding of the global methane budget the last 25 years.

#### 4.1.1.1 Measuring methane from space

Atmospheric CH<sub>4</sub> measurements from satellites would have been very useful to understand the natural sources but the available products particularly in the Arctic region are currently not good enough: restricted to daytime, poor temporal and spatial resolution and estimates of column abundance only. Some infrared measurements providing night time observations have

---

<sup>4</sup> This means that with current atmospheric chemical distribution a 10 % increase in emission of methane, the atmospheric composition increases will reach 14 %.

recently become available, but these also have poor temporal and spatial resolutions. There is a strong need to develop new methods and instrumentation for CH<sub>4</sub> measurements and deploy these in the Arctic.

Myhre et al. (2009) show that close to Zeppelin are currently SCIAMACHY, AIRS and IASI satellite measurements of CH<sub>4</sub> not capable of providing the temporal and spatial resolution needed in order to quantify and understand near-surface variations in CH<sub>4</sub>. The analyses done with the measurements from the Zeppelin observatory shows clearly that the satellite data are neither suitable nor of sufficient resolution to understand processes there, or provide valuable information for validation. A similar conclusion may be made for the AIRS, IASI and GOSAT data; however a more detailed analysis needs to be done.

#### 4.1.2 First observations of Nitrous Oxide at the Zeppelin Observatory

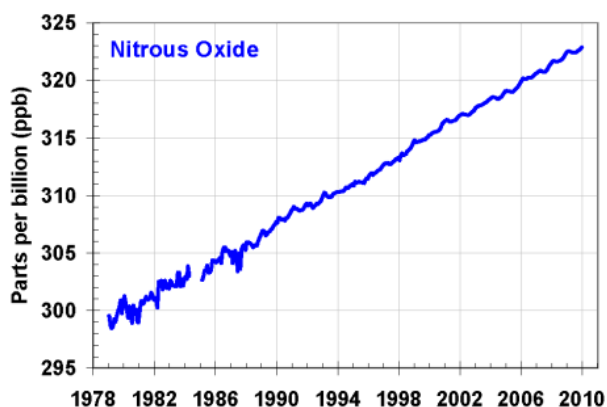
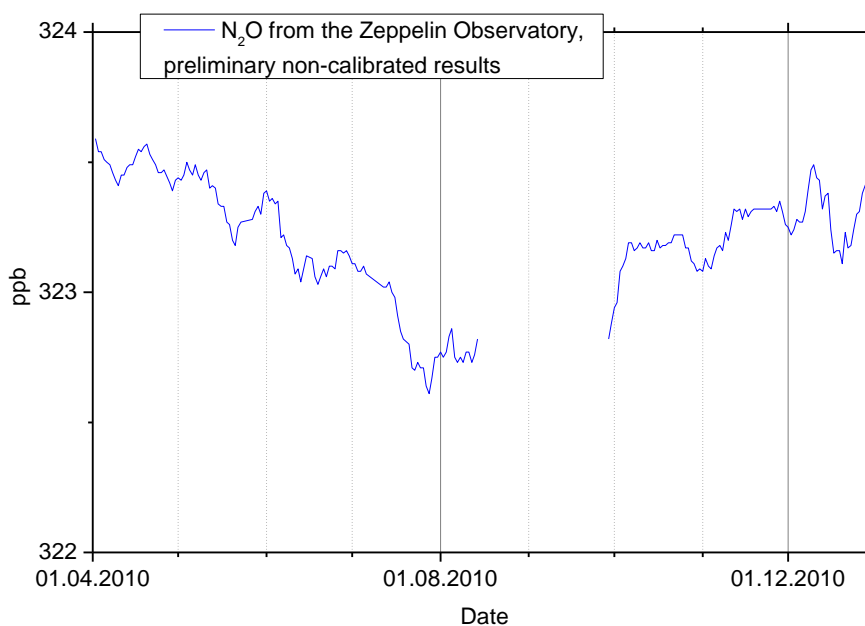


Figure 8: Global average abundances of, nitrous oxide from the NOAA global air sampling network are plotted since the beginning of 1979. <http://www.esrl.noaa.gov/gmd/aggi/>

Nitrous Oxide (N<sub>2</sub>O) is a greenhouse gas with both natural and anthropogenic sources. The sources include oceans, tropical forests, soil, biomass burning, cultivated soil and use of fertilizer, and various industrial processes. There are large uncertainties in the major soil, agricultural, combustion and oceanic sources of N<sub>2</sub>O and also frozen peat soils in Arctic tundra is recently reports as a potential significant source (Repo et al., 2009). N<sub>2</sub>O has a lifetime of ca 114 years and the GWP is 310 (Forster et al., 2007). Thus N<sub>2</sub>O is an important greenhouse gas contributing around 5-6 % to the overall long lived greenhouse gas forcing over the industrial era, and

the gas is regulated through the Kyoto protocol. Additionally, N<sub>2</sub>O is also the major source of the ozone-depleting nitric oxide (NO) and nitrogen dioxide (NO<sub>2</sub>) in the stratosphere thus the component is also influencing the stratospheric ozone layer WMO (2007).

N<sub>2</sub>O has increased from around 270 ppb prior to industrialization and up to an average global mean of 322.5 ppb in 2009 (WMO, 2010). Figure 8 is taken from NOAA and shows the average global development of N<sub>2</sub>O since 1978. The mean growth rate has been 0.77 ppb/yr the last 10 according to WMO (WMO, 2010). The NOAA observations are based on flask samples with mostly weekly or lower time resolution. There are few continuous observations of N<sub>2</sub>O, and particularly in the Arctic region. In 2009 NILU installed a new instrument at Zeppelin to measure N<sub>2</sub>O with high time resolution; 15 mins. The instrument was in full operation in April 2010 and the first results are presented in Figure 9.



*Figure 9: First results of the measurements of N<sub>2</sub>O at the Zeppelin Observatory. Note that this is preliminary non calibrated results for 2010.*

#### **4.1.3 Observations of Carbon Dioxide (CO<sub>2</sub>) in the period 1988-2009**

CO<sub>2</sub> is the most important greenhouse gases with a radiative forcing of 1.66 W m<sup>-2</sup> since 1750 and an increase in the forcing of as much as 0.2 W m<sup>-2</sup> since the IPCC report from 2001 (Forster et al., 2007). CO<sub>2</sub> is the end product in the atmosphere of the oxidation of all main organic compounds and has shown an increase of as much as 38 % since the pre industrial time (WMO, 2009).

Norway do not perform own measurements of CO<sub>2</sub> at the Zeppelin Observatory. The atmospheric CO<sub>2</sub> concentration measured at Zeppelin Observatory for the period 2001-2009 is presented in Figure 10. These data are provided by ITM University of Stockholm and we acknowledge the effort they are doing in monitoring CO<sub>2</sub> at the site. Note that the data are preliminary and have not undergone a full quality assurance.

The results show a continues increase since the start of the observations and in Figure 11 is the development of the annual mean concentrations measured at Zeppelin observatory for the period 1988-2009 shown.

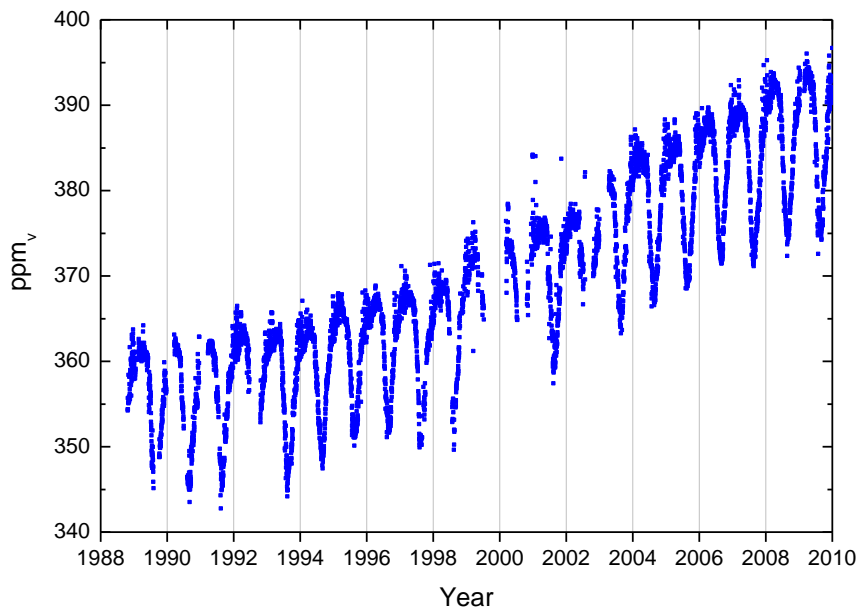


Figure 10: The CO<sub>2</sub> concentration measured at Zeppelin Observatory for the period 2001-2009.

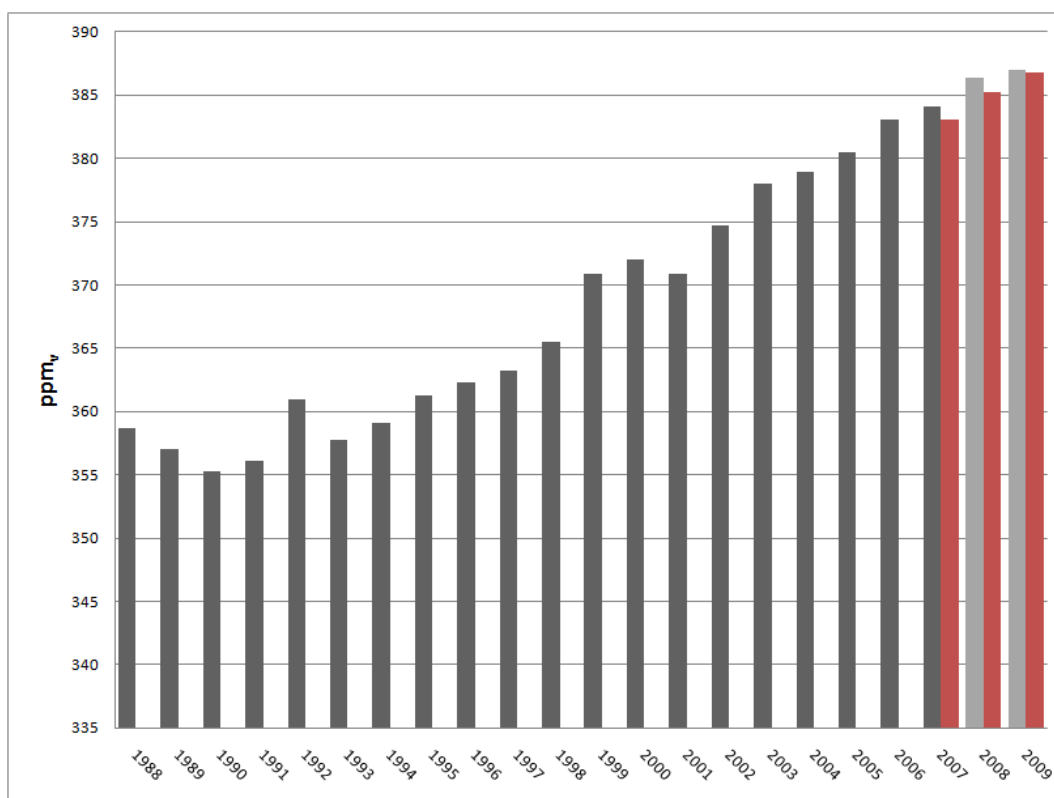


Figure 11: Development of the annual mean mixing ratio of CO<sub>2</sub> measured at Zeppelin observatory for the period 1988-2009. The light grey bars are the preliminary results for 2008 and 2009, and the red bars show the global annual mean for 2007-2009 (WMO, 2010).

The results show that 2009 is a new record year for the annual mixing ratio of CO<sub>2</sub> at Zeppelin, although the increase is smaller than the global mean increase. Unfortunately ITM University of Stockholm have not completed their analysis of the observations yet, thus the mean values for 2008 and 2009 are preliminary. It is shown as a light grey bars in the Figure. The preliminary results indicate that there is an increase of 0.6 ppb since 2008. The global mean value for 2009 is 386.8 ppb (WMO, 2010). This is an increase of 1.6 ppb since 2008. The main reason why the CO<sub>2</sub> level is higher at Zeppelin than globally is that in general the CO<sub>2</sub> emissions are lower in the Southern hemisphere, and the global mixing takes a certain time.

#### 4.1.4 Observations of Methyl Chloride in the period 2001-2009

Methyl chloride (CH<sub>3</sub>Cl) is the most abundant halocarbon in the atmosphere. The main sources of Methyl Chloride in the atmosphere are natural and dominating source is thought to be the algae in the ocean, with biomass burning as the second largest source. But also emissions from warm coastal land, particularly from tropical islands are shown to be a significant source. Due to the dominating natural sources, this compound is not regulated through any of the Montreal or Kyoto protocols, but is an important natural source of Chlorine to the stratosphere.

The results of the observation of this substance for the period 2001-2009 are shown in Figure 12.

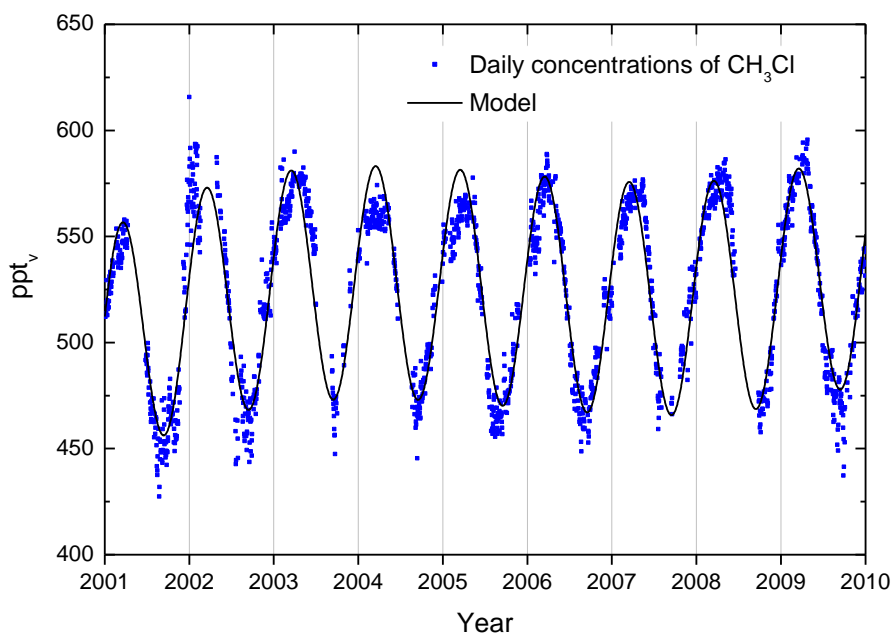


Figure 12: Observations of methyl chloride, CH<sub>3</sub>Cl, for the period 2001-2009 at the Zeppelin observatory. Dots: daily averaged concentrations from the observations, solid line: modelled background mixing ratio.

The lifetime of the compound is only 1.3 year resulting in large seasonal fluctuations as shown in the Figure. Thus the degradation of the compound is dependent on solar intensity. To reach the stratosphere, the lifetime in general needs to be in the order of 2-4 years to have significant chlorine contribution. However, Methyl Chloride has relatively high mixing ratios, and contributes to the stratospheric Chlorine burden. With respect to the warming potential this substance is 16 times stronger than CO<sub>2</sub> per kg gas emitted.

By use of the model described in Appendix I we have calculated the annual trend, and the change in the trend is also given in Table 2. The trend for the period 2001-2009 is 1.38 ppt per year, and the change in the trend is -0.86, much weaker than last year, a slowdown and change in the development.

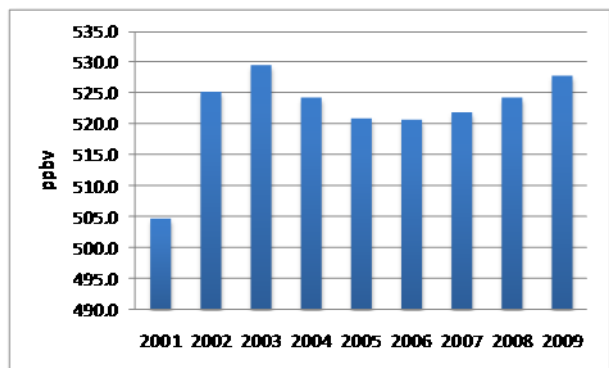


Figure 13: Development of the annual means methyl chloride measured at the Zeppelin Observatory for the period 2001-2009.

The development of the annual means of methyl chloride for the period 2001-2009 is presented in Figure 13. The last years there has been a stabilisation of the level of this gas, but from 2006 there is an increase of 1.4%. As one of the main sources of this compound is algae from the ocean, it is interesting to note the development the last years as the sources might be indirectly related to sea ice cover in the Arctic region, and thus also to the temperatures in the region. A closer study of this is recommended as another sources is biomass burning which might also changed the last years.

#### 4.1.5 Observations of Methyl Bromide in the period 2001-2009

The sources of Methyl Bromide ( $\text{CH}_3\text{Br}$ ) are both from natural and anthropogenic activities. The natural sources such as the ocean, plants, and soil, can also be a sink for this substance. Additionally there are also significant anthropogenic sources; it is used in a broad spectrum of pesticides in the control of pest insects, nematodes, weeds, pathogens, and rodents. It is also used in agriculture primarily for soil fumigation, as well as for commodity and quarantine treatment, and structural fumigation. While methyl bromide is a natural substance, the additional methyl bromide added to the atmosphere by humans contributes to the man made thinning of the ozone layer. Total organic bromine from halons and methyl bromide peaked in 1998 and has declined since (WMO, 2007). This observed decrease was solely a result of declines observed for methyl bromide. Bromine (Br) from halons continues to increase, but at slower rates in recent years, see section 4.2.4 on page 39.

The results of the daily averaged observations of this compound for the period 2001-2009 are shown in Figure 14.

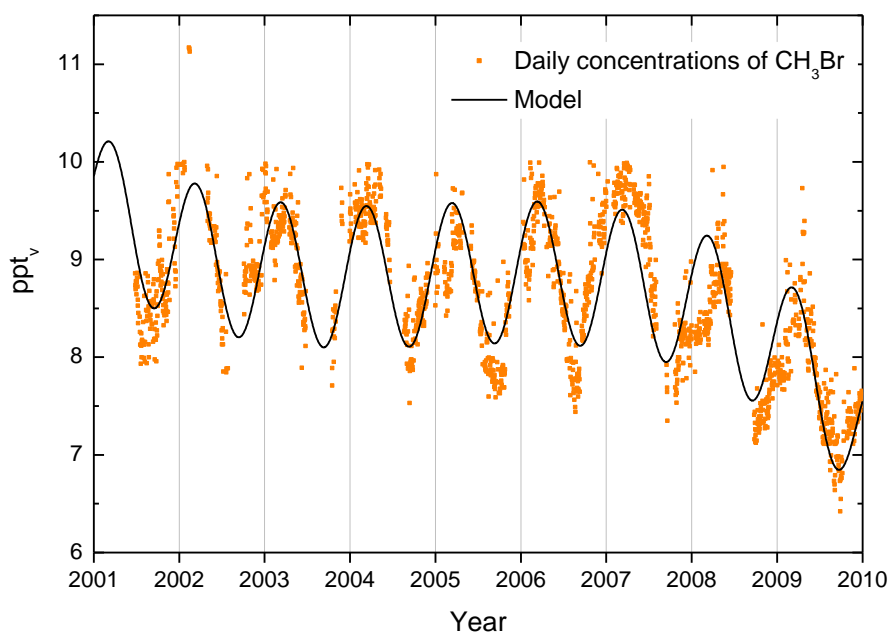


Figure 14: Observations of methyl bromide,  $\text{CH}_3\text{Br}$ , for the period 2001-2009 at the Zeppelin observatory. Dots: daily averages mixing ratios from the observations, solid line: modelled background mixing ratio.

A relatively large change is evident after the year 2007, a reduction of 13%. Methyl bromide is a greenhouse gas with a lifetime of 0.7 years and it is 5 times stronger than  $\text{CO}_2$ , if the amount emitted of both gases were equal. The short life time explains the large annual and seasonal variations of this compound.

We have calculated the annual trend by use of the model described in Appendix I. The trend and change in the trend is given in Table 2. For the period 2001-2009 there is a reduction in the mixing ratio of -0.14 ppt per year, with acceleration in the trend of -0.04. However, note that the observed changes are small and the time period relatively short thus the seasonal and annual variations of the trends are uncertain.

The development of the annual means for the period 2001-2009 is presented in Figure 15, clearly illustrating the decrease the last years. In general atmospheric amounts of methyl bromide have declined since the beginning in 1999 when industrial production was reduced. By mid-2004, mixing ratios had declined globally with 1.3 ppt (14%) from the peak of 9.2 ppt measured before 1999 (WMO, 2007). Global averaged mixing ratios and development the last years are not available for comparison.

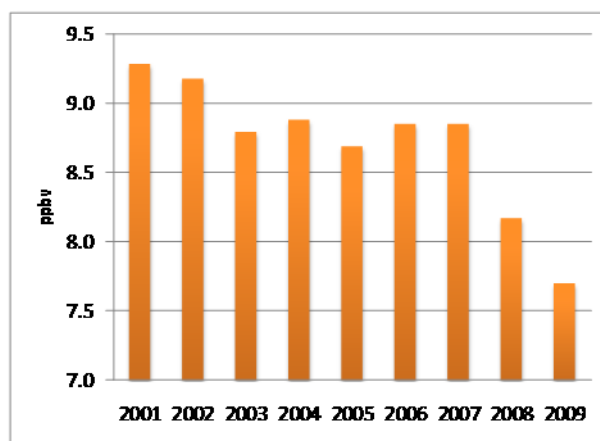


Figure 15: Development of the annual means of Methyl Bromide measured at the Zeppelin Observatory for the period 2001-2009.

#### 4.1.6 Observations of tropospheric ozone in the period 1990-2009

Tropospheric ozone (which is the ozone in the lower part of the atmosphere) is a natural constituent of the atmosphere and plays a vital role in many atmospheric processes. It also a greenhouse gas with a radiative forcing of  $+0.35 \text{ W m}^{-2}$  (IPCC, 2007) due to changes in the concentrations since 1750. This is 10% of the overall global radiative forcing since 1750. There are no direct anthropogenic sources for ozone; thus the component is not regulated by the Kyoto protocol. Ozone is not emitted directly to the atmosphere, but it is rather produced from precursor gases; the formation of ozone is due to a large number of photochemical reactions taking place in the atmosphere and depends on the temperature, humidity and solar radiation as well as the primary emissions of nitrogen oxides and volatile organic compounds. Anthropogenic emissions of VOC and nitrogen oxides have increased the photochemical formation of ozone in the troposphere. Until the end of the 1960s the problem was basically believed to be one of the big cities and their immediate surroundings. In the 1970s, however, it was found that the problem of photochemical oxidant formation is much more widespread. The ongoing monitoring of ozone at rural sites throughout Europe shows that episodes of high concentrations of ground-level ozone occur over most parts of the continent every summer.

The 1999 Gothenburg Protocol is designed for a joint abatement of acidification, eutrophication and ground-level ozone. The critical levels defined by ECE for protection of vegetation are  $150 \mu\text{g}/\text{m}^3$  for hourly mean,  $60 \mu\text{g}/\text{m}^3$  for eight-hour mean and  $50 \mu\text{g}/\text{m}^3$  for seven-hour mean (9 a.m. -4 p.m.) averaged over the growing season (April-September).

The observed ozone mixing ratios at the Zeppelin Observatory for the period 1990-2009 are shown in Figure 16.

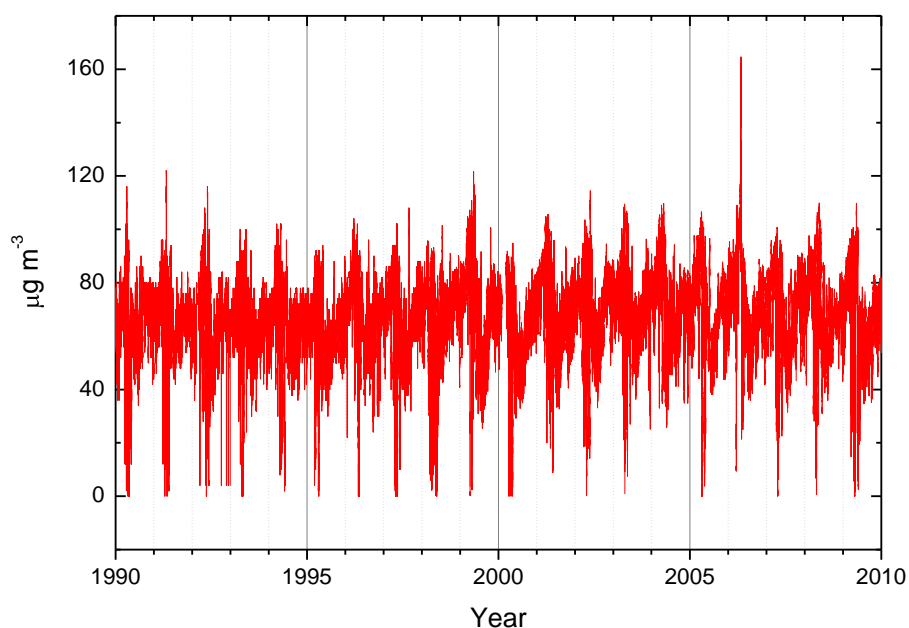


Figure 16: Observations of ozone in the troposphere for the period 1990-2009 at the Zeppelin observatory. Red dots: hourly average concentrations.

Monthly mean concentrations show large seasonal variations. In 2006 there was an extreme episode with transport of pollution into the Arctic region and ozone levels as high as  $\sim 160 \mu\text{g m}^{-3}$ . This was above all critical levels. In 2009 there have been few strong episodes, and the maximum ozone level observed was  $109 \mu\text{g m}^{-3}$  at 8<sup>th</sup> of May 2009.

#### 4.1.7 Observations of CO in the period 2001-2009

Carbon monoxide (CO) is not considered as a direct greenhouse gas, mostly because it does not absorb terrestrial thermal IR energy strongly enough. However, CO is able to modulate the level of methane and production tropospheric ozone which are both very important climate components. The CO sources and emissions have influence on the increasing tropospheric ozone and methane concentrations. CO is closely linked to the cycles of methane and ozone and, like methane; CO plays a key role in the control of the OH radical.

The observed CO mixing ratio for the period September 2001-2009 is shown in Figure 10

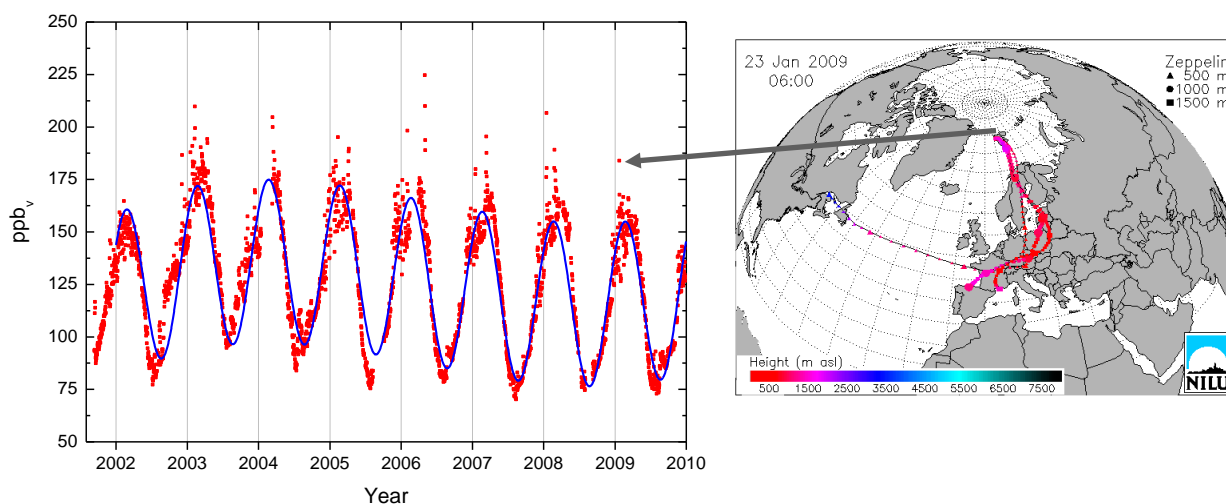


Figure 17: Observations of carbon monoxide (CO) from the September 2001 to 31.12.2009 at the Zeppelin observatory. Red dots: daily averaged observed mixing ratios. The solid line is the modelled background mixing ratio. The maximum value in 2009 is caused by transport of pollution from Europe as illustrated to the right.

Monthly mean concentrations of CO show a seasonal variation with large amplitudes in the Northern Hemisphere and small ones in the Southern Hemisphere. This seasonal cycle is driven by variations in OH concentration as a sink, emission by industries and biomass burning, and transportation on a large scale.

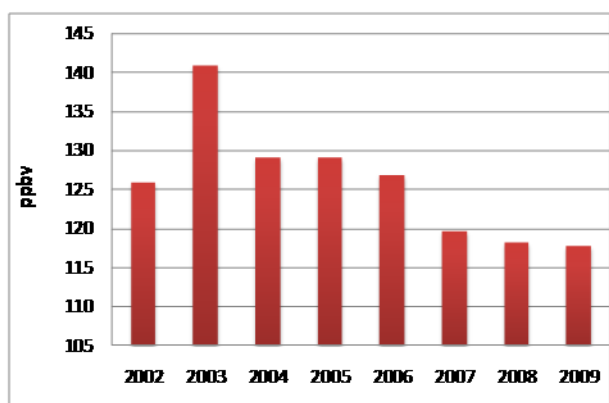


Figure 18: Development of the annual means of CO measured at the Zeppelin Observatory for the period 2001-2009.

The maximum daily average value in 2009 was observed on the 23<sup>th</sup> of January and was 183.9 ppb. The maximum value is caused by transport of pollution from Europe as illustrated to the right in the Figure. The highest mixing ratio ever observed at Zeppelin; is 217.2 ppb on the 2<sup>nd</sup> of May 2006. These peak values were due to transport of polluted air from lower latitudes; urban pollution (e.g. combustion of fossil fuel) and CO is also an excellent tracer for transport of smoke from agricultural- or forest fires. In general the CO concentrations measured at Zeppelin show a decrease during the period and 2009 has the lowest for the period

investigated. The difference in the mixing ratio of CO between the peak year 2003 and 2009 is 16%. CO is very important to monitor as the sources of CO are numerous and complex, and the level of this compound is important for the ozone and methane levels. Atmospheric CO sources are oxidation of various organic gases (volatile organic compounds, VOC) from sources as fossil fuel, biomass burning, and also oxidation of methane is important. Additionally emissions from plants and ocean are important sources.

The global levels of CO were increasing until the mid-1980s. Thereafter the levels have declined with an averaged global growth rate  $-0.9$  ppb/year for the period from 1992 to 2001. The variability of the growth rates is large. High positive growth rates and subsequent high negative growth rates were observed in northern latitudes and southern low latitudes from 1997 to 1999. We calculated a trend at Zeppelin of  $-2.5$  ppb per year for the period 2002-2009. The development of the annual means for the period 2002-2009 is presented in Figure 18, clearly illustrating a maximum in the year of 2003, and a decrease from 2003-2009.

## 4.2 Greenhouse gases with solely anthropogenic sources

All the gases presented in this chapter have solely anthropogenic sources. These are the man-made greenhouse gases and are called CFCs, HCFCs, HFCs PFCs, SF<sub>6</sub> and halons and most of the gases did not exist in the atmosphere before the 20<sup>th</sup> century. All these gases except for SF<sub>6</sub> are halogenated hydrocarbons. Although the gases have much lower concentration levels than most of the natural gases mentioned in the previous section, they are strong infrared absorbers, many of them with extremely long atmospheric lifetimes resulting in high global warming potentials; see Table 1 on page 7. Together as a group the gases contribute 11% to the overall global radiative forcing since 1750.

Some of these gases are ozone depleting, and consequently regulated through the Montreal protocol. Additional chlorine and bromine from CFCs, HCFCs and halons added to the atmosphere contributes to the thinning of the ozone layer, allowing increased UV radiation to reach the earth's surface, with potential impact not only to human health and the environment, but to agricultural crops as well. In 1987 the Montreal Protocol was signed in order to reduce the production and use of these ozone-depleting substances (ODS) and the amount of ODS in the troposphere reached a maximum around 1995. The amount of most of the ODS in the troposphere is now declining slowly and one expects to be back to pre-1980 levels around year 2050. In the stratosphere the peak is reached somewhat later, around the year 2000, and observations until 2004 confirm that the level of stratospheric chlorine has not continued to increase (WMO, 2007).

The CFCs, consisting primarily of CFC-11, -12, and -113, accounted for ~62% of total tropospheric Chlorine in 2004 and accounted for a decline of 9 ppt Chlorine from 2003-2004 (or nearly half of the total Chlorine decline in the troposphere over this period) (WMO, 2007).

There are two generations of substitutes for the CFCs, the main group of the ozone depleting substances. The first generation substitutes is now included in the Montreal protocol as they also influence the ozone layer. This comprises the components called HCFCs listed in Table 1 and Table 2. The second-generation substitutes, the HFCs, are included in the Kyoto protocol. The situation now is that the CFCs have started to decline, while their substitutes are increasing, and many of them have a steep increase.

#### 4.2.1 Observations of Chlorofluorocarbons (CFCs) in the period 2001-2009

This section includes the results of the observations of the CFCs: CFC-11, CFC-12, CFC-113, CFC-115. These are the main ozone depleting gases, and the anthropogenic emissions started around 1930s and were restricted in the first Montreal protocol. Figure 19 shows the daily averaged observed mixing ratios of these four CFCs. The current instrumentation is not in accordance with recommendations and criteria of AGAGE for measurements of CFCs and there are larger uncertainties in the observations of these compounds, see also Appendix I. As a result also the trends are connected with larger uncertainties. From September 2009 we have new and improved instrumentation installed at Zeppelin providing better observations of these compounds.

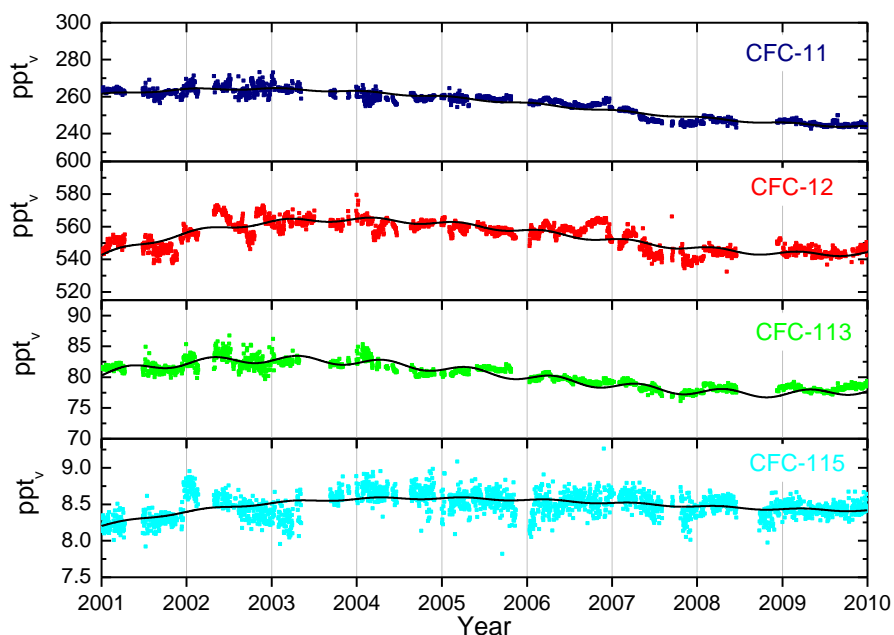


Figure 19: Daily averaged mixing ratios of the monitored CFCs: CFC-11 (dark blue), CFC-12 (red), CFC-113 (green) and CFC-115 (light blue) for the period 2001-2008 at the Zeppelin observatory. The solid lines are modelled background mixing ratio.

The main sources of these compounds were foam blowing, aerosol propellant, temperature control (refrigerators), solvent, and electronics industry. The highest production of the observed CFCs was around 1985 and maximum emissions were around 1987. The life times of the compounds is long as given in Table 1, and also the GWP due to the life time and strong infrared absorption properties is very high.

We have used the model described in Appendix I in the calculation of the annual trends, and changes in the trends. The trends per year for the substances CFC-11, CFC12 and CFC-113 are now all negative given in Table 2, and the changes in the trends are also negative indicating acceleration in the decline. For the compound CFC-115 the trend is still slightly positive, +0.01 ppt/year, but the change in trend is negative and thus we expect the trend for 2001-2010 to be negative. In total the development of the CFC levels at the global background site Zeppelin is now very promising.

According to WMO (WMO, 2007) the CFC-11 mixing ratios are decreasing at approximately 1.9 ppt/year and CFC-113 are decreasing by approximately 0.8 ppt/yr up to 2005 as a global mean. This is relatively close to our results at Zeppelin for CFC-113 for the period 2001-2009

(-0.7 ppt/yr for 2001-2009), but we find larger reduction for CFC-11, approximately 2.6 ppt/year. In Europe the growth rates for CFC-11 was -2.7 for 2003-2004, in agreement with our results. The difference might be explained by the geographical distribution of the sources, the very remote location of the Zeppelin observatory or uncertainties in the measurements.

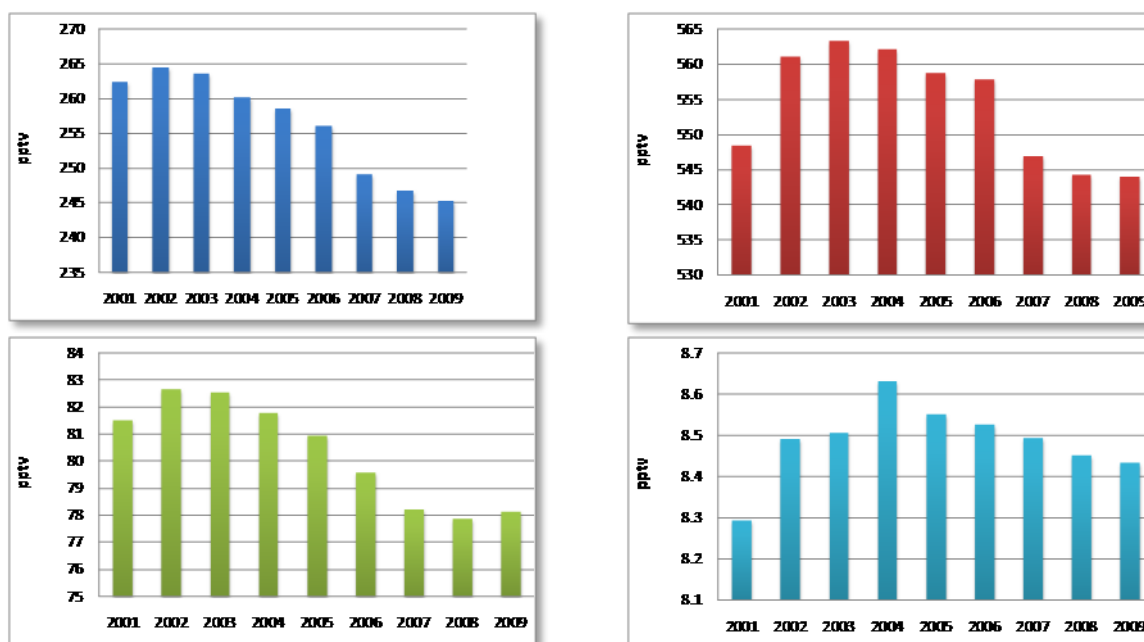


Figure 20: Development of the annual means all the observed CFCs at the Zeppelin Observatory for the period 2001-2009. Upper left panel: CFC-11, upper right panel: CFC-12, lower left panel: CFC-113, lower right panel: CFC-115. Please see appendix I for data quality and uncertainty.

The development of the annual means for all the observed CFCs is shown in Figure 20, and it shows a similar tendency for all the compounds; a weak increase in the beginning of the period and a decrease the recent years. The results of CFC-113 show an increase from 2008-2009, which is not expected. This might be due to low precision of the observations and too few observations the last part of 2008, resulting in a too low annual mean for 2008. As described in Appendix I there is now a new instrument at Zeppelin giving better and more accurate observations of CFCs. The old and new observations will be harmonised and a more detailed analysis of the CFCs will be performed with the data from the new instrument available. CFC-12 (the red diagram) is the gas with the highest GWP of the CFCs, 10600, and the second highest of all gases observed at Zeppelin. This means that the warming potential of 1 kg emitted CFC-12 gas has 10600 times stronger warming effect than 1 kg emitted CO<sub>2</sub> gas. The global averaged atmospheric mixing ratio of CFC-12 has been constant within 1% (5 ppt) since 2000 and some *in situ* column measurements at Northern Hemisphere show that peak values were attained in 2003 (WMO, 2007). This fits well with our observations as illustrated in Figure 20 as CFC-12 has the maximum in 2003-2004, but the variations since 2001 is larger than the global average variation, and there seem to be a clear reduction the last years.

#### 4.2.2 Observations of Hydrochlorofluorocarbons (HCFCs) in the period 2001-2009

This chapter includes the observations of the following components: HCFC-22, HCFC-141b and HCFC-142b. These are all first generation replacement gases for the CFCs and their lifetimes are rather long. This means that they have potentially strong warming effects,

depending on their concentrations and absorption properties; their GWPs are high (see Table 1). The compound HCFC-142b is the strongest of these gases, and the warming potential is 2400 times stronger than CO<sub>2</sub>, per kg gas emitted. These gases do also contain chlorine, and thus are contributing to the depletion of the ozone layer. The HCFCs accounted for 6% of the total tropospheric chlorine in 2004 versus 5% of the total in 2000 (WMO, 2007).

The daily averaged observations of these gases are shown in Figure 21 for the period 2001-2009.<sup>5</sup> As a result also the trends are connected with larger uncertainties. From September 2009 we have new and improved instrumentation installed at Zeppelin providing better observations of these compounds.

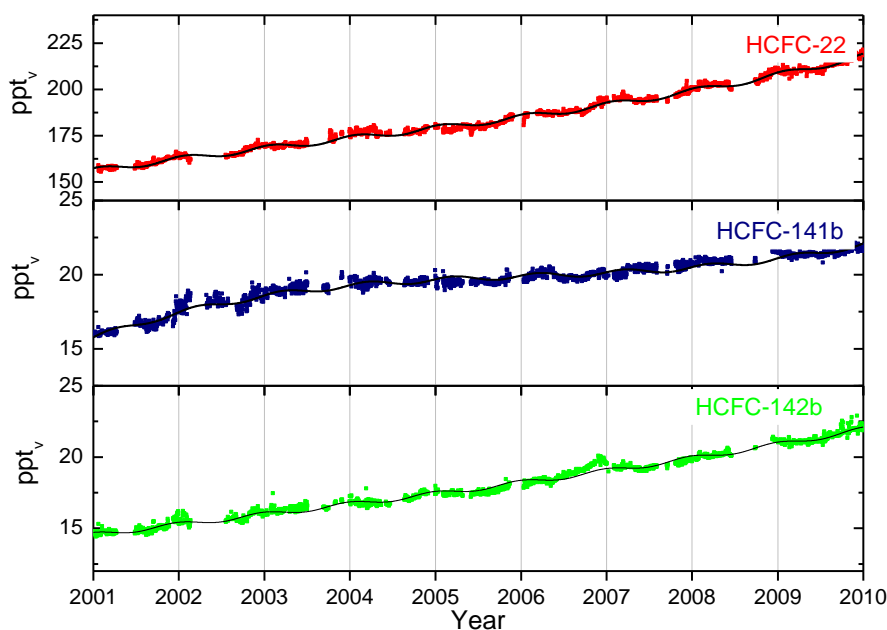


Figure 21: Daily average mixing ratios of the monitored HCFCs: HCFC-22 (red), HCFC-141b (dark blue) HCFC-142b<sup>4</sup> (green) for the period 2001-2009 at the Zeppelin observatory. The solid lines are modelled background mixing ratio.

The trends per year for the compounds HCFC-22, HCFC-141b and HCFC-142b are all positive, particularly for HCFC-22 as given in Table 2. HCFC-22 is the most abundant of the HCFCs and is currently increasing at a rate of 6.5 ppt/year over the period 2001-2009. In comparison, the global mean increase for 2000-2004 was +4.9 ppt/year according to WMO, (WMO, 2007). The mixing ratios of HCFC-141b and HCFC-142b have increased by 0.5 ppt/yr and 0.8 ppt/year, respectively over the same period.

It is worth mentioning that the changes in trends are negative for HCFC-22 and HCFC-141b, indicating that the yearly increases in the concentrations are slowing down. This is not the case for HCFC-142b, which still has a slight acceleration in the trend. The rates of increase

<sup>5</sup> The current instrumentation is not in accordance with recommendations and criteria of AGAGE for measurements of the HCFC-142b and there are larger uncertainties in the observations of this compound, see also Appendix I.

for all three of these HCFC substances are significantly lower than projected in the previous Ozone Assessment (WMO, 2007).

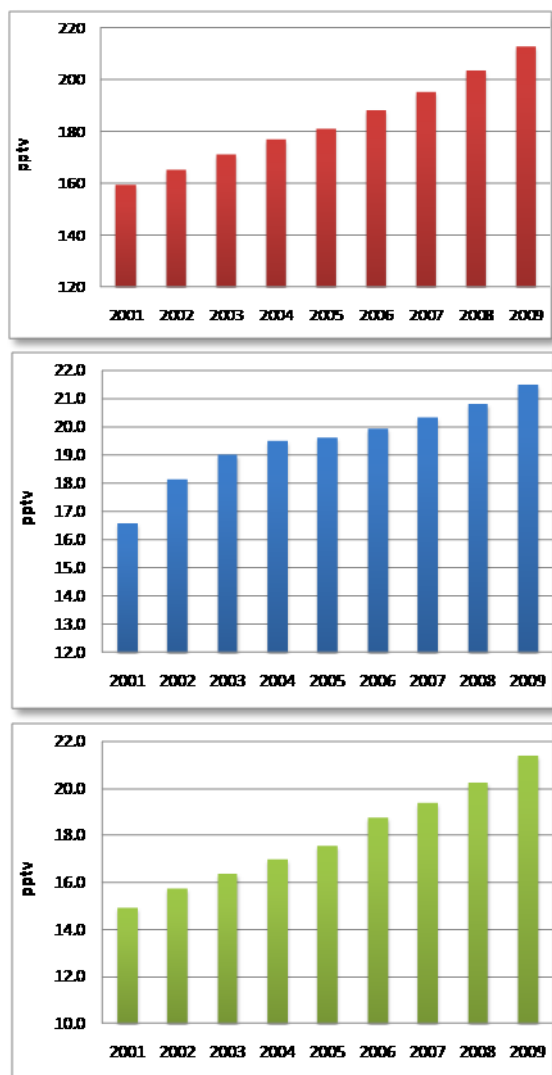


Figure 22: Development of the annual means the observed HCFCs at the Zeppelin Observatory for the period 2001-2009. Red: HCFC-22, Blue: HCFC-141b, and green: HCFC-142b.

Figure 22 shows the annual means for the full period for all these compounds, clearly illustrating the development; and increase which now shows signs of slowing down. The main sources of these gases are temperature control (refrigerants), foam blowing and solvents, as for the CFCs, which they suppose to replace. All these gases are regulated through the Montreal protocol as they all contain Chlorine. The use of the gases is now frozen, but they are not completely phased out. With lifetimes in the order of 10-20 years it is central to monitor the levels in the future as they have an influence both on the ozone layer, and are strong climate gases.

#### 4.2.3 Observations of hydrofluorocarbons (HFCs) in the period 2001-2009

The substances called HFCs are the so called second generation replacements of CFCs, which means that they are considered as better alternatives to the CFCs with respect to the ozone layer than HCFCs described in the previous section. This sub-section includes the following components: HFC-125, HFC-134a, HFC-152a with lifetimes in the order of 1.4-30 years. These substances do not contain chlorine thus they do not have a direct influence on the ozone layer, but they are infrared absorbers and contribute to the global warming.

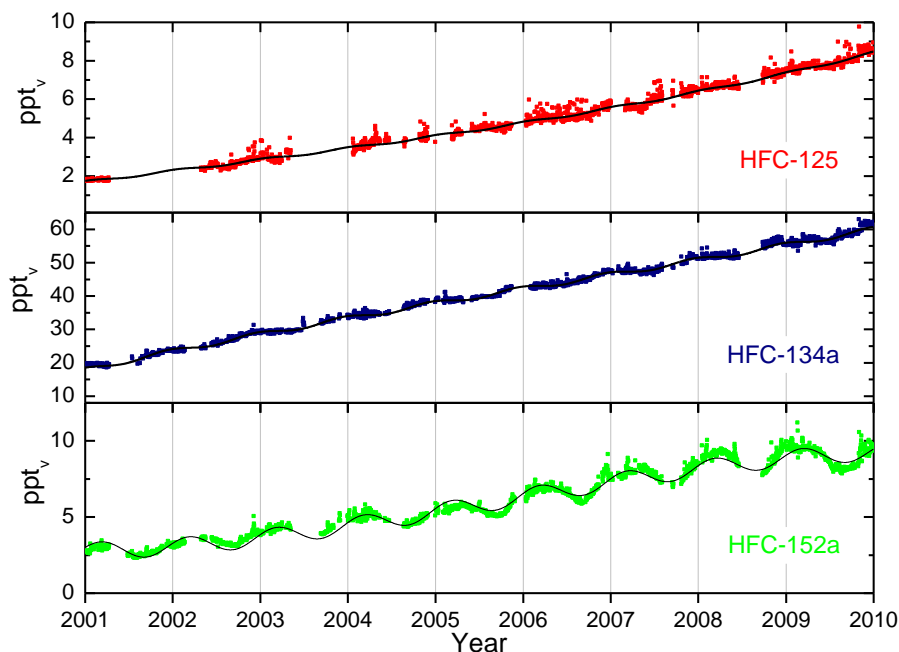


Figure 23: Daily average concentrations of the monitored CFCs: HFC-125 (red), HFC-134a (dark blue), HFC-152a (green) for the period 2001-2009 at the Zeppelin observatory. The solid lines are modelled background mixing ratio.

HFC-152a has the shortest life time and is mainly destroyed in the lowest part of the atmosphere by photolysis and reactions with OH. The seasonal cycle in the observed mixing ratios of these substances is caused by the variation in the incoming solar radiation and is clearly visible in the time series shown in Figure 23 for HFC-152a.

Even if these compounds are better alternatives for the protection of the ozone layer as they do not contain chlorine or bromine, they are still highly potent greenhouse gases. 1 kg of the gas HFC-125 is as much as 3400 times more powerful greenhouse gas than CO<sub>2</sub>. Still their mixing ratios are rather low, but the background mixing ratios are increasing steeply as our results show. This is also clearly illustrated in Figure 24 showing the development of the annual means. The gases are continuously increasing at a constant rate per year as earlier.

The three main HFCs are HFC-23 (measured at Zeppelin from 2010), HFC-134a and HFC-152a, with HFC-134a being the most widely used refrigerant (temperature control), and in air conditioners in cars. Since 1990, when it was almost undetectable in the atmosphere, concentrations of HFC-134a have risen massively. For the period 2001-2009 we find an annual increase per year of 4.6 ppt, which leaves this compound as the one with the second highest change per year of the all the halocarbons observed at Zeppelin. The mixing ratios of HFC-125, HFC-134a and HFC-152a have increased by as much as 299%, 178% and 224% respectively since 2001. This is a rapid average increase in the interval from ~20-33 % per year.

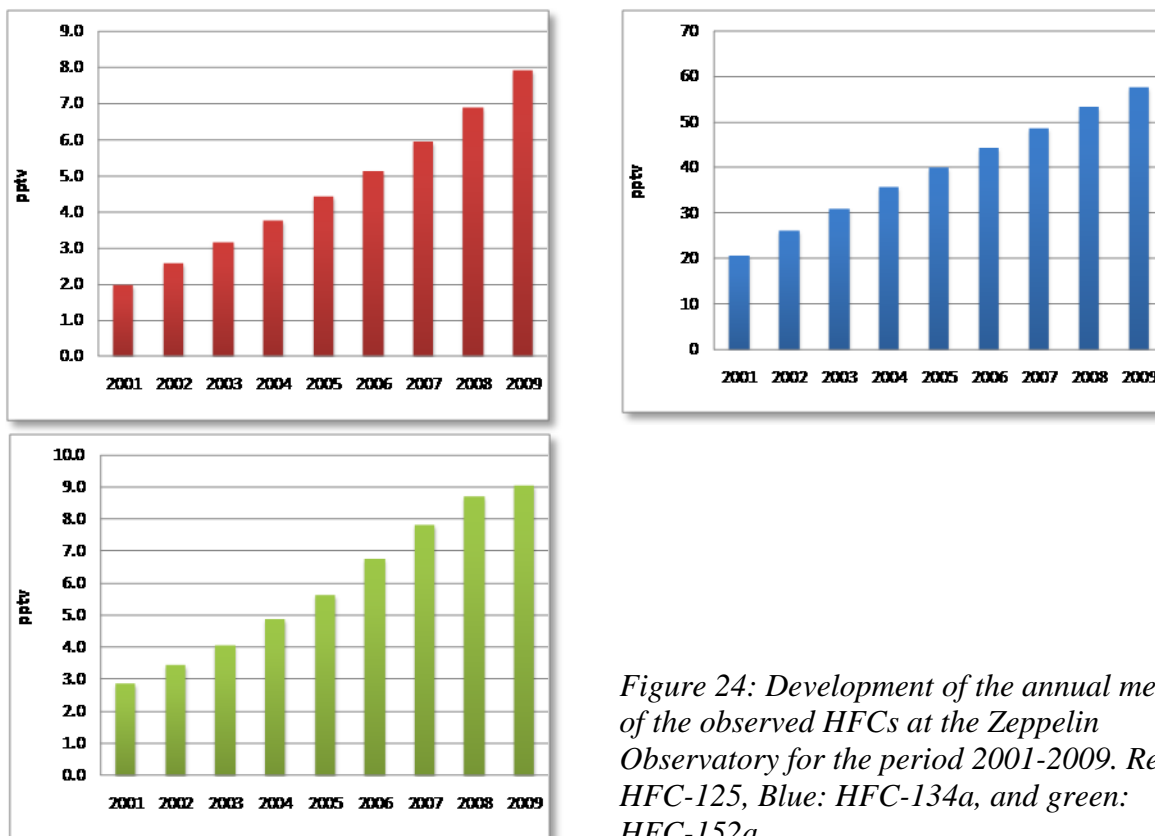


Figure 24: Development of the annual means of the observed HFCs at the Zeppelin Observatory for the period 2001-2009. Red: HFC-125, Blue: HFC-134a, and green: HFC-152a.

In Figure 25 we have included the development of the emissions of HFC-134a for the period 2001-2005 divided in source (left) and region (right) for Europe and Russia. Emission data are from the EDGAR data base, version 4.1 (EDGAR, 2010). As can be seen there is an increase year by year, with a larger change from 2001-2002. This seems to be reflected in the annual mean at Zeppelin for this component. The change from 2001-2002 was 5.3 ppt at Zeppelin, and after that absolute change have been between 4.2 and 4.9 ppt. OECD-Europe is the region with the absolute highest emissions over this period.

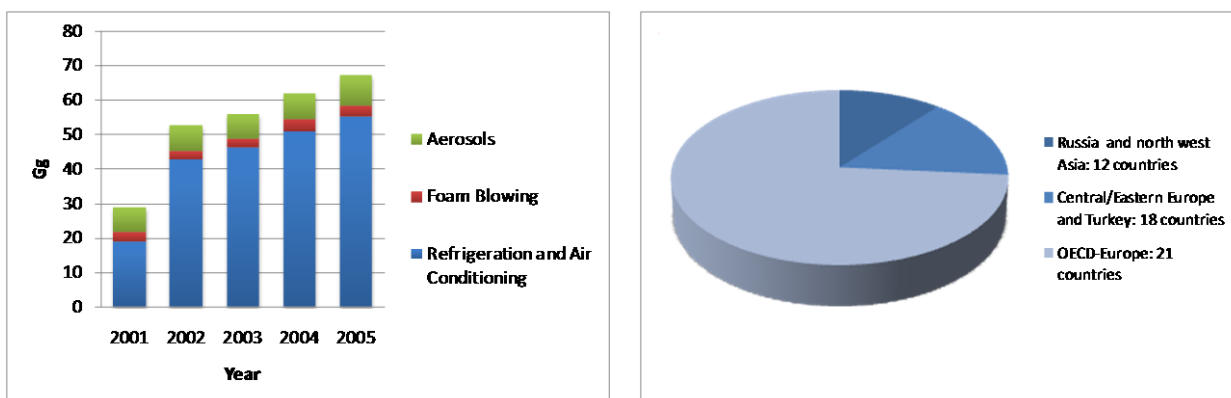


Figure 25: The development of the emissions of HFC-134a for the period 2001-2005 divided in source (to the right) and region (to the left) for Europe and Russia.

Due to the large increase in these compounds it is relevant to calculate the radiative forcing of these observed changes. Based on the assumption that these changes are the same at all locations (constant geographical distribution) we find that the total radiative forcing for these three gases since the start of the emissions is  $0.012 \text{ W m}^{-2}$  for. Thus the contribution from the recent man made emissions of these gases is still considered as small. This is explained by the (still) low mixing ratios of the compounds. It is important to follow the development of these gases due to the rapid annual growth.

#### 4.2.4 Observations of halons in the period 2001-2009

Halons include the following components: H-1301, H-1211. These climate gases contain bromine, also contribution to the depletion of the ozone layer. Actually, bromine is even more effective in destroying ozone than chlorine. The halons are regulated through the Montreal protocol, and are now phased out. The main source of these substances was fire extinguishers. Figure 26 presents the daily average concentrations of the monitored halons at Zeppelin<sup>6</sup>.

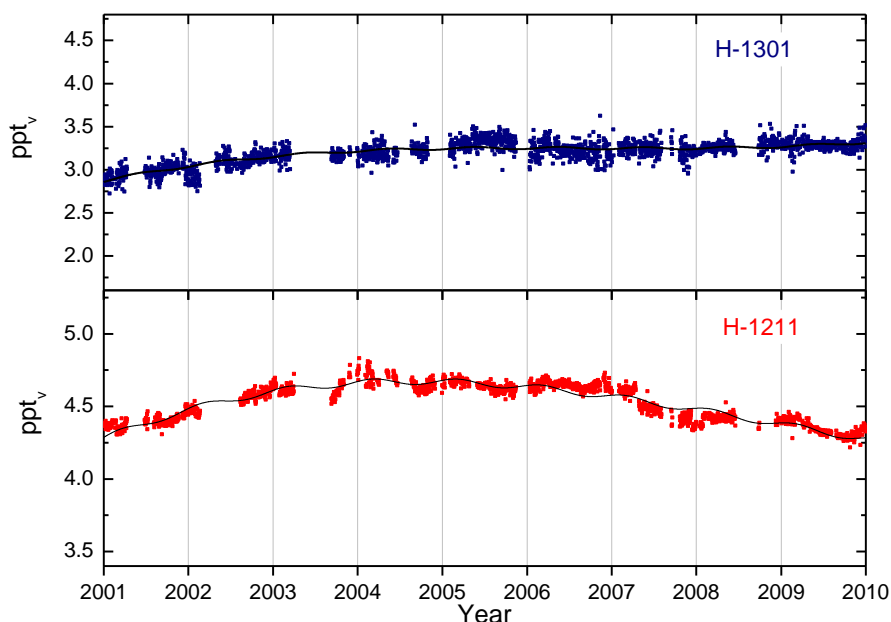


Figure 26: Daily average concentrations of the monitored halons: H-1301 (blue in the upper panel) and H-1211<sup>5</sup> (Red in the lower panel) for the period 2001-2009 at the Zeppelin observatory. The solid lines are modelled background mixing ratio.

By use of the model described in Appendix I we have calculated the annual trends, and changes in trends, given in Table 2. The trends for the period 2001-2009 shows a small increase for both substances in total, with a very small reduction in the rates indicating that the trend is expected to be lower the next years (if there are no abrupt changes in sources and sinks).

<sup>6</sup> The current instrumentation is not in accordance with recommendations and criteria of AGAGE for measurements of the Halon-1211 and there are larger uncertainties in the observations of this compound, see also Appendix I.

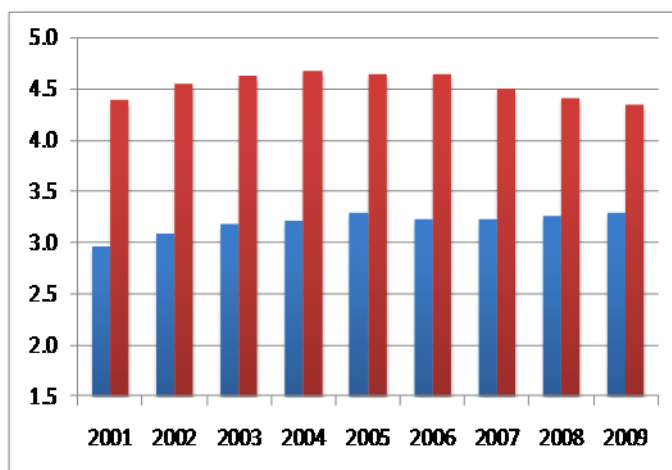


Figure 27: Development of the annual means the observed Halons at the Zeppelin Observatory for the period 2001-2009. Red: Halon-1211, Blue: H-1301.

The development of the annual means are shown in the Figure to the left, and as can be seen the mixing ratios are quite stable over the measured period explained by low emissions and relatively long lifetimes (11 years for H-1211 and 65 years for H-1301.) According to the last Ozone Assessment (WMO, 2007) it is currently unclear whether atmospheric mixing ratios of halon-1301 continue to increase. The global atmospheric increase in halon-1211 was 0.06 ppt/year in average in 2000-2004 which is about half the change for the period 1996-2000. This agrees well with our observations in the Arctic region.

#### 4.2.5 Observations of other chlorinated hydrocarbons in the period 2001-2009

This section includes observations of the components: trichloromethane (also called methyl chloroform,  $\text{CH}_3\text{CCl}_3$ ), dichloromethane ( $\text{CH}_2\text{Cl}_2$ ), chloroform ( $\text{CHCl}_3$ ), trichloroethylen ( $\text{CHClCCl}_2$ ), perchloroethylene ( $\text{CCl}_2\text{CCl}_2$ ). The main sources of all these substances are solvents. Note that Chloroform also have natural sources and the largest single source being in offshore sea water. The daily averaged concentrations are shown in Figure 28.

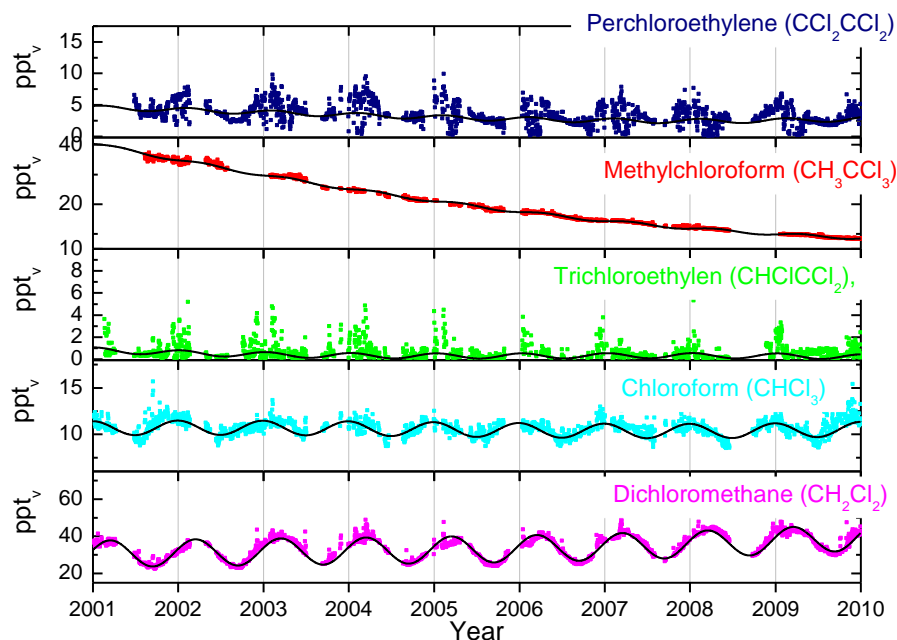


Figure 28: Daily average concentrations chlorinated hydrocarbons: From the upper panel: perchloroethylene (dark blue) methylchloroform (red), trichloroethylen (green), chloroform (light blue) and dichloromethane (pink) for the period 2001-2009 at the Zeppelin observatory. The solid lines are the modelled background mixing ratio.

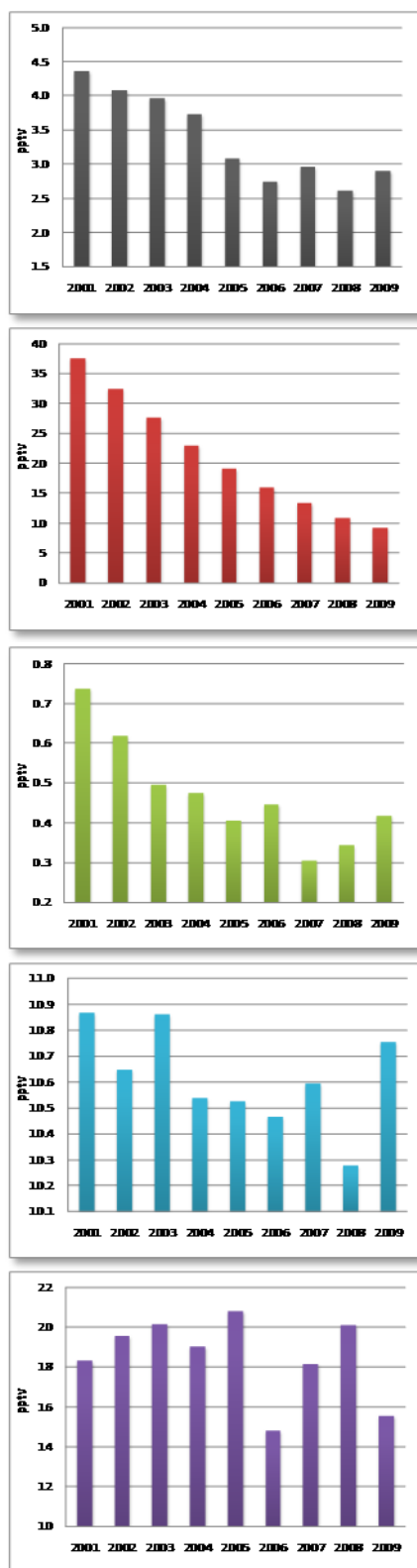


Figure 29: Annual means of the chlorinated hydrocarbons. From the upper panel: perchloroethylene (grey), trichloromethane (red), trichloroethylen (green), chloroform (blue) and dichloromethane (violet) for the period 2001-2009.

Trichloromethane ( $\text{CH}_3\text{CCl}_3$ ) has continued to decrease and contributed 13.5 ppt, or more than half, of the overall decline observed for total tropospheric Cl in 2003-2004. It is currently still the largest contributor to the decline in tropospheric chlorine. Globally averaged surface mixing ratios were 22.6 ppt in 2004 versus 46.4 ppt in 2000 (WMO, 2007). Our measurements at Zeppelin show now that the component has further decreased and is more than halved since 2004.

#### 4.2.6 Perfluorinated compounds

The only perfluorinated compound measured at Zeppelin is sulphurhexafluoride,  $\text{SF}_6$ . This is an extremely strong greenhouse gas emitted to the atmosphere mainly from the production of magnesium and electronics industry. The atmospheric lifetime of this compound is as much as 3200 years, and the global warming potential is 22200, which means that the emission of 1 kg of this gas has a warming potential which is 22200 times stronger than 1 kg emitted  $\text{CO}_2$ .

The other perfluorinated compounds are also very powerful greenhouse gases thus NILU plan to extend the monitoring programme with Carbon tetrafluoride ( $\text{CF}_4$ ) and possibly also hexafluoroethane ( $\text{C}_2\text{F}_6$ ) from 2010, when we have new and improved instrumentation installed at Zeppelin.

The current instrumentation is not well suited for measurements of SF<sub>6</sub> thus there are larger uncertainties for this compounds mixing ratios than for most of the other compounds reported<sup>7</sup>. The daily averaged concentration of SF<sub>6</sub> is presented in Figure 30. The compound is increasing with a rate of 0.3 ppt/year, and has increased by 40% since the start in 2001. Note that the variations through the year is not due to seasonal variations, but rather to instrumental adjustments.

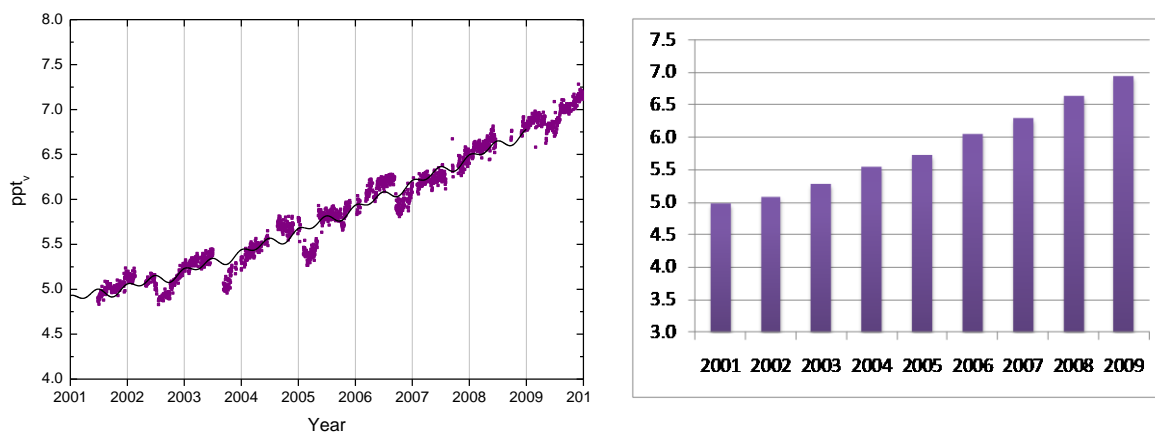


Figure 30: Daily average concentrations of SF<sub>6</sub> for the period 2001-2009<sup>6</sup> to the left, and the development of the annual mean concentrations in the right panel.

<sup>7</sup> The current instrumentation is not in accordance with recommendations and criteria of AGAGE for measurements of the SF<sub>6</sub> and there are larger uncertainties in the observations of this compound, see also Appendix I.

## 5. Observations of greenhouse gases observed at the Birkenes Observatory in Aust-Agder

In 2009 NILU upgraded and extended the observational activity at the Birkenes Observatory in Aust-Agder. Until 2009 the only Norwegian site measuring greenhouse gases was Zeppelin, but from mid May 2009 there are also continues measurements of CO<sub>2</sub> and CH<sub>4</sub> at Birkenes. The first results are presented below.

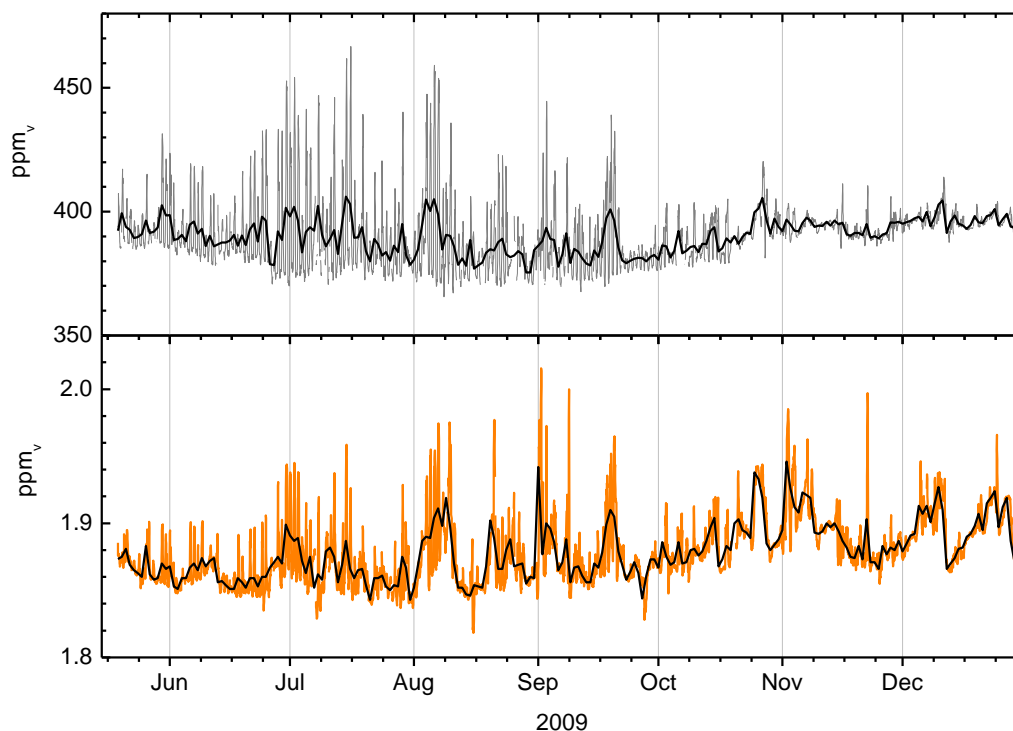


Figure 31: Greenhouse gas measurements at Birkenes Observatory from 19. May-31. December 2009. Upper panel: CO<sub>2</sub> measurements, grey line: hourly mean, black line: daily mean. Lower panel: CH<sub>4</sub> from Birkenes, orange line: hourly mean, black line: daily mean. Note that the observations are not calibrated, see Appendix I.

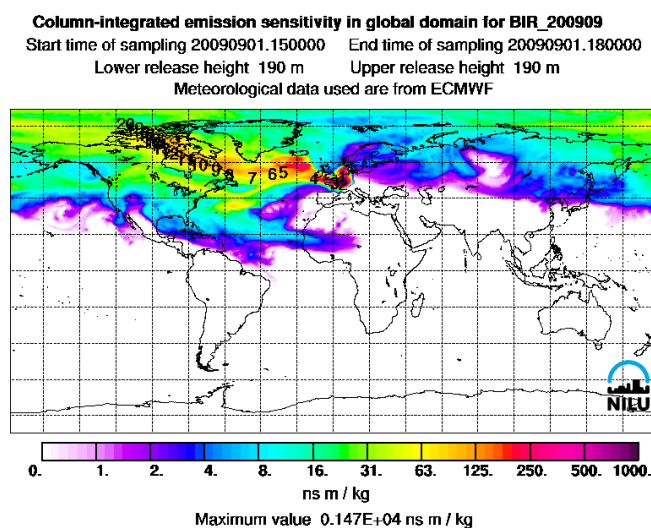


Figure 32: Transport pattern of air to Birkenes at 1 September.

The upper panel shows the daily (black line) and hourly (grey line) variations in CO<sub>2</sub>. It is clear that the variations are largest during the summer months. In this period there is a clear diurnal variation with high values during the night and lower values during daytime. This is mainly due to the plant respiration, but also the meteorological situation during summer contributes to larger variations in the compound. In the lower panel is the CH<sub>4</sub> measurements shown. The diurnal variation for this compound is smaller, but the variations are still largest during summer and early autumn. In addition to the diurnal

variations, there are also episodes with higher levels of both components due to transport of pollution from various regions. In general there are high levels when the meteorological situation results in transport from Central Europe.

The highest CO<sub>2</sub> measurements are during summer and particularly warm periods. The maximum value of CH<sub>4</sub> is on 1 September and 22 November. In both periods there are slightly elevated levels of CO<sub>2</sub> as well, but not particularly high. Figure 32 shows the results of the FLEXPART simulation for Birkenes on 1 September. At this day the air masses were arriving from northern US and across central and northern Europe towards Birkenes during a 20 period. This transport pattern resulted in the highest observed methane value at Birkenes and also elevated values of CO<sub>2</sub>.

Figure 33 show the monthly mean variations for both CO<sub>2</sub> and CH<sub>4</sub> at Birkenes. There is a clear minimum in the summer months and a maximum in the fall/winter as expected.

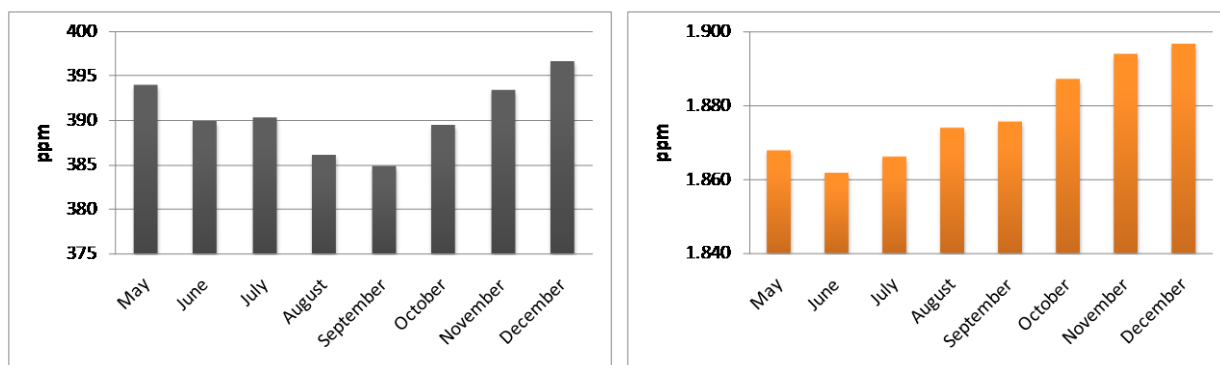


Figure 33: Monthly mean variations for CO<sub>2</sub> (to the left) and CH<sub>4</sub> (to the right) at Birkenes Observatory.

## **6. Aerosols and climate: Observations from Zeppelin and Birkenes Observatory**

In the investigations of climate change, aerosols are of vital interest, as they cause significant effects on the radiative balance of the Earth, both directly, through scattering and absorption of short-wave and long-wave radiation, and indirectly, by acting as condensation nuclei. Calculations of the effects of aerosols still have a high level of uncertainty despite the huge scientific focus during the last decades (IPCC, 2007). It is more complicated to represent aerosol climate effects in climate models than the climate effect of greenhouse gases. The greenhouse gas radiative forcing is only a function of the gas concentration. For carbon dioxide, long and reliable concentration records dating back several 100000 years exist, and the physics of interaction between greenhouse gas and atmospheric radiation is rather well understood. For atmospheric aerosol, the longest continuous time series date back not more than around 4 decades. The aerosol radiative forcing depends on a number of aerosol properties, e.g. particle size distribution, chemical composition, optical properties, morphology in addition to the concentration and evolution in time.

The low understanding of the atmospheric aerosol influence on climate is one of the reasons for the large uncertainty range of the global average surface temperature increase predicted in the IPCC 4<sup>th</sup> assessment report, e.g. a range of 1.4 – 6.4°C by 2100 in the rapid economic growth scenario A1. Comprehensive aerosol measurements at selected supersites are necessary for improving the modelling and knowledge of aerosol climate interaction. This is the first year the national Klif programme includes aerosol observations from Birkenes.

Aerosols vary considerably by regions and respond quickly to changes in emissions as their lifetime is short, in the order of days-weeks. Major sources of anthropogenic aerosols are fossil fuel and biomass burning. Aerosols like sulphate, biomass burning aerosols and fossil fuel organic carbon results in negative radiative forcing (cooling), while black carbon from fossil fuel and fires has a positive forcing (warming effect). Natural aerosols like sea salt, dust and sulphate and carbon aerosols from natural emissions are expected to increase as a result of climate change.

In Polar Regions with high surface albedo due to snow and ice, aerosols can produce appreciable warming at the surface. Shindell and Faluvegi (2009) conclude that decreasing concentrations of sulphate aerosols and increasing concentrations of black carbon at mid latitudes may have substantially contributed to rapid Arctic warming during the past three decades. Interestingly, Eleftheriadis et al (2009) report decreased levels of black carbon at Svalbard in the period 1998-2007. Improving our knowledge of polar aerosols and their radiative impacts is important in order to arrive at a more realistic evaluation of changes in the Earth's radiative balance, especially as the polar albedo can change because of reductions in sea ice and changes in snow cover.

### **6.1 Observations of aerosol properties in Norway in a global context**

Observations of aerosol properties are made at ground sites (with comprehensive variable set and excellent temporal coverage), as well as satellite platforms (with reduced variable set and moderate temporal, but excellent spatial coverage) and aircraft (with comprehensive variable set in the whole atmospheric column, but low temporal and spatial coverage). The surface observations need to follow established operating and quality assurance procedures, and need to be collected in one place with easy access. Subsequently, these datasets are aggregated as input or evaluation data for climate models. Over the past 5-10 years, several top-down and

bottom-up initiatives have achieved a considerable organization of this information chain. Within Europe, the EU-project “European Supersites for Atmospheric Aerosol Research” (EUSAAR) has established operating standards, quality assurance procedures, and a data collection and dissemination infrastructure (including near-real-time) for ground based aerosol observations. The same is currently being done at the international level by the aerosol programme of the WMO Global Atmosphere Watch (GAW) project. For satellite data, a new GAW virtual data centre (World Data Centre for Remote Sensing of the Atmosphere, WDC-RSAT) has been established for providing a common portal to the various satellite aerosol products. On the side of the climate models, the “Aerosol Comparisons between Observations and Models” (AeroCom) bottom-up initiative has been rather successful in connecting to the observation community and in integrating the observations into their model tools. Quantifying the aerosol climate effect has thus become a complex project with rather specialised and internationally distributed tasks which is nevertheless well integrated.

NILU contributes in several ways to this international project. Since January 2010, NILU hosts the GAW World Data Centre for Aerosol (WDCA), collecting and disseminating the observations of aerosol variables from the ground-based GAW network from currently over 40 stations worldwide. In this function, NILU is active in the respective international bodies of WMO GAW, CLRTAP-EMEP, but also connects to the modelling community of the AeroCom project. Since 2010, a significant part of the AeroCom project is also hosted in Norway, by the Norwegian Meteorological Institute, allowing for an inner-Norwegian synergy to be developed. In addition, NILU itself operates three atmospheric observatories, one each at Zeppelin Mountain, Svalbard, at Birkenes in Southern Norway, and at Troll Station, Queen Maud Land, Antarctica. The programme of aerosol variables observed at these stations follows the GAW recommendations.

*Table 3: Aerosol observations at the Zeppelin, Birkenes and Troll Observatory following the GAW recommendations.*

	Zeppelin/Ny-Ålesund	Birkenes	Troll
<b>Particle Number Size Distribution</b>	fine mode ( $0.01 \mu\text{m} < D_p < 0.8 \mu\text{m}$ ) in collaboration with Stockholm University	fine and coarse mode ( $0.01 \mu\text{m} < D_p < 10 \mu\text{m}$ )	fine mode ( $0.03 \mu\text{m} < D_p < 0.8 \mu\text{m}$ )
<b>Aerosol Scattering Coefficient</b>	spectral at 450, 550, 700 nm, in collaboration with Stockholm University	spectral at 450, 550, 700 nm	spectral at 450, 550, 700 nm
<b>Aerosol Absorption Coefficient</b>	single wavelength at 525 nm, in collaboration with Stockholm University	single wavelength at 525 nm	single wavelength at 525 nm
<b>Aerosol Optical Depth</b>	spectral at 368, 412, 500, 862 nm in collaboration with WORCC	spectral at 340, 380, 440, 500, 675, 870, 1020, 1640 nm, in collaboration with Univ. Valladolid	spectral at 368, 412, 500, 862 nm
<b>Aerosol Chemical Composition</b>	main components (ion chromatography), heavy metals (inductively-coupled-plasma mass-spectrometry)	main components (ion chromatography), heavy metals (inductively-coupled-plasma mass-spectrometry)	main components (ion chromatography)
<b>Particle Mass Concentration</b>	---	PM <sub>2.5</sub> , PM <sub>10</sub>	PM <sub>10</sub>

These variables have been selected for their relevance to assessing the aerosol climate effect, for their feasibility of being operated long-term with manageable maintenance, and for synergy aspects with air quality and health effect questions. This report covers the

observations at Birkenes and Zeppelin observatories which are supported by KLIF (marked in green).

## 6.2 Aerosol properties measured at Birkenes in 2009

The fundamental physical and optical properties of aerosols are measured at the Birkenes Observatory. Auxiliary instruments were installed at the new Birkenes station in summer 2009. At the same time, the existing instruments were moved from the old to the new station. During summer and fall 2009 up to the official opening of the improved station, the auxiliary instruments were operated in a pre-operational mode to verify proper operating conditions. One instrument, the integrating nephelometer measuring aerosol scattering and hemispheric backscattering coefficient, was affected by electromagnetic interferences in this period, which affected data quality to a degree that the data had to be removed during quality assurance.

Figure 34 and Figure 35 show the aerosol physical and optical data available for 2009, combined for new and old station at Birkenes. Figure 34 depicts the time series of the particle number size distribution in the particle diameter range of  $0.019 \mu\text{m} < D_p < 0.55 \mu\text{m}$  measured by differential particle mobility analysis. These colour surface plots have the time in days of year (DOY) on the x-axis, the particle diameter on the logarithmic y-axis, and the particle concentration per logarithmic diameter interval  $dN / d \log D_p$  on the logarithmic colour code. This chart type is the commonly accepted way of illustrating this variable, which is inherently dense in information, and thus needs some time to get acquainted with. Figure 35 contains the corresponding time series of the aerosol optical properties measured at Birkenes, i.e. aerosol scattering coefficient, aerosol absorption coefficient, and single scattering albedo.

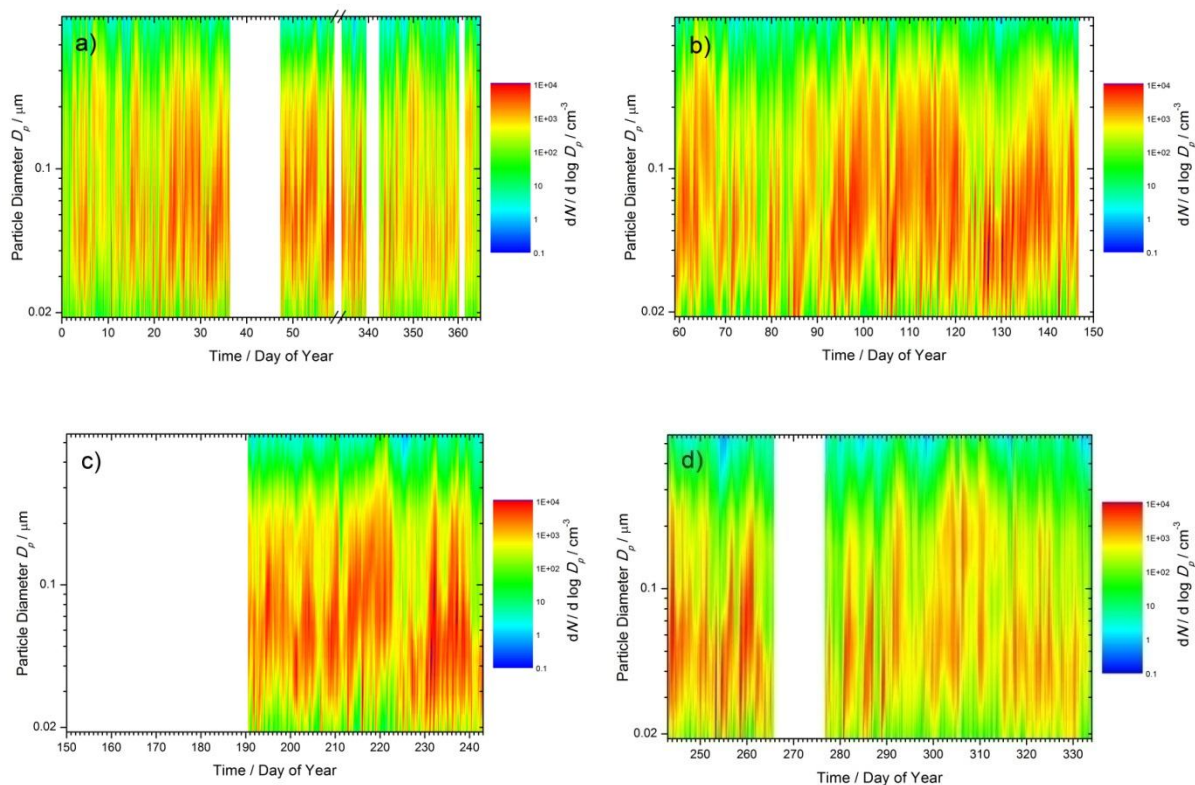


Figure 34: 2009 time series of particle number size distribution at Birkenes, panel a) winter, panel b) spring, panel c) summer, panel d) autumn. The gap in June (DOY 150 – 190) is caused by participating in a off-site system intercomparison workshop for QA purposes. The other gaps result from power outages.

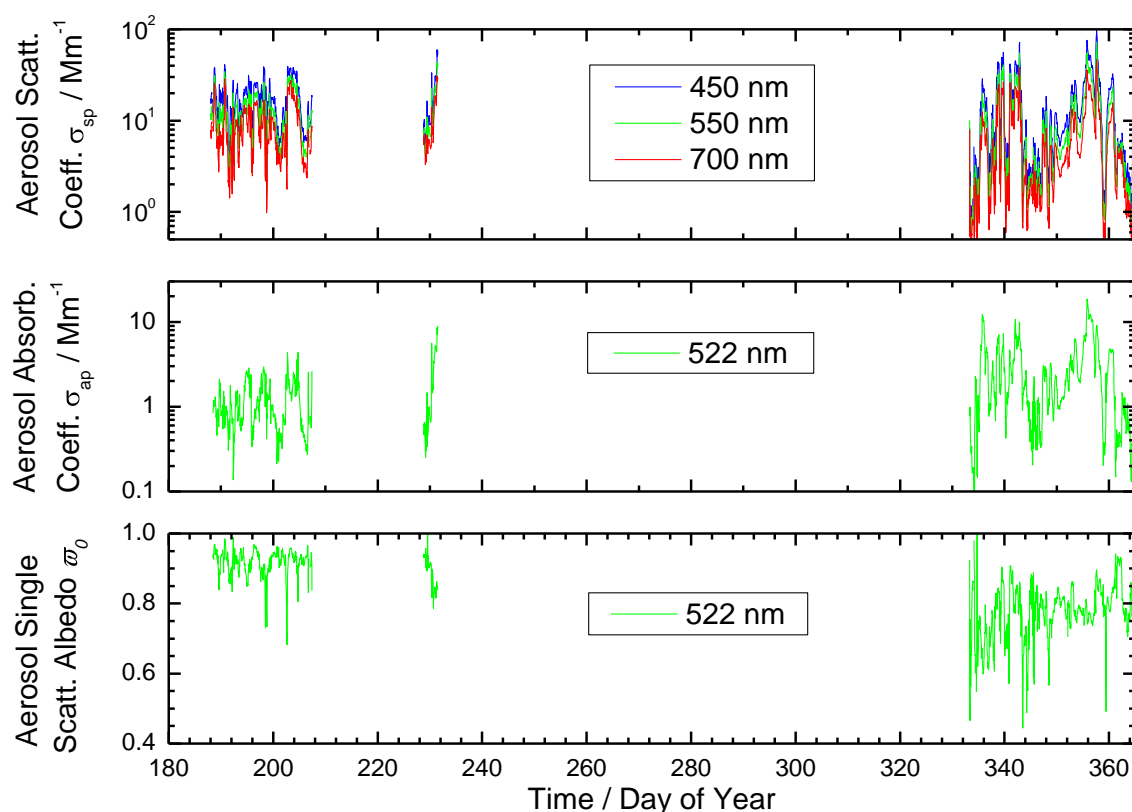


Figure 35: Time series of aerosol optical properties measured in 2009 at the new Birkenes station during the pre-operational phase and after opening of the station on day 333.

The single scattering albedo is the fraction of light scattered by the particles rather than absorbed. Thus it is an indication of the aerosol's ability to absorb the radiation and heat the atmosphere. This variable, in combination with other variables, allows conclusions about the aerosol type. Figure 35 plots the optical variables after opening of the station (on day 333) and of the pre-operational phase if it passed quality assurance. For a detailed analysis of aerosol origin and climate effects, the full variable set including particle size distribution and optical properties will be necessary. However, already with the limited set of variables from the pre-operational period, we can assemble an aerosol phenomenology which will be elaborated in the forthcoming years.

For the phenomenology, we will primarily look at the time series of the particle number size distribution, and elaborate the findings by selecting typical examples. The particle size distribution is probably the most fundamental aerosol property, both for the aerosol climate and health effects. The shape of the particle size distribution is not unique, but characteristic for aerosols of a given age and origin. Particles in different size ranges differ in their characteristic life time.

Aerosols are commonly separated into a fine (particle diameter  $D_p < 1 \mu\text{m}$ ) and a coarse fraction ( $D_p > 1 \mu\text{m}$ ), which are governed by different microphysical processes (Raes et al., 2000). Aerosols in the coarse size range are commonly created by break up of bulk material, e.g. sea water for sea spray aerosol, plant / microbial components for primary biogenic aerosol, minerals for mineral dust. Fine fraction aerosols are created by condensation of

vapours from the gas phase. The vapours either condense onto pre-existing particles, or form new particles in the size range  $D_p \leq 0.02 \mu\text{m}$  (nucleation mode). The newly formed particles either evaporate again, or grow by further uptake of material from the gas phase into the Aitken size range ( $0.02 \mu\text{m} < D_p \leq 0.08 \mu\text{m}$ ). For particles in the Aitken size range, the processes of coagulation and cloud processing become important in addition to growth from the gas phase. Aitken size range particles that coagulate with each other or larger particles, or grow by cloud processing, end up in the accumulation mode size range ( $0.08 \mu\text{m} < D_p \leq 1 \mu\text{m}$ ). In this size range, the particles are stable unless they are removed by cloud activation and precipitation or dry removal. Each size range is usually dominated by one, log-normally shaped peak in the particle number size distribution. The average life time of nucleation mode particles is not larger than 1 hour, for Aitken mode particles on the order of a couple of hours, and for accumulation mode particles up to a week. Thus particles in the accumulation mode are the only ones that can be transported on a regional or long-range scale.

When looking at the 2009 fine fraction particle number size distribution time series from Birkenes observatory depicted in Figure 34, it is apparent that the aerosol characteristics often change abruptly between low background particle concentrations of  $\leq 400 \text{ cm}^{-3}/\text{dlog}D_p$  and high concentrations of  $> 4000 \text{ cm}^{-3}/\text{dlog}D_p$  that peak in the Aitken and / or accumulation mode. In interpreting these episodes and attributing them to a source, the trajectory tool FLEXTRA (Stohl et al., 1995; Stohl & Seibert, 1998) and the Lagrangian backward plume model FLEXPART (Stohl et al., 1998; Stohl et al., 2005) are used in addition to the characteristics of the particle size distribution. Panel a) of Figure 36 compares the particle size distributions of two early spring air masses, one of clean background air of North Atlantic / Arctic origin, and an air mass that previously passed over Poland and Russia. Apart from generally higher particle concentrations in the continental case, both size distributions show distinct Aitken and accumulation modes.

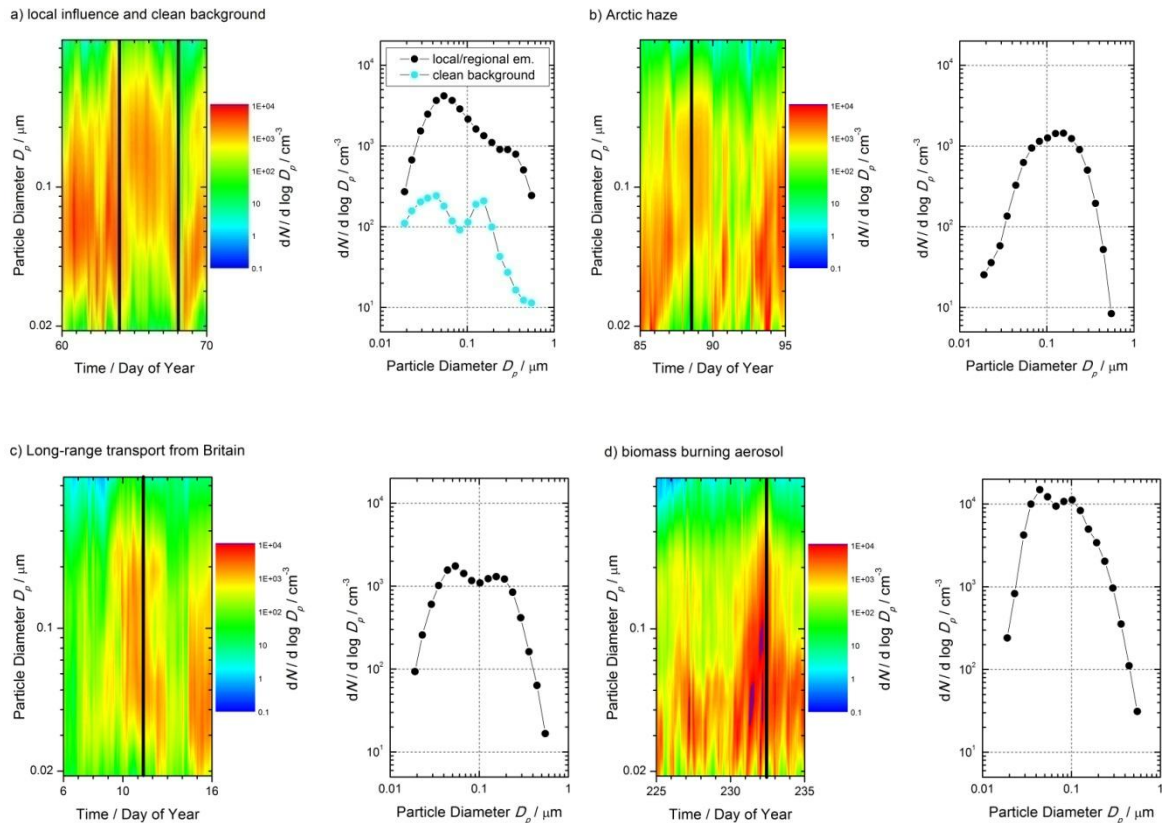


Figure 36: Particle size distributions of typical aerosol cases encountered at Birkenes: a) locally influenced and clean background; b) Arctic haze; c) continental long-range transported; d) long-range transported biomass burning. Each panel shows the particle size distribution as classical x-y plot for one point in time on the right hand side, as well as the corresponding excerpt from the particle size distribution time series colour surface plot on the left hand side. The particle size distribution plotted as x-y plot is marked in the time series with a thick black vertical line.

In the background air, the accumulation mode peaks at  $D_p = 0.15 \mu\text{m}$ , whereas in the continental air, it peaks at the larger value of  $D_p = 0.24 \mu\text{m}$ . This shift to larger particle size in continental air, along with higher particle concentrations, is the result of higher precursor emissions (natural and anthropogenic aerosol precursor gases) over the continent, and more intense microphysical processing, i.e. gas-to-particle conversion and coagulation. Moreover, the particle concentration in the Aitken mode relative to the accumulation is much higher in the continental case than in the background case. It may be tempting to attribute this also to continental emissions, but such a conclusion would be premature. Particles in the Aitken size range have a lifetime of a couple of hours before they coagulate with each other or with accumulation mode particles. If these Aitken mode particles were of continental origin, they would have vanished while the aerosol was transported from the continent to Norway. The Aitken mode particles in the “continental” case are therefore of regional or local origin, likely from domestic heating. Further information would be necessary to confirm this assumption, e.g. measurements of optical properties, since aerosol from domestic heating is more absorbing and has a lower single scattering albedo than background aerosol. These were not available at this time. However, the available time series of 2009 aerosol optical properties at

Birkenes in Figure 35 shows on average smaller single scattering albedos, i.e. larger particle absorption, in winter than in summer, which supports the hypothesis.

The next example in Figure 36, panel b), shows the particle number size distribution in another aerosol originating from the North Atlantic / Arctic. Here, the Aitken mode is almost absent; the distribution consists nearly exclusively of a single accumulation mode. The particle concentration is elevated as compared with the Arctic background aerosol in panel a) of the same figure and, in the accumulation mode size range, comparable to that of the continental aerosol in panel a). These features are typically encountered in well-aged Arctic haze aerosol (Heintzenberg, 1980). While the air mass was captured in the Arctic winter vortex, microphysical processes had ample time to finish processing of precursors emitted in the vortex into accumulation mode particles by gas-to-particle conversion and coagulation. The air mass was observed in Birkenes in spring when the Arctic vortex decays and the previously isolated air is transported southward.

Panel c) of Figure 36 shows another example of a particle size distribution in an aerosol of continental origin. The trajectory analysis indicates that the concerned air mass passed over Southern Britain on its way to Birkenes. The size distribution is bi-modal just as the “Poland / Russia” continental distribution shown in panel a), but the accumulation mode peaks at  $D_p = 0.15 \mu\text{m}$  instead of  $D_p = 0.24 \mu\text{m}$ , indicating less precursor gases and less microphysical processing. The nature of the Aitken mode in the aerosol passing over Britain is inconclusive. It may be the result of incomplete microphysical processing into the accumulation mode under transport, but may also be of regional origin. The last case example in Figure 36, in panel d), features an also bi-modal aerosol with particle concentrations in excess of  $4000 \text{ cm}^3/\text{dlog}D_p$ , which is rather unusual for Birkenes. Backward plume calculations over 20 days indicate that this air mass passed over forest fires in Southern Alaska about 18-19 days prior to arriving at Birkenes. This is consistent with results analysing the weekly particle filter samples from Birkenes, which indicate a levoglucosan concentration 5 times higher than average at this location for the corresponding week. Levoglucosan is a tracer species for the combustion of wood. However, the particle size distribution also features an Aitken mode with higher particle concentrations than the accumulation mode. For reasons already explained, this is highly unusual for aerosols that had ample time for self-processing. The reason can be found by consulting the particle size distribution time series in panel d) of Figure 36. The graph shows numerous events where the concentration of the smallest particles in the observed size range suddenly increases and the particle diameter corresponding to the concerned peak increases in the following couple of hours. Such an event is superimposed onto the biomass burning aerosol originating from Alaska.

Figure 37 shows a higher resolution time series of two such events, which are termed particle formation events. These occur if the concentration of condensable precursor gases increases to supersaturation and the existing particle surface is not sufficient to take up the condensing vapour, which then creates new particles (Kulmala et al., 2004). These particles subsequently grow by taking up more mass from the gas phase, leading to an, at first, rapid then decelerating increase of the peak particle diameter of the thus created nucleation mode. This forms to the classical “banana-shaped” appearance in the size distribution time series plot.

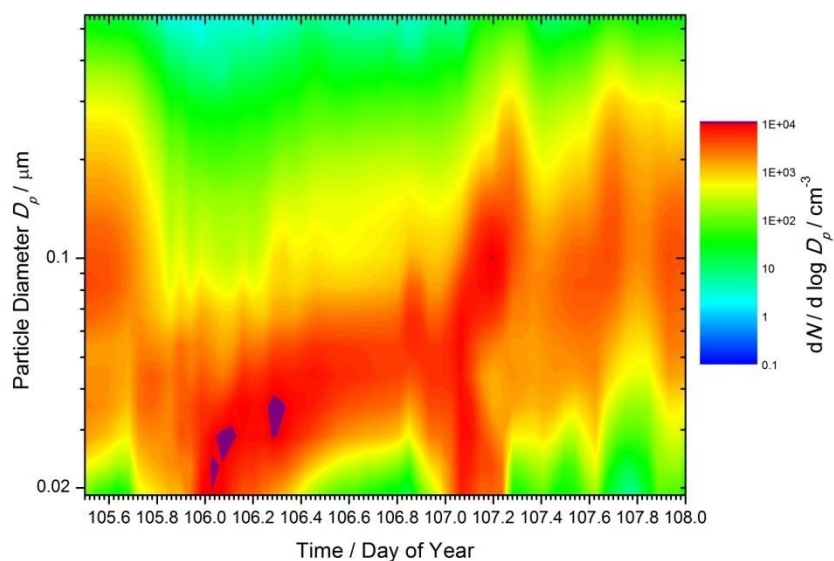


Figure 37: Particle number size distribution time series of two new particle formation events observed at Birkenes in spring 2009.

Figure 37 shows two such events, one with a well developed “banana-shape”, and one where this shape is cut off. This may occur when air masses with pre-existing particle surface are advected that take up the condensing vapour. Particle formation events depend on the photochemical creation of condensable vapours. This is why Figure 34 shows an increasing frequency of such events in spring, a peak in summer, a decreasing frequency in fall, and the absence of such events in winter. Particle formation events occur either during midday when the photochemical activity creating condensable vapours is highest, or in the middle of the night when radiative cooling increases the supersaturation of these vapours. It has to be kept in mind that the air sampled at a ground station is constantly exchanged by advection. Observing a particle formation event therefore implies that this is a phenomenon occurring not on a local, but on a regional scale. At Birkenes, particle formation events occur almost daily in summer, sometimes even twice per day. This supports findings of other investigators stating that particle formation due to biogenic precursors is a major, but poorly quantified contribution to the aerosol particle number budget at boreal latitudes. When considering that the number concentration of particles with  $D_p > 0.06 - 0.08 \mu\text{m}$  is an essential variable for quantifying the indirect aerosol climate effect, it is apparent this particle source needs to be understood and quantified better for improving the quality of climate predictions at boreal latitudes.

### 6.3 Observations of the total aerosol load above Zeppelin and Birkenes observatories

Aerosol optical depth (AOD) is an effective measure of the total aerosol load in the atmospheric column above the observation site. It is a measure of the attenuation of the radiation due to scattering and absorption of visible light by particles in a vertical column of the atmosphere. AOD is proportional to the total concentration of particulates in the atmosphere. The AOD wavelength dependence is linked to the aerosol particle size predominance and contains also information about the aerosol type. This is described by the

Ångström exponent (AE), with high values for small particles and low values representative for large particles.

During the last years, the awareness of the importance of total column aerosol measurements has increased. This is reflected in the increase of the instruments operated, clearly seen in Figure 38, which shows the development of the networks of sun-photometer in Scandinavia (Toledano et al., 2010). Photos of the standard instruments and characteristics are shown in Figure 50 on page 75.

Since 2002 aerosol optical depth observations have been made in Ny-Ålesund. These are part of the global network of AOD observations, which started in 1999 on behalf of the WMO GAW program. Classic extinction measurements at the recommended 4 WMO wavelengths 368, 415, 500 and 862 are performed as collaboration between PMOD/WRC and NILU, using a Precision Filter Radiometer (PFR, *Wehrli*, 2000 and 2005). Calibration is performed annually at PMOD/WRC. NRT data are displayed at [www.pmodwrc.ch/worcc](http://www.pmodwrc.ch/worcc) and can be downloaded from the WDCA site ([ebas.nilu.no](http://ebas.nilu.no))

In spring 2009 a CIMEL sun-photometer was put in operation at the new Birkenes observatory. This is an automatic sun and sky radiometer, with spectral interference filters centered at selected wavelengths: 340, 380, 440, 500, 675, 870, 1020, and 1640 nm. The CIMEL type CE-318 is a standard instrument of the Aerosol Robotic Network AERONET network (Holben et al., 1998; NASA, 2011). Measurements are made in collaboration with the University of Valladolid (Spain), who perform annual calibration (RIMA-AERONET sub-network). NRT data are displayed at AERONET website ([aeronet.gsfc.nasa.gov](http://aeronet.gsfc.nasa.gov)).

Additional Norwegian AOD observations (not reported here) are made at the Antarctic Troll observatory (contributing to GAW-PFR network) and Andenes (NILU, in collaboration with Univ. Valladolid (Spain) and ARR (contributing to AERONET)).

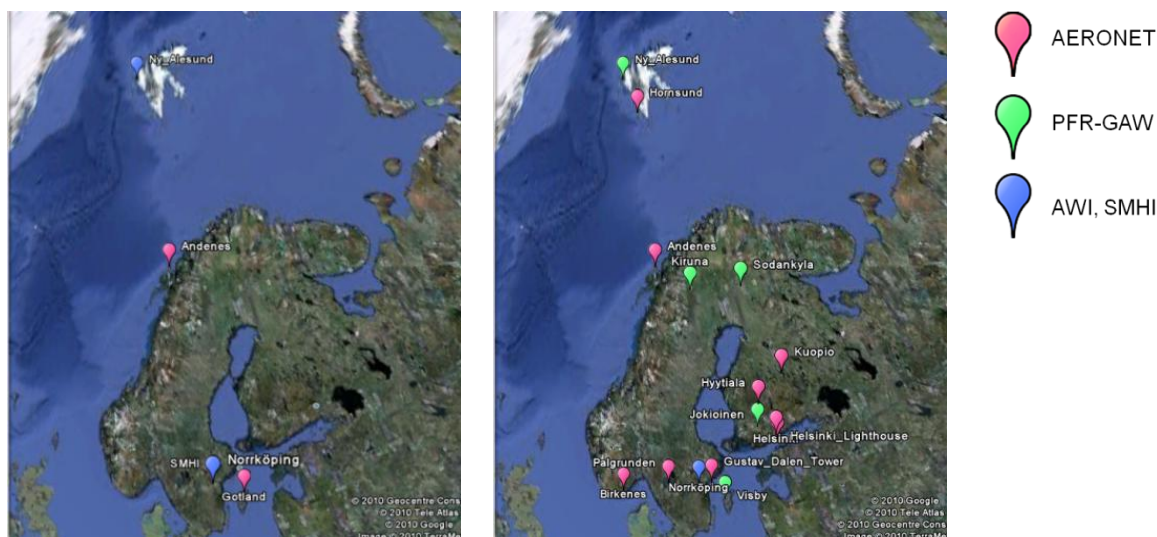


Figure 38: Scandinavian sun photometer measurements before 2003 (left panel) and 2007 – 2010 (right panel). Figure adapted from Toledano et al. (2010).

### 6.3.1 Measurements of the total aerosol load above the Birkenes observatory

Aerosol optical depth measurements started at the new Birkenes observatory in spring 2009, utilizing an automatic sun and sky radiometer (CIMEL type CE-318).

Atmospheric measurements have been made in the time period 30 April to 19 October 2009. The retrieval method is that of the AERONET version 2 direct sun algorithm (for details, see <http://aeronet.gsfc.nasa.gov>). All aerosol optical depth data shown here, have reached the AERONET Level 2.0. Level 2.0 data are quality assured data, to which pre- and post-field calibration have been applied. In addition they were automatically cloud cleared and manually inspected. The associated AOD uncertainty is 0.01-0.02 (larger for shorter wavelengths). The Ångström exponent (AE) is calculated in the range between 440 and 870 nm.

The time-series of the total AOD in 2009 is given in Figure 39<sup>8</sup>. Besides the total AOD, the coarse mode AOD is shown. Low coarse mode AOD is observed especially during the summer months, which can also be expressed as predominance of fine mode fraction. The yearly averaged fine mode fraction for 2009 was  $71 \pm 15$  %. Values were clear above 80% during the summer months. Although it is too early to draw climatological conclusions, it seems that the AOD and coarse mode fraction show a clear seasonality, with higher total AOD and lower coarse mode AOD in summer 2009. On top of stable spring background conditions with low AOD between 0.05 and 0.01, several episodes with high aerosol load can be seen.

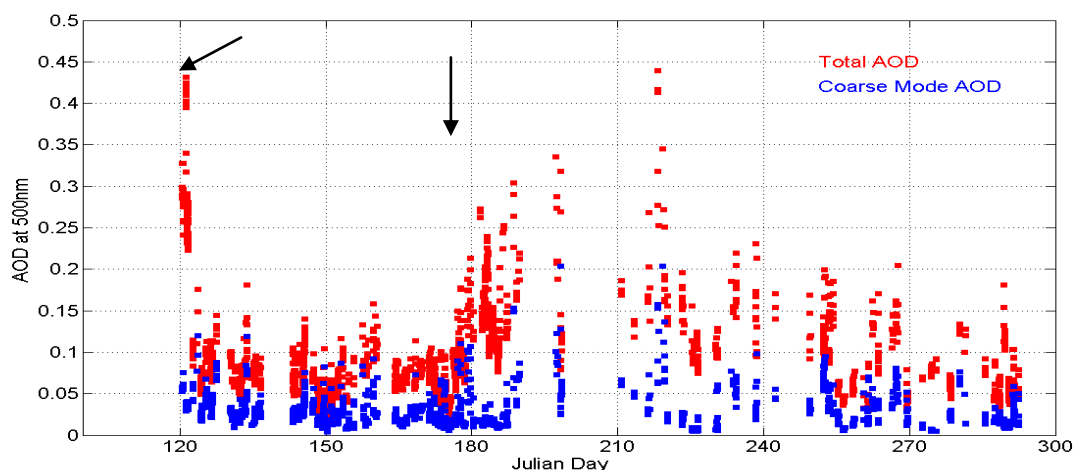


Figure 39: Time-series of total and coarse mode AOD measured during the first year of operation, in 2009, at the Birkenes observatory.

In Table 4 the data are presented as monthly mean averages of the aerosol optical depth at 500 nm, the Ångström exponent, precipitable water (PW), the associated standard deviations ( $\sigma$ ), and the number of days (N) in 2009 are given. The data are visualized in Figure 40.

<sup>8</sup> The data displayed are from the AERONET-SDA Version 4.1 data set (for a description of the SpectralDeconvolution Algorithm see O'Neill et al, 2003, O'Neill, 2005), which are derived from pre- and post-field calibrated and manually inspected AOD data

Table 4: Aerosol optical depth at 500 nm, Ångström exponent ( $\alpha_{440-870}$ ), precipitable water (PW), the associated standard deviations ( $\sigma$ ), the number of days ( $N$ ) in 2009.

Averages of	AOD <sub>500</sub>	$\sigma$	$\alpha_{440-870}$	$\sigma$	PW	$\sigma$	$N$
MAY	0.09	0.05	1.16	0.31	0.97	0.28	22
JUN	0.09	0.05	1.42	0.27	1.26	0.38	25
JUL	0.18	0.06	1.43	0.44	2.02	0.25	11
AUG	0.17	0.07	1.14	0.20	1.57	0.44	13
SEP	0.10	0.04	0.96	0.24	1.32	0.30	15
OCT	0.08	0.03	1.05	0.18	0.75	0.19	12

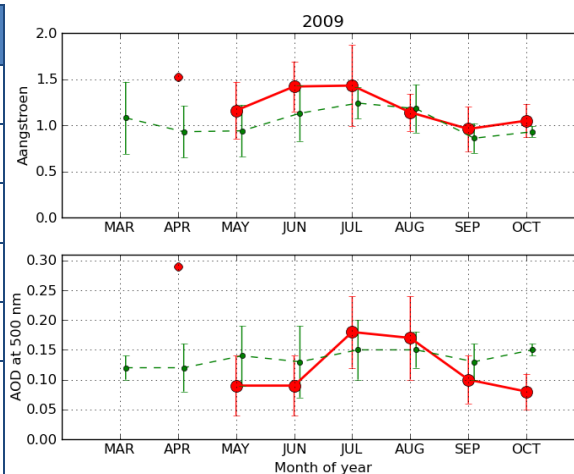


Figure 40: Monthly mean values ( $\pm$  standard deviation) of Ångström exponent (upper panel) and Aerosol Optical Depth in 2009 (lower panel). Red: data from Birkenes; Green: data from Andenes.

The monthly averaged data show a maximum aerosol load during summer period. Compared to values from the Northern Norwegian site Andenes (green dashed line in Figure 40), averaged AOD values at Birkenes (red marks in Figure 40) were lower in spring and autumn, but higher during the summer month July and August. The larger Ångström exponent between May and July indicate a predominance of fine particulates in Southern Norway during this time of 2009. The annual cycle can be linked to long-range transport patterns from e.g. the European continent, but a one year dataset is not sufficient to draw conclusions about seasonality of the aerosol optical depth at the site.

Figure 41 shows the 2-d density distribution of AOD and AE. The relative frequency distribution shows two distinct branches: one peaking at AOD of about 0.06 and AE below 1.5, the other one has slightly higher AOD and larger AE (predominance of smaller particles). Whether this can be linked to different transport patterns and/or local contribution to the aerosol load needs to be further investigated, preferable with a larger statistical base of data.

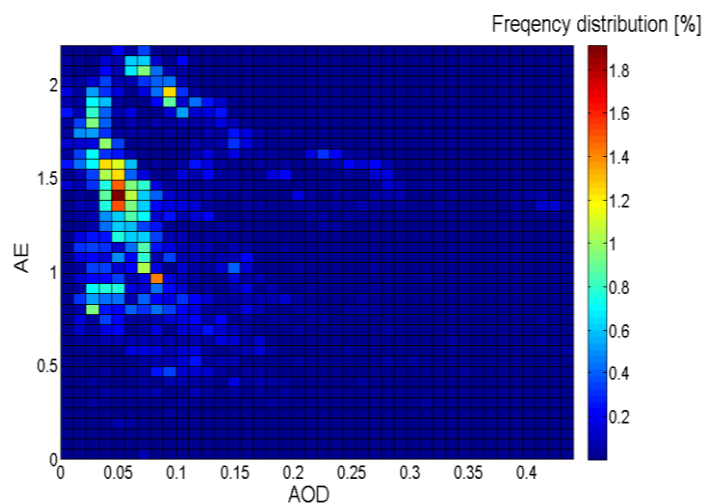


Figure 41: 2d density distribution of AOD and AE (from the SDS-dataset) observed during 2009.

Besides AOD and AE, the AERONET retrieval derives products from the inversion of sun-sky radiances (Dubovik et al., 2000 and 2002), which can be used to characterize the aerosol microphysical properties: particle size distributions, volume concentrations, effective radii and fine mode volume fraction. While these products are retrieved in all turbidity conditions, optical properties, such as single scattering albedo (SSA) and refractive index, derived from inversion require mode rate AOD ( $>0.4$  at 440 nm) to be retrieved with sufficient accuracy. Figure 42 (left panels) provides as an example, we show the size distribution for two periods with episodes of enhanced aerosol optical depth seen at Birkenes. Directly at the start of the observations, on 30 April / 1 May 2009, very high AOD values and a dominance of small particles were seen. Back-trajectories from NOAA's HySPLIT model for 1 May 08 UTC (middle panel

Figure 42) and daily averaged MODIS Terra AOD for 30 April/1 May, indicate transport of aerosol rich air-masses from SW and SE Europe reaching Birkenes at both lower and elevated altitudes. During the summer episodes (around day 183), with moderate AOD around 0.2 and a very distinct predominance of fine particles, the air masses seem to have been more confined to Northern Europe / Southern Scandinavia (see trajectories below 2 km). The MODIS Terra AOD shows typical moderate AOD levels in Norway and enhanced aerosol load in various regions in Europe. With more data to be obtained during the coming years, an aerosol characterization in Southern Norway and its relationship to transport patterns will be established by further analysis of the columnar optical properties obtained at the Birkenes site.

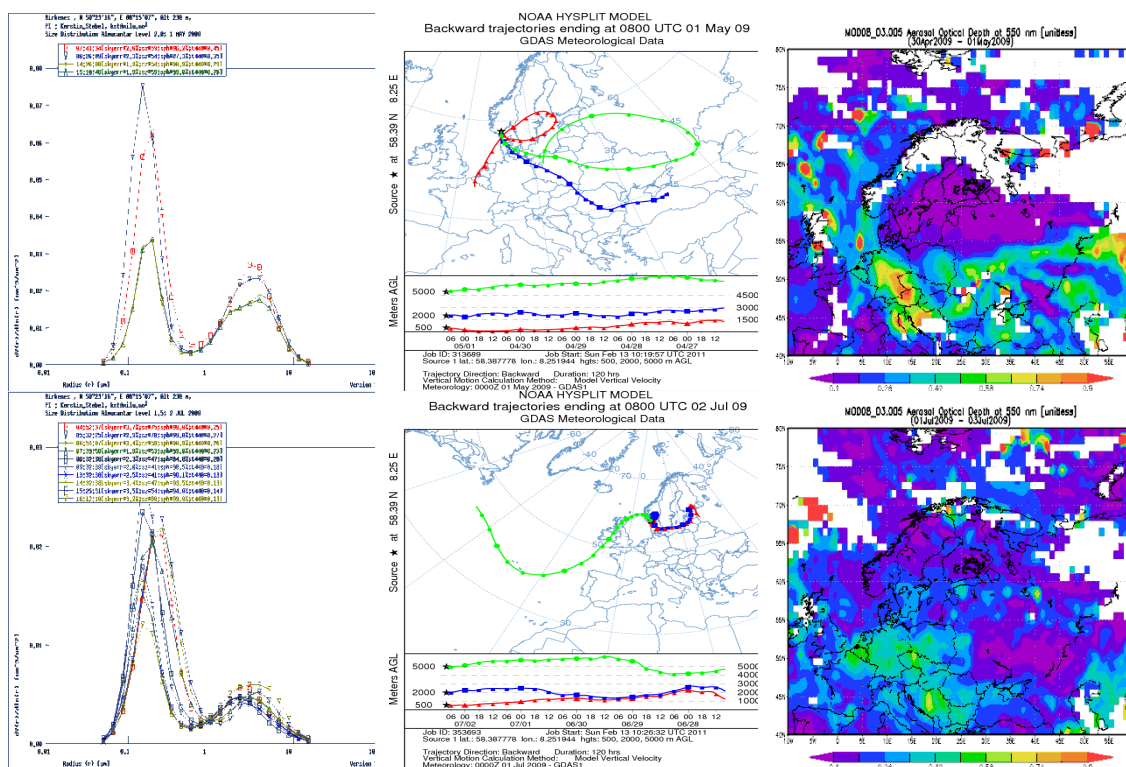


Figure 42: Episodes, with high aerosol load and small particle dominance, observed at Birkenes, around 30 April/1 May and 1-3 July 2009. Left panel: Particle size distribution on 1 May and 2 July 2009. Middle panel: Back-trajectories calculated with NOAA's HySPLIT model for 1 May 08 UTC and 2 July 08 UTC. Right panel: MODIS Terra AOD, averaged for 30 April/1 May and 1-3 July 2009.

### 6.3.2 Measurements of the total aerosol load above Ny-Ålesund

Measurements of the aerosol optical depth in Ny-Ålesund started in May 2002. The observations are part of the global network of AOD observations, which started in 1999 on behalf of the WMO GAW program. The measurements contributed to the POLAR-AOD network and first results can be found in Tomasi et al. (2007). The instrument is located on the roof of the Sverdrup station, Ny-Ålesund, close to the Zeppelin Observatory. Using a Precision Filter Radiometer (PFR, Wehrli, 2000 and 2005) direct solar radiation in four narrow spectral bands at 862, 501, 411, and 368 nm is obtained. One minute samples are recorded. Data quality control includes instrumental control like detector temperature and solar pointing control as well as objective cloud screening. SCIAMACHY TOSOMI ozone columns and meteorological data from Ny-Ålesund were used in the retrieval of the aerosol optical depth. The Ångström coefficient AE is derived for each set of measurements using all four PFR channels (Note: the wavelength region for calculation from AE (PFR) is slightly different from the one used for calculation of AE (CIMEL; which is 440 to 870 nm). The PFR is annually calibrated at PMOD/WRC. The most recent calibration date is January 2009.

In Ny-Ålesund the polar night lasts from 26<sup>th</sup> October to 16<sup>th</sup> February, leading to short observational seasons. However during the summer it would be possible to measure day and night if the weather conditions are satisfactory, unless bad weather conditions – cloudy or foggy – inhibit the observations of direct solar radiation.

In Table 5 and Table 6 monthly mean and sunlight-season average values of AOD at 500 nm and Ångström coefficient measured in Ny-Ålesund between 2002 and 2009 are summarized. The data are visualized in

Figure 43 and Figure 44. The 2009 measurements started in March. Due to instrumental related problems and overcast weather, AOD results only cover the period May to September. Monthly mean data are calculated from hourly averaged values with more than 10% of valid observations included. The results show clear inter-annual variability. Individual episodes have a large impact on observed monthly averages. Huge emissions from boreal forest fires in North America, with light absorbing aerosol containing BC, were transported into the region and very likely explain the elevated AOD levels end of July 2004 (Stohl *et al.* 2006). Agricultural fires in Eastern Europe resulted in elevated pollution levels in Arctic in spring 2006 (Stohl *et al.*, 2007) and Myhre *et al.* (2007) found that these aerosol had a strong cooling effect on the Arctic during this period, with a moderate warming effect when the aerosol layer were above snow covered surface areas.

*Table 5: Monthly mean and sunlight-season average values of AOD at 500 nm measured in Ny-Ålesund between 2002 and 2009. The values given are mean and standard deviation.*

Month / Year	2002	2003	2004	2005	2006	2007	2008	2009	2002-2009
March		0.15 ±0.12	0.06±0.00	0.08±0.03	0.12±0.03		0.14±0.07		0.12±0.07
April	0.06±0.01	0.11±0.05	0.12±0.08	0.12±0.07	0.16±0.07	0.10±0.05	0.15±0.08		0.13±0.07
May	0.08±0.03	0.15±0.06	0.13±0.09	0.10±0.03		0.10±0.12	0.15±0.05	0.11±0.03	0.12±0.07
June	0.06±0.02	0.10±0.03	0.06±0.01	0.05±0.02	0.04±0.00	0.07±0.03	0.06±0.02	0.08±0.02	0.06±0.02
July	0.07±0.12	0.04±0.01	0.10±0.07	0.05±0.02	0.05±0.02	0.05±0.01	0.06±0.03	0.11±0.04	0.07±0.05
August	0.07±0.08	0.05±0.02	0.05±0.02	0.04±0.03	0.05±0.04	0.05±0.02		0.10±0.02	0.06±0.04
September	0.06±0.05	0.06±0.03	0.04±0.02	0.03±0.01	0.04±0.03	0.04±0.03		0.09±0.01	0.05±0.03
Mar – Sep	0.07±0.05	0.09±0.06	0.08±0.07	0.08±0.05	0.09±0.07	0.07±0.06	0.12±0.07	0.13±0.05	0.09±0.07

*Table 6: Monthly mean and sunlight-season average values of Ångström coefficient AE measured in Ny-Ålesund in the period between 2002 and 2009. The values given are mean and standard deviation.*

Month/Year	2002	2003	2004	2005	2006	2007	2008	2009	2002-2009
March		0.9±0.5	1.3±0.1	1.1±0.3	0.9±0.1		1.4±0.3		1.3±0.4
April	0.9±0.1	1.3±0.3	1.2±0.3	1.4±0.4	0.9±0.3	1.4±0.4	1.3±0.3		1.3±0.4
May	1.4±0.1	1.3±0.2	1.4±0.5	1.0±0.2		1.4±0.6	1.4±0.2	1.3±0.4	1.3±0.4
June	1.2±0.3	1.5±0.1	1.7±0.2	1.6±0.3	1.7±0.2	1.7±0.2	1.5±0.4	1.4±0.2	1.5±0.3
July	1.2±0.2	1.5±0.3	1.6±0.4	1.7±0.2	1.4±0.3	1.6±0.2	1.5±0.3	1.3±0.3	1.5±0.3
August	1.3±0.4	1.4±0.5	1.5±0.3	1.4±0.7	1.3±0.6	1.7±0.3		1.2 ±0.1	1.4±0.4
September	1.2±0.5	1.4±0.3	1.3±0.3	1.5±0.4	1.4±0.3	1.5±0.4		1.1±0.1	1.4±0.4
Mar-Sep	1.3±0.3	1.3±0.4	1.4±0.4	1.3±0.4	1.2±0.4	1.5±0.4	1.4±0.3	1.3±0.3	1.4±0.4

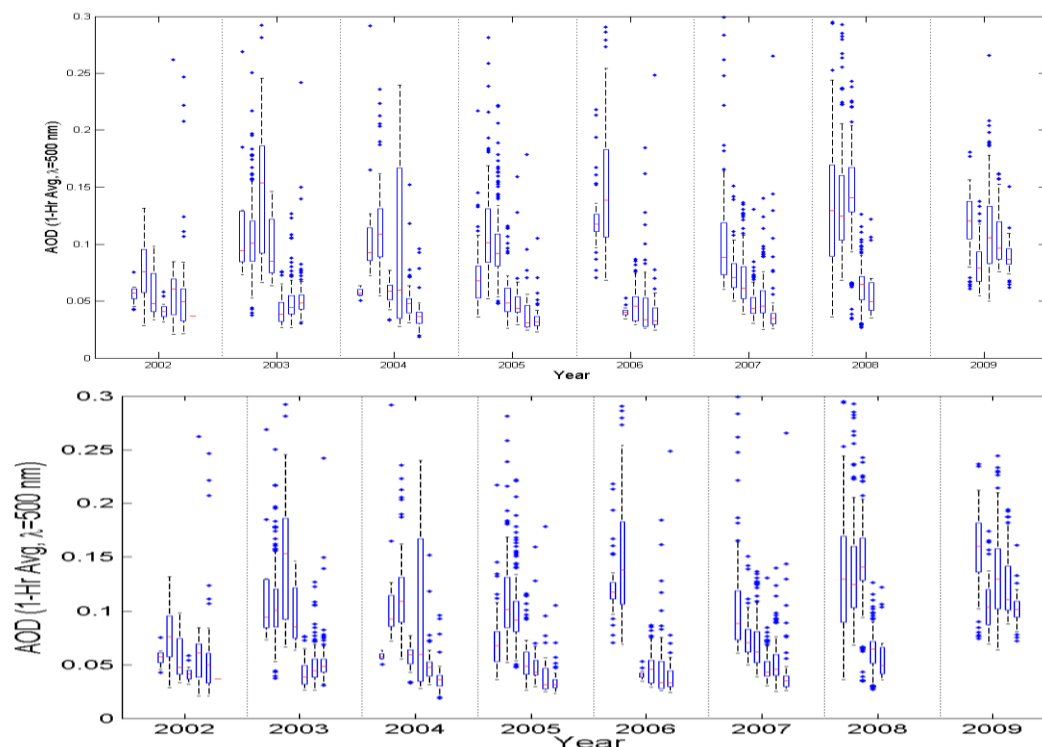


Figure 43: Monthly average Ångström exponent (upper panel) and aerosol optical depth (AOD at 500 nm) (lower panel) measured in Ny-Ålesund during the sunlight time periods in 2002 - 2009. On each box, the central mark is the median, the edges of the box are the 25th and 75th percentiles, the whiskers extend to the most extreme data points not considered outliers, and outliers (in terms of monthly averages, although not considered outlier in terms of pollutions events with high aerosol loads) are plotted individually.

Seasonal variations for AOD and Ångström coefficient are shown in Figure 43. The measurements reveal the expected pattern, larger AOD, equivalent to higher aerosol-load during the Arctic haze period in spring than in summer, where background conditions were seen with low aerosol column concentration. The Ångström coefficients increase from spring to summer with large loading of fine aerosols seen in summer. The AOD data show lowest scatter and highest AE in June. Autumn values show again higher scatter and on average somewhat lower AE than during the mid-summer period. In 2009 slightly higher than averages AOD and lower than averages Ångström coefficient have been measured in summer and autumn. Nevertheless the values are within the scatter of the long-term observation data set 2002-2009.

The transition from spring-time to summer has been analysed using multi-year observations of aerosols at Svalbard (Engvall et al., 2008). The authors show the transition from an accumulation-dominated (90-630 nm) to an Aitken-dominated distribution (22-90 nm) occurs over the period April through June and suggest that the aerosol microphysical properties are not only the result of transport, but of a delicate balance between incoming solar radiation, transport, and condensational sink processes. The observations from Engvall et al. (2008) show that it's an open question how and to what extent processes in the boundary layer and the free troposphere is inter-linked in the Arctic. How these findings can help to understand the total column aerosol observations is yet unclear, as both particle ranges reported by the

authors have to be considered as small (the smallest wavelengths channel of the PFR is 368 nm). In order to get better insight into this phenomenon, further investigations are necessary.

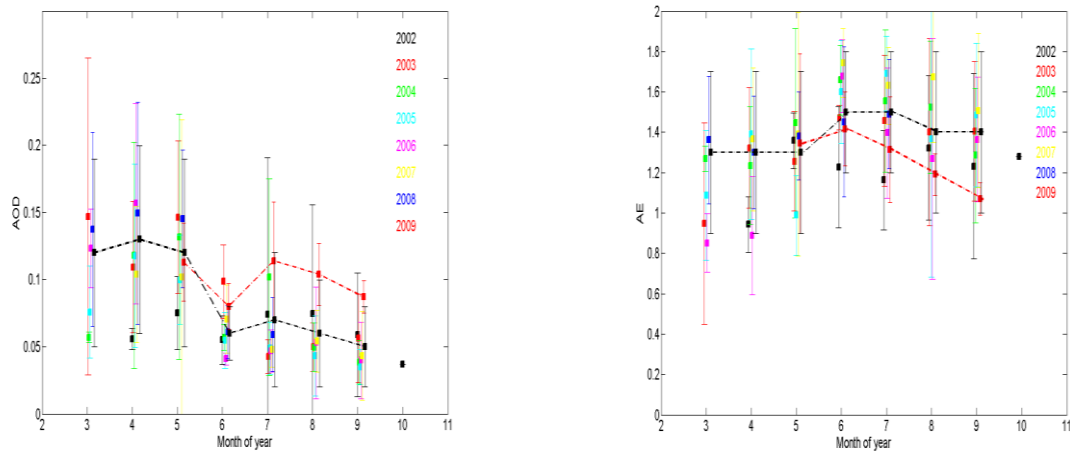


Figure 44: Monthly mean values ( $\pm$  standard deviation) of Ångström exponent (upper panel) and Aerosol Optical Depth during 2002 - 2009 (lower panel). Black dotted line: data averaged over all years. Red: data from 2009.

In

Figure 44 the 2d relative frequency distribution of hourly averaged AOD and Ångström coefficients seen in Ny-Ålesund is shown. All data obtained between 2002 and 2009 (left panel) are compared to the 2009 data set (right panel). Small particles with low aerosol optical depth below 0.05 and AE above 1.6 are dominating the frequency distribution – for comparison: the all year mean AOD is  $0.09 \pm 0.07$  with AE  $1.4 \pm 0.4$ . In 2009 the frequency distribution is shifted to slightly higher AE. As the observational period does in 2009 not cover the early spring Arctic haze period, more general conclusions are not drawn yet.

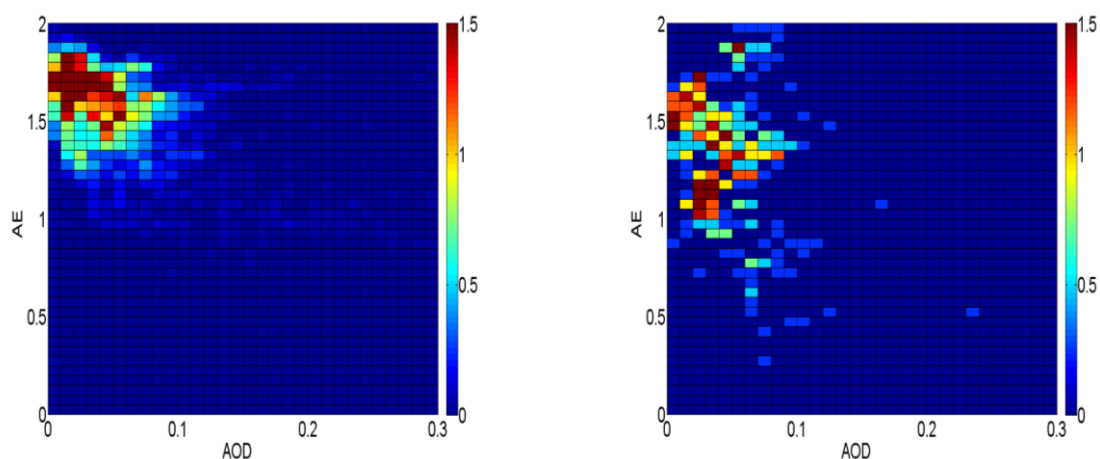


Figure 45: The 2d relative frequency distribution of hourly averaged AOD and Ångström coefficient during 2002 to 2009 (left panel) and during May – September 2009 (right panel).

## 7. Transport of pollution to the Zeppelin Observatory and the influence on the observations

We have performed an analysis and assessment of the source regions of the air masses arriving at Zeppelin in the period 2001-2009. Analyses of the air mass origin are important for the understanding of the observed levels of the gases and aerosols. We have analysed the origin of the air arriving at Zeppelin in 2009. Air mass trajectories are calculated using the FLEXTRA trajectory model (<http://www.nilu.no/trajectories/>) and using meteorological data provided from European Centre for Medium Range Weather Forecasts (ECMWF). 7 days backward trajectories from ECMWF have been used to investigate the major transport pathways into the region.<sup>9</sup> The origin of the air arriving at Zeppelin is categorised in following 6 sectors:

- **Arctic region:** Clean Arctic air: Air mass trajectories with all trajectory points north of 65°N
- **Atlantic sector:** Clean marine air: Air mass trajectories with all trajectory points between 10°W and 70°W and from south of 60°N.
- **North American sector:** Polluted air: If at least 50% of the trajectory points are between 70°W and 180°W, and from south of 60°N.
- **European sector:** Polluted air: If at least 50% of the trajectory points were between 10°W and 30°E, and from south of 60°N.
- **Russian sector:** Polluted air: If air mass trajectories with all points between 30°E and 180°E and from south of 60°N.
- **Undefined sector:** 20% the trajectories do not come from a distinct sector.

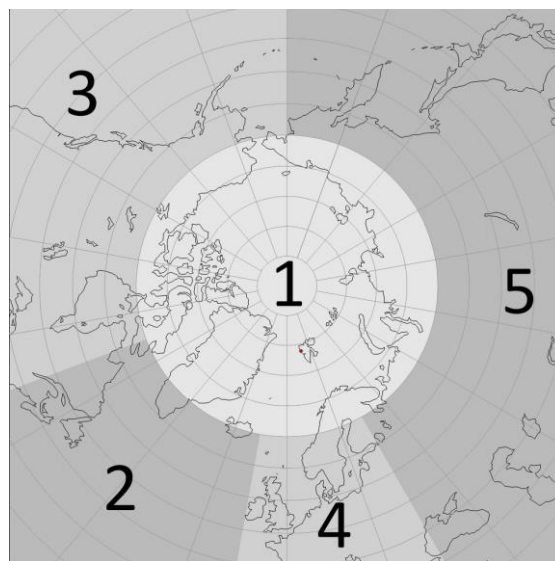


Figure 46: The sectors used to classify the air arriving at the Zeppelin Observatory. 1 is Arctic sector, 2 is Atlantic sector, 3 is North American sector, 4 is European sector and 5 is Russian sector.

Air from the Arctic and Atlantic sector is assumed to contain minimal influence of pollution. There are almost no industrial sources in these areas, and one can say that the air is ‘clean’. Background values of the greenhouse gases components are defined from those ‘clean air’ areas with 6 out of 8 trajectories (sampling day +/- 12 hours) within the sector, as described above.

Figure 47 shows the share of polluted and clean air arriving at the Zeppelin observatory for the years 2001-2009. The most striking result of this analysis is that in particularly 2007 and

<sup>9</sup> The spatial resolution is T106, which correspond to a latitude/longitude resolution of 1x1 degrees, the temporal resolution is 6 hours, and 91 levels (60 levels before February 2006) are available in the vertical direction. The data sets used are so-called analysis, which is a combination of observations and numerical calculations. This includes measurements from satellites, radio sondes, buoys, weather stations, etc. which are assimilated into a meteorological model that produce an estimate of the state of the atmosphere at a given time.

2008 the fraction of air arriving at Zeppelin categorized as clean marine and Arctic air was clearly higher than the previous years. As described in section 4.1 the CH<sub>4</sub> concentration has increased since 2005. This can point in the direction of a possible Arctic source or accumulation of methane in the Arctic, particularly during late summer and autumn. Also the year 2003 with high methane concentration had a large fraction of clean air arriving at Zeppelin. 2009 is a somewhat different. In 2009 there were many episodes with polluted air transported to Zeppelin but no episodes as extreme as the record one observed in spring 2006 (Stohl et al., 2007; Myhre et al 2007). In contrast to the last years the site experienced higher influence of polluted air masses from central Europe and from the Russian sector in 2009. Clean arctic marine air dominated only on 59% of the days which is considerable lower than previous years. At the same time the category with mixed air from various sectors has increased slightly, thus the results are connected with uncertainty.

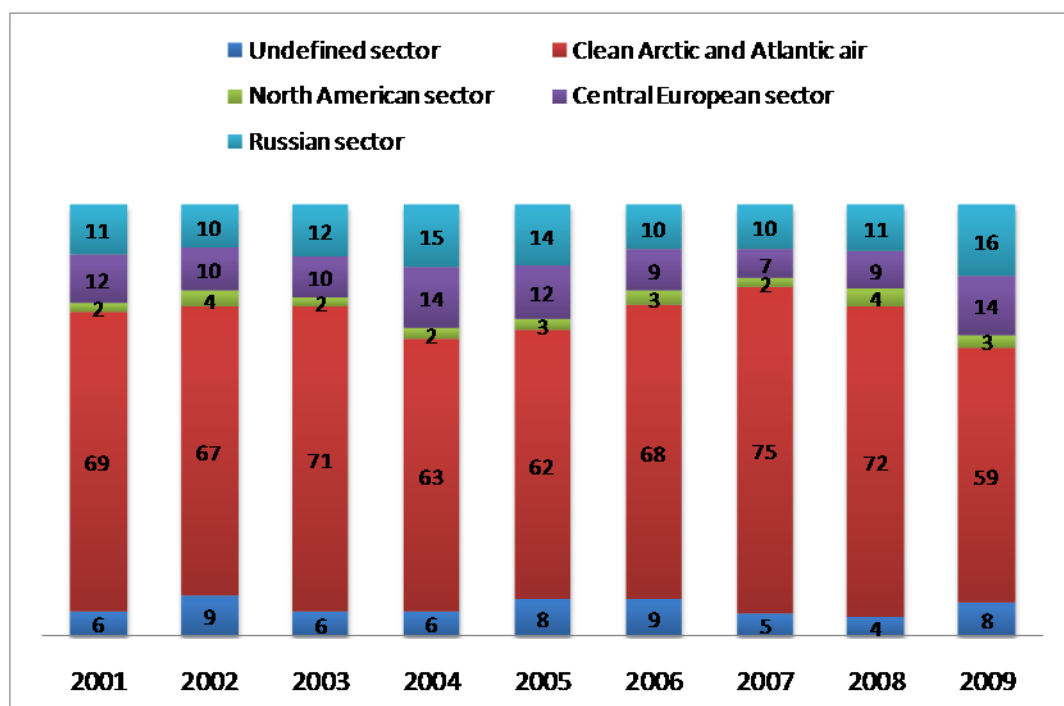
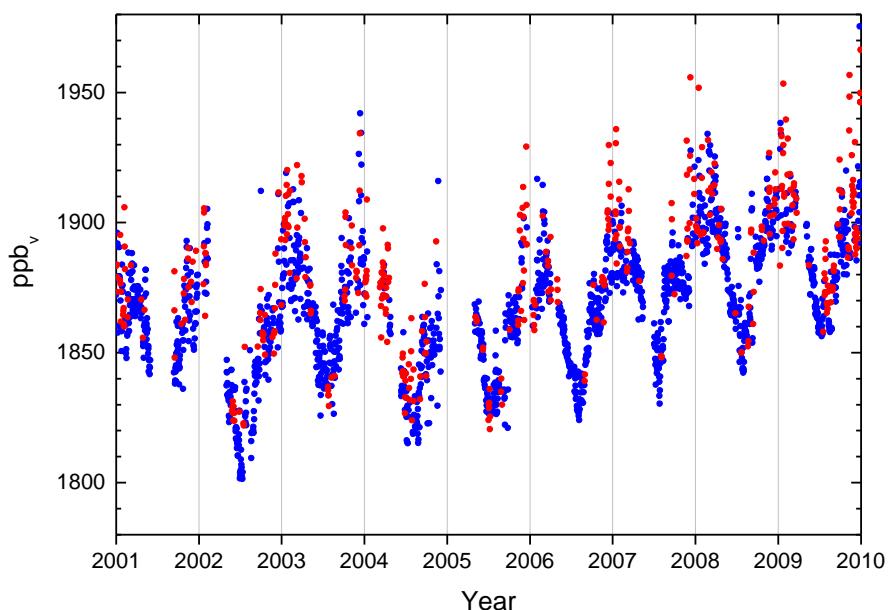


Figure 47: The percentage of polluted and clean air arriving at Zeppelin in the period 2001-2009 from the various sectors.

## 7.1 Regional emissions and the influence on methane levels

For the year 2009 we have performed a more detailed analysis of the air masses for selected days and periods with elevated methane levels. In Figure 48 are methane observations for the period 2001-2009 shown together with an indication of the air masses which are considered as clean Arctic and Atlantic air or polluted air.



*Figure 48: Observations of methane for the period 2001-2009 at the Zeppelin observatory. Blue dots: air mass origin is from a clean sector, red dots: the air mass origin is from a polluted sector.*

The blue dots represent the background methane level, which means that the air masses originating from the Arctic or Atlantic region. The red dots represent the methane observations when the air masses arriving at Zeppelin originate from a polluted region: North America, Europe or Russia. As can be seen in 2007 and 2008 a large portion of the air masses arriving at Zeppelin originate from the Arctic and Atlantic sector. Further, the peak episodes are due to pollution transported from lower latitudes. In 2009 there are particularly many episodes with polluted air the last part of the year.

We have analysed a selection of the peak episodes in 2009 in methane further by use of the FLEXPART model (<http://transport.nilu.no/flexpart>). In the upper panel of Figure 49 are the observations for 2009 shown together with indications of sources regions for the episodes and in the lower panel are FLEXPART simulations for 30<sup>th</sup> July shown.

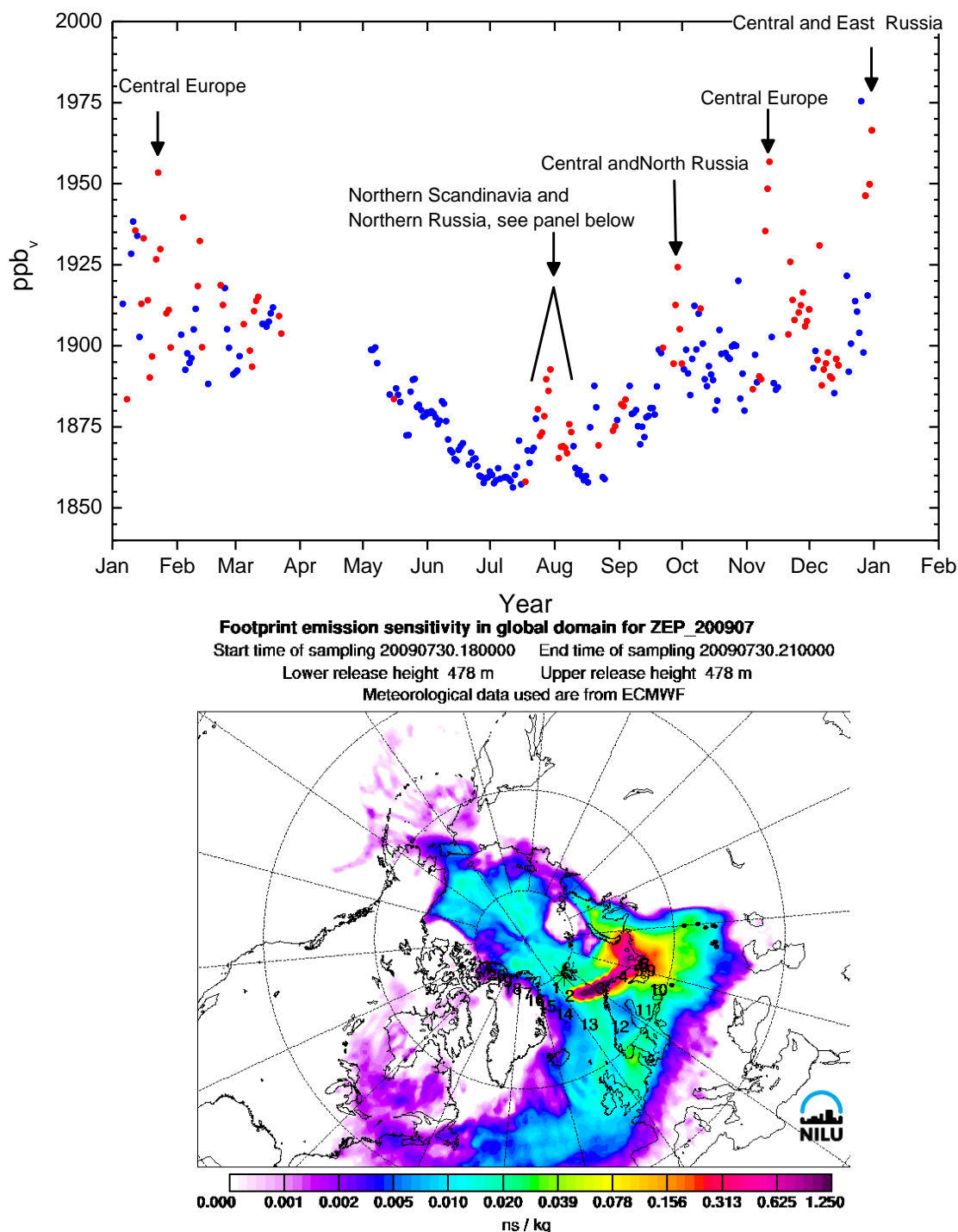


Figure 49: Upper panel: Methane observations for 2009 with an indication of source regions for the elevated episodes. Lower panel: FLEXPART simulations for 30<sup>th</sup> July.

An approximate indication of the source region of the episodes is included in Figure 49. This is based on an analysis of FLEXTRA simulations for the selected days. In the lower panel are FLEXPART simulations for 30<sup>th</sup> July shown. In this period there were high levels of CH<sub>4</sub>, slightly enhanced levels of CO at one day, but low ozone values. Ozone and CO are suitable tracers for urban pollution and fires and combustion processes, respectively. There are also elevated levels of CH<sub>3</sub>Cl but few other components. The main sources of CH<sub>3</sub>Cl are ocean and biomass burning. There were not possible to observe fires the in region in this period, and the main cause of this episode is not clear.

## 8. References

- Andreae, M.O., Jones, C.D., Cox, P.M. (2005) Strong present-day aerosol cooling implies a hot future. *Nature*, 435, 1187–1190.
- Bergamaschi, P., Frankenberg, C., Meirink, J.F., Krol, M., Dentener, F., Wagner, T., Platt, U., Kaplan, J. O., Körner, S., Heimann, M., Dlugokencky, E.J., Goede, A. (2007) Satellite cartography of atmospheric methane from SCIAMACHY onboard ENVISAT 2. Evaluation based on inverse model simulations. *J. Geophys. Res.*, 112, D02304, doi:10.1029/2006JD007268.
- Dubovik, O., Holben, B. N., Eck, T. F., Smirnov, A., Kaufman, Y. J., King, M. D., Tanre, D., Slutsker, I. (2002) Variability of absorption and optical properties of key aerosol types observed in worldwide locations, *J. Atmos. Sci.*, 59, 590–608.
- Dubovik, O., Smirnov, A., Holben, B.N., King, M.D., Kaufman, Y.J., Eck, T.F., Slutsker, I. (2000) Accuracy assessments of aerosol optical properties retrieved from Aerosol Robotic Network (AERONET) Sun and sky radiance measurements. *J. Geophys. Res.*, 105, 9791–9806.
- EDGAR (2010) European Commission, Joint Research Centre (JRC)/Netherlands Environmental Assessment Agency (PBL). Emission Database for Global Atmospheric Research (EDGAR), release version 4.1. URL: <http://edgar.jrc.ec.europa.eu>
- Eleftheriadis, K., Vratolis, S., Nyeki, S. (2009) Aerosol black carbon in the European Arctic: Measurements at Zeppelin station, Ny-Ålesund, Svalbard from 1998–2007. *Geophys. Res., Lett.*, 36, L02809, doi:10.1029/2008GL035741.
- Engvall, A.-C., Krejci, R., Ström, J., Treffeisen, R., Scheele, R., Hermansen, O., Paatero, J. (2008) Changes in aerosol properties during spring-summer period in the Arctic troposphere. *Atmos. Chem. Phys.*, 8, 445–462.
- Forster, P., Ramaswamy, V., Artaxo, P., Berntsen, T., Betts, R., Fahey, D.W., Haywood, J., Lean, J., Lowe, D.C., Myhre, G., Nganga, J., Prinn, R., Raga, G., Schulz, M., Van Dorland, R. (2007) Changes in atmospheric constituents and in radiative forcing. In: *Climate Change 2007: The physical science basis. Contribution of Working Group I to the fourth assessment report of the Intergovernmental Panel on Climate Change*. Ed. by Solomon, S., D. Qin, M. Manning, Z. Chen, M. Marquis, K.B. Averyt, M. Tignor, H.L. Miller. Cambridge, Cambridge University Press.
- Heintzenberg, J. (1980) Particle size distribution and optical properties of arctic haze. *Tellus*, 32, 251–260.
- Holben, B., Eck, T., Slutsker, I., Tanré, D., Buis, J., Setzer, A., Vermote, E., Reagan, J., Kaufman, Y. (1998) AERONET- a federated instrument network and data archive for aerosol characterization. *Remote Sens. Environ.*, 66, 1-16.
- IPCC (2007) Summary for Policymakers. In: *Climate Change 2007: The Physical Science Basis. Contribution of Working Group I to the Fourth Assessment Report of the Intergovernmental Panel on Climate Change*. Ed.d by Solomon, S., D. Qin, M. Manning, Z. Chen, M. Marquis, K.B. Averyt, M. Tignor, H.L. Miller. Cambridge, United Kingdom and New York, Cambridge University Press.
- Isaksen, I.S.A., Hov, Ø. (1987) Calculation of trends in the tropospheric concentration of O<sub>3</sub>, OH, CO, CH<sub>4</sub> and NO<sub>x</sub>. *Tellus*, 39B, 271-285.

- Isaksen, I.S.A., Gauss, M., Myhre, G., Walter Anthony, K.M., Ruppel, C. (2010) Strong atmospheric chemistry feedback to climate warming from Arctic methane emissions. *Global Biogeochem. Cycles*, 25, GB2002, doi: 10.1029/2010GB003845.
- Keppeler, F., Hamilton, J.G., Bra, M., Röckmann, T. (2006) Methane emissions from terrestrial plants under aerobic conditions. *Nature*, 439, 187-191.
- Kiehl, J.T. (2007) Twentieth century climate model response and climate sensitivity. *Geophys. Res. Lett.*, 34, L22710, doi: 10.1029/2007GL31383.
- Kulmala, M., Vehkamäki, H., Petäjä, T., DalMaso, M., Lauri, A., Kerminen, V.-M., Birmili, W., McMurry, P.H. (2004) Formation and growth rates of ultrafine atmospheric particles: a review of observations. *J. Aerosol Sci.*, 35, 143 – 176.
- Myhre, C.L., Hermansen, O., Fjæraa, A.M., Lunder, C., Schmidbauer, N., Stebel, K., Prata, F. (2010) Greenhouse monitoring at the Zeppelin station - annual report 2008. Kjeller (Statlig program for forurensningsovervåking. Rapport 1071/2010) (TA 2633/2010) (NILU OR 24/2010).
- Myhre, C.L., Toledano, C., Myhre, G., Stebel, K., Yttri, K.E., Aaltonen, V., Johnsrud, M., Frioud, M., Cachorro, V., de Frutos, A., Lihavainen, H., Campbell, J.R., Chaikovsky, A.P., Shiobara, M., Welton, E.J., Tørseth, K. (2007) Regional aerosol optical properties and radiative impact of the extreme smoke event in the European Arctic in spring 2006. *Atmos. Chem. Phys.*, 7, 5899-5915.
- NASA Goddard Space Flight Center (2011) AERONET Aerosol Robotic Network. **URL:** <http://aeronet.gsfc.nasa.gov/> [2011-06-09]
- O'Neill, N., Eck, T., Smirnov, A., Holben, B. (2008) Spectral Deconvolution Algorithm (SDA), Technical memo, version 4.1. AERONET, NASA. **URL:** [http://aeronet.gsfc.nasa.gov/new\\_web/PDF/tauf\\_tauc\\_technical\\_memo.pdf](http://aeronet.gsfc.nasa.gov/new_web/PDF/tauf_tauc_technical_memo.pdf)
- O'Neill, N.T., Eck, T.F., Smirnov, A., Holben, B.N., Thulasiraman, S. (2003) Spectral discrimination of coarse and fine mode optical depth. *J. Geophys. Res.*, 108, 4559, doi:10.1029/2002JD002975.
- Prather, M. et al. (2001) Atmospheric chemistry and greenhouse gases. In: *Climate Change 2001: The Scientific Basis, Contribution of Working Group I to the Third Assessment Report of the Intergovernmental Panel on Climate Change*. Ed. by J.T. Houghton et al. Cambridge, Cambridge University Press. pp. 239-287.
- Raes, F., Van Dingenen, R., Vignati, E., Wilson, J., Putaud, J.-P., Seinfeld, J. H., Adams, P. (2000) Formation and cycling of aerosols in the global troposphere. *Atmos. Environ.*, 34, 4215–4240.
- Repo, M.E., Susiluoto, S., Lind, S.E., Jokinen, S., Elsakov, V., Biasi, C., Virtanen, T., Pertti, J., Martikainen, P.J. (2009) Large N<sub>2</sub>O emissions from cryoturbated peat soil in tundra. *Nature Geosci.*, 2, 189–192.
- Rigby, M., Prinn, R.G., Fraser, P.J., Simmonds, P.G., Langenfelds, R.L., Huang, J., Cunnold, D.M., Steele, L.P., Krummel, P.B., Weiss, R.F., O'Doherty, S., Salameh, P.K., Wang, H.J., Harth, C.M., Mühle, J., Porter, L.W. (2008) Renewed growth of atmospheric methane. *Geophys. Res. Lett.*, 35, L22805, doi:10.1029/2008GL036037.
- Rodríguez, E., Toledano, C., Cachorro, V.E., Ortiz, P., Stebel, K., Berjón, A., Blindheim, S., Gausa, M., de Frutos, A.M. (2011) Aerosol characterization at the sub-Arctic site Andenes (69°N, 16°E), by the analysis of columnar optical properties. Submitted to the *Quart. J. Roy. Meteorol. Soc.*

- Schuur, E.A.G., Bockheim, J., Canadell, J., Euskirchen, E., Field, C.B., Goryachkin, S.V., Hagemann, S., Kuhry, P., Lafleur, P., Lee, H., Mazhitova, G., Nelson, F.E., Rinke, A., Romanovsky, V., Shiklomanov, N., Tarnocai, C., Venevsky, S., Vogel, J.G., Zimov, S.A. (2008) Vulnerability of permafrost carbon to climate change: implications for the global carbon cycle. *Bioscience*, 58, 701–714.
- Shindell, D., Faluvegi, G. (2009) Climate response to regional radiative forcing during the twentieth century. *Nature Geosci.*, 2, 294–300.
- Simmonds, P.G., Manning, A.J., Cunnold, D.M., Fraser, P.J., McCulloch, A., O'Doherty, S., Krummel, P.B., Wang, R.H.J., Porter, L.W., Derwent, R.G., Grealley, B., Salameh, P., Miller, B.R., Prinn, R.G., Weiss, R.F. (2006) Observations of dichloromethane, trichloroethene and tetrachloroethene from the AGAGE stations at Cape Grim, Tasmania, and Mace Head, Ireland. *J. Geophys. Res.*, 111, D18304, doi: 10.1029/2006JD007082.
- Stohl, A., Seibert, P. (1998) Accuracy of trajectories as determined from the conservation of meteorological tracers. *Quart. J. Roy. Meteorol. Soc.*, 124, 1465–1484.
- Stohl, A., Andrews, E., Burkhardt, J.F., Forster, C., Herber, A., Hoch, S.W., Kowal, D., Lunder, C., Mefford, T., Ogren, J.A., Sharma, S., Spichtinger, N., Stebel, K., Stone, R., Strom, J., Tørseth, K., Wehrli, C., Yttri, K.E. (2006) Pan-Arctic enhancements of light absorbing aerosol concentrations due to North American boreal forest fires during summer 2004. *J. Geophys. Res.*, 111, D22214, doi: 10.1029/2006JD007216.
- Stohl, A., Berg, T., Burkhardt, J.F., Fjæraa, A.M., Forster, C., Herber, A., Hov, Ø., Lunder, C., McMillan, W.W., Oltmans, S., Shiobara, M., Simpson, D., Solberg, S., Stebel, K., Ström, J., Tørseth, K., Treffeisen, R., Virkkunen, K., Yttri, K.E. (2007) Arctic smoke – record high air pollution levels in the European Arctic due to agricultural fires in Eastern Europe in spring 2006. *Atmos. Chem. Phys.*, 7, 511–534.
- Stohl, A., Forster, C., Frank, A., Seibert, P., Wotawa, G. (2005) Technical note: The lagrangian particle dispersion model flexpart version 6.2. *Atmos. Chem. Phys.*, 5, 2461–2474.
- Stohl, A., Hittenberger, M., Wotawa, G. (1998) Validation of the lagrangian particle dispersion modell FLEXPART against large scale tracer experiment data. *Atmos. Environ.*, 32, 4245–4264.
- Stohl, A., Wotawa, G., Seibert, P., Kromp-Kolb, H. (1995) Interpolation errors in wind fields as a function of spatial and temporal resolution and their impact on different types of kinematic trajectories. *J. Appl. Meteor.*, 34, 2149–2165.
- Toledano, C., Cachorro, V., Gausa, M., Stebel, K., Aaltonen, V., Berjón, A., Ortiz, P., de Frutos, A., Bennouna, Y., Blindheim, S., Myhre, C.L., Rodriguez, E., de Leeuw, G., Zibordi, G., Wehrli, C., Krazter, S., Hakansson, B., Carlund, T. (2010) Overview of sun photometer measurements of aerosol properties in Scandinavia and Svalbard. Oral presentation at IPY Oslo Science Conference. Oslo, Norway. **URL:** <http://ipy-osc.no/abstract/385694>
- Tomasi, C., Vitale, V., Lupi, A., Di Carmine, C., Campanelli, M., Herber, A., Treffeisen, R., Stone, R.S., Andrews, E., Sharma, S., Radionov, V., von Hoyningen-Huene, W., Stebel, K., Hansen, G.H., Myhre, C.L., Wehrli, C., Aaltonen, V., Lihavainen, H., Virkkula, A., Hillamo, R., Ström, J., Toledano, C., Cachorro, V.E., Ortiz, P., de Frutos, A.M., Blindheim, S., Frioud, M., Gausa, M., Zielinski, T., Petelski, T., Yamanouchi, T. (2007) Aerosols in polar regions: A historical overview based on optical depth and in situ observations. *J. Geophys. Res.*, 112, D16205, doi:10.1029/2007JD008432.

- Walter, K.M., Edwards, M.E., Grosse, G., Zimov, S.A., Chapin III, F.S. (2007) Thermokarst lakes as a source of atmospheric CH<sub>4</sub> during the last deglaciation. *Science*, 318, 633–636.
- Wehrli, C. (2000) Calibrations of filter radiometers for determination of atmospheric optical depth. *Meteorologia*, 37, 419-422.
- Wehrli, C. (2005) GAWPFR: A network of Aerosol Optical Depth observations with Precision Filter Radiometers. In: *WMO/GAW Experts workshop on a global surface based network for long term observations of column aerosol optical properties*. Geneva, World Meteorological Organization (GAW Report No. 162, WMO TD No. 1287).
- WMO (2007) Scientific assessment of ozone depletion: 2006. Geneva, World Meteorological Organization (Global Ozone Research and Monitoring Project – Report No. 50).
- WMO (2009) Greenhouse Gas Bulletin. The state of greenhouse gases in the atmosphere using global observations through 2008. Geneva (Bulletin No. 5, 23 November 2009).  
**URL:** [http://www.wmo.int/pages/prog/arep/gaw/ghg/documents/ghg-bulletin2008\\_en.pdf](http://www.wmo.int/pages/prog/arep/gaw/ghg/documents/ghg-bulletin2008_en.pdf)
- WMO (2010) Greenhouse Gas Bulletin. The state of greenhouse gases in the atmosphere using global observations through 2009. Geneva (Bulletin No. 6, 24 November 2010).  
**URL:** [http://www.wmo.int/pages/prog/arep/gaw/ghg/documents/GHG\\_bull\\_6en.pdf](http://www.wmo.int/pages/prog/arep/gaw/ghg/documents/GHG_bull_6en.pdf)

## **Appendix I: Description of instruments, methods and trend analysis**

In this appendix are the instrumental methods used for the measurements of the various greenhouse gases presented. Additionally we explain the theoretical methods used in the calculation of the trends. In the end of the section we show how the annual mean values presented in Table 2 are calculated.

### **Details about greenhouse gas measurements and recent improvement and extensions**

NILU performs measurements of halogenated greenhouse gases as well as methane and carbon monoxide using automated gas chromatographs with high sampling frequencies at Zeppelin. A mass spectrometric detector is used to determine more than 20 halogenated compounds, automatically sampled 6 times per day. Methane and CO are sampled 3 times per hour. This high sampling frequency gives valuable data for the examination of episodes caused by long-range transport of pollutants as well as a good basis for the study of trends and global atmospheric change. Close cooperation with AGAGE-partners on the halocarbon instrument and audits on the methane and CO-instruments (performed by EMPA on the behalf of GAW/WMO) results in data of high quality.

At the Birkenes Observatory a very different approach is used. At this site Picarro Cavity Ring-Down Spectroscopy (CRDS) is employed. This is a state of the art infrared spectrometer for field measurements with very high time resolution and precision. The Picarro CRDS are utilizing a near-infrared laser to measure spectral signatures of the molecule. Gas is introduced in an optical measurement cavity with an effective path length of up to 20 km making it possible to measure very low concentrations. The CRDS technology allows monitoring of CO<sub>2</sub> and CH<sub>4</sub> in moist air. During post-processing concentrations are re-calculated for dry air. This is required to remove the variability of moisture in the atmosphere, and to make the monitoring results comparable with traditional FTIR monitoring methods.

Table 7: Instrumental details for greenhouse gas measurements at Zeppelin and Birkenes.

Component		Instrument and method	Time res.	Calibration procedures	Comment
<b>Methane (Zeppelin)</b>	CH <sub>4</sub>	GC-FID	15 min	Hourly, working std. calibrated vs. GAW std.	Data coverage 2009: 87%
<b>Methane (Birkenes)</b>	CH <sub>4</sub>	Picarro CRDS G1301 CO <sub>2</sub> /CH <sub>4</sub> /H <sub>2</sub> O	5 s	Waiting for calibration gases from NOAA. Currently only initial calibration from Picarro.	Measurements started 19. May 2009
<b>Methane (Zeppelin)</b> <b>Nitrous oxide (Zeppelin)</b>	CH <sub>4</sub> N <sub>2</sub> O	GC-FID-ECD	15 min	Hourly, working std. calibrated vs. GAW std.	First data in September 2009. There were some necessary adjustments during the first months at Zeppelin. The instrument was in full operation from spring 2010
<b>Carbon monoxide</b>	CO	GC-MgO/UV	20 min	Every 2 hours, working std. calibrated vs. GAW std.	Data coverage 2009: 94%
<b>Carbon dioxide (Zeppelin)</b>	CO <sub>2</sub>		1 h		CO <sub>2</sub> measurements performed by ITM Stockholm University (SU)
<b>Carbon dioxide (Birkenes)</b>	CO <sub>2</sub>	Picarro CRDS G1301 CO <sub>2</sub> /CH <sub>4</sub> /H <sub>2</sub> O	5 s	Waiting for calibration gases from NOAA. Currently only initial calibration from Picarro.	Measurements started 19. May 2009
<b>CFC-11</b> <b>CFC-12</b> <b>CFC-113</b> <b>CFC-115</b> <b>HFC-125</b> <b>HFC-134a</b> <b>HFC-152a</b> <b>HFC-365mfc (new)</b> <b>HCFC-22</b> <b>HCFC-141b</b> <b>HCFC-142b</b> <b>H-1301</b> <b>H-1211</b>	CFCl <sub>3</sub> CF <sub>2</sub> Cl <sub>2</sub> CF <sub>2</sub> ClCFCl <sub>2</sub> CF <sub>3</sub> CF <sub>2</sub> Cl CHF <sub>2</sub> CF <sub>3</sub> CH <sub>2</sub> FCF <sub>3</sub> CH <sub>3</sub> CHF <sub>2</sub> CF <sub>3</sub> CH <sub>2</sub> CHF <sub>2</sub> CH <sub>3</sub> CHF <sub>2</sub> Cl CH <sub>3</sub> CFCl <sub>2</sub> CH <sub>3</sub> CF <sub>2</sub> Cl CF <sub>3</sub> Br CF <sub>2</sub> ClBr	ADS-GC-MS	4 h	Every 4 hours, working std. calibrated vs. AGAGE std.	Data coverage 2009: 83%  The measurements of the CFCs, HCFC-142b, Halon-1212, and SF <sub>6</sub> have higher uncertainty and are not within the required precision of AGAGE. See next section for details.

Table 7, cont.

Component		Instrument and method	Time res.	Calibration procedures	Comment
<b>Methyl Chloride</b>	CH <sub>3</sub> Cl				
<b>Methyl Bromide</b>	CH <sub>3</sub> Br				
<b>Methylenedichloride</b>	CH <sub>2</sub> Cl <sub>2</sub>				
<b>Chloroform</b>	CHCl <sub>3</sub>				
<b>Methylchloroform</b>	CH <sub>3</sub> CCl <sub>3</sub>				
<b>TriChloroethylene</b>	CHClCCl <sub>2</sub>				
<b>Perchloroethylene</b>	CCl <sub>2</sub> CCl <sub>2</sub>				
<b>Sulphurhexafluoride</b>	SF <sub>6</sub>				
<b>Tetrafluormethane</b>	CF <sub>4</sub>	Medusa	2 h	Every 2	Start September
<b>PFC-116</b>	C <sub>2</sub> F <sub>6</sub>	No. 19		hours,	2009. The instrument
<b>PFC-218</b>	C <sub>3</sub> F <sub>8</sub>			working std.	will run in parallel with
<b>PFC-318</b>	c-C <sub>4</sub> F <sub>8</sub>			calibrated vs.	ADS-GC-MS for one
<b>Sulphurhexafluoride</b>	SF <sub>6</sub>			AGAGE std	year. This instrument
<b>Sulfuryl fluoride</b>	SO <sub>2</sub> F <sub>2</sub>				gives much better
<b>HFC-23</b>	CHF <sub>3</sub>				precision and also
<b>HFC-32</b>	CH <sub>2</sub> F <sub>2</sub>				measures more
<b>HFC-125</b>	CHF <sub>2</sub> CF <sub>3</sub>				components than the
<b>HFC-134a</b>	CH <sub>2</sub> FCF <sub>3</sub>				ADS-GC-MS. The
<b>HFC-143a</b>	CH <sub>3</sub> CF <sub>3</sub>				uncertainty in the
<b>HFC-152a</b>	CH <sub>3</sub> CHF <sub>2</sub>				measurements of
<b>HFC-227ea</b>	CF <sub>3</sub> CHFCF <sub>3</sub>				CFCs, HCFC-142b,
<b>HFC-236fa</b>	CF <sub>3</sub> CH <sub>2</sub> CF <sub>3</sub>				Halon-1212, and SF <sub>6</sub>
<b>HFC-245fa</b>	CF <sub>3</sub> CH <sub>2</sub> CHF <sub>2</sub>				will be reduced.
<b>HFC-365mfc</b>	CF <sub>3</sub> CH <sub>2</sub> CHF <sub>2</sub> CH <sub>3</sub>				
<b>HCFC-22</b>	CHF <sub>2</sub> Cl				
<b>HCFC-124</b>	CHClFCF <sub>3</sub>				
<b>HCFC-141b</b>	CH <sub>3</sub> CFC <sub>2</sub>				
<b>HCFC-142b</b>	CH <sub>3</sub> CF <sub>2</sub> Cl				
<b>CFC-11</b>	CFCl <sub>3</sub>				
<b>CFC-12</b>	CF <sub>2</sub> Cl <sub>2</sub>				
<b>CFC-113</b>	CF <sub>2</sub> CICFCl <sub>2</sub>				
<b>CFC-114</b>	CF <sub>2</sub> CICF <sub>2</sub> Cl				
<b>CFC-115</b>	CF <sub>3</sub> CF <sub>2</sub> Cl				
<b>H-1211</b>	CF <sub>3</sub> Br				
<b>H-1301</b>	CF <sub>2</sub> ClBr				
<b>H-2402</b>	CF <sub>2</sub> BrCF <sub>2</sub> Br				
<b>Methyl Chloride</b>	CH <sub>3</sub> Cl				
<b>Methyl Bromide</b>	CH <sub>3</sub> Br				
<b>Methyl Iodide</b>	CH <sub>3</sub> I				
<b>Methylenedichloride</b>	CH <sub>2</sub> Cl <sub>2</sub>				
<b>Chloroform</b>	CHCl <sub>3</sub>				
<b>Methylchloroform</b>	CH <sub>3</sub> CCl <sub>3</sub>				
<b>Dibromomethane</b>	CH <sub>2</sub> Br <sub>2</sub>				
<b>Bromoform</b>	CHBr <sub>3</sub>				
<b>TriChloroethylene</b>	TCE				
<b>Perchloroethylene</b>	PCE				
<b>Ethane</b>	C <sub>2</sub> H <sub>6</sub>				
<b>Benzene</b>	C <sub>6</sub> H <sub>6</sub>				
<b>Carbonyl Sulfide</b>	COS				
<b>Ozone</b>	O <sub>3</sub>		5 min		

**CO<sub>2</sub> measurements performed by ITM Stockholm University (SU)**

At the Zeppelin station carbon dioxide (CO<sub>2</sub>) and atmospheric particles are measured by Stockholm University (Institute of Applied Environmental Research, ITM).

SU maintains a continuous infrared CO<sub>2</sub> instrument, which has been monitoring since 1989. The continuous data are enhanced by the weekly flask sampling programme in co-operation with NOAA CMDL. Analysis of the flask samples provides CH<sub>4</sub>, CO, H<sub>2</sub>, N<sub>2</sub>O and SF<sub>6</sub> data for the Zeppelin station.

***Data quality and uncertainties***

In general the ADS-GCMS can measure a wide range of hydrochlorofluorocarbons, hydrofluorocarbons (HCFC-141b, HCFC-142b, HFC-134a etc.), methyl halides (CH<sub>3</sub>Cl, CH<sub>3</sub>Br, CH<sub>3</sub>I) and the halons (e.g. H-1211, H-1301) with a good scientific quality. The system can also measure other compounds like the chlorofluorocarbons, but the quality and the precision of these measurements are not at the same level. Table 8 shows a list over those species measured with the ADS-GCMS at Zeppelin Observatory. The species that are in blue are of acceptable scientific quality and in accordance with recommendations and criteria of AGAGE for measurements of halogenated greenhouse gases. Those listed in red have higher uncertainty and are not within the required precision of AGAGE. There are various reasons for this increased uncertainty; unsolved instrumental problems e.g. possible electron overload in detector (for the CFC's), influence from other species, detection limits (CH<sub>3</sub>I, CHClCCl<sub>2</sub>) and unsolved calibration problems (HCFC-22, HCFC-142b, H-1211, CHBr<sub>3</sub>).

*Table 8: ADS-GCMS measured species. Good scientific quality data in Blue; Data with reduced quality data in Red. The data are available through <http://ebas.nilu.no>. Please read and follow the stated data policy upon use.*

Compound	Typical precision (%)	Compound	Typical precision (%)
SF <sub>6</sub>	1,5	H1301	1,5
HFC134a	0,4	H1211	0,4
HFC152a	0,6	CH <sub>3</sub> Cl	0,6
HFC125	0,8	CH <sub>3</sub> Br	0,8
HFC365mfc	1,7	CH <sub>3</sub> I	5,1
HCFC22	0,2	CH <sub>2</sub> Cl <sub>2</sub>	0,4
HCFC141b	0,5	CHCl <sub>3</sub>	0,3
HCFC142b	0,5	CHBr <sub>3</sub>	15
HCFC124	2,3	CCl <sub>4</sub>	0,5
CFC11	0,3	CH <sub>3</sub> CCl <sub>3</sub>	0,6
CFC12	0,3	CHClCCl <sub>2</sub>	1,2
CFC113	0,2	CCl <sub>2</sub> CCl <sub>2</sub>	0,7
CFC115	0,8		

### **New Medusa instrument installed at Zeppelin and improved air inlet system**

To have the suitable and necessary scientific quality of the GHG measurements and fulfill the requirements of AGAGE NILU installed a new Medusa at the Zeppelin station Autumn 2010. The instrument is developed to provide more accurate measurements of halocarbon gases and also extending the range of compounds monitored.

The new Medusa instruments not only extend the number of species measured by original ADS instruments to 40 species, but also improve the quality and precision in measurements of most of the species, especially the CFC's. But even though the improvements, there are still a few issues related to the measurements of the CFC's and a few others of the 40 species that are unresolved. Therefore, the AGAGE network has decided to report their CFC data measured with their old GC-MD system from the AGAGE stations that both have a GC-MD and a Medusa.

Table 9 gives an overview over the species measured with the Medusa and GC-MD systems at the AGAGE stations and the typical precision with the different instruments. With the installation of Medusa instrument at Zeppelin Observatory the Observatory will be part of the AGAGE network and the measurements will meet the same criteria as shown in Table 9.

There has also been improved air inlet for the GHG observations at Zeppelin to reduce possible influence from the station and visitors at the stations.



*NILU engineer Are Bäcklund about to install a new air inlet for the Medusa instrument.  
Photo: Ove Hermansen, NILU*

Table 9: AGAGE measured species. *Medusa in Blue; GC-MD green; Both: Red.*

Compound	Typical precision (%)	Compound	Typical precision (%)
CF <sub>4</sub>	0.15	H1301	1.5
C <sub>2</sub> F <sub>6</sub>	0.9	H1211	0.5
C <sub>3</sub> F <sub>8</sub>	3	H2402	2
SF <sub>6</sub>	0.4	CH <sub>3</sub> Cl	0.2
SO <sub>2</sub> F <sub>2</sub>	1.6	CH <sub>3</sub> Br	0.5
HFC23	0.7	CH <sub>3</sub> I	2
HFC32	5	CH <sub>2</sub> Cl <sub>2</sub>	0.8
HFC134a	0.4	CHCl <sub>3</sub>	0.6
HFC152a	1.2	CHBr <sub>3</sub>	0.6
HFC125	1	CCl <sub>4</sub>	1
HFC143a	1.2	CH <sub>3</sub> CCl <sub>3</sub>	0.7
HFC365mfc	10	CHClCCl <sub>2</sub>	2.5
HCFC22	0.3	CCl <sub>2</sub> CCl <sub>2</sub>	0.5
HCFC141b	0.4	C <sub>2</sub> H <sub>2</sub>	0.5
HCFC142b	0.6	C <sub>2</sub> H <sub>4</sub>	2
HCFC124	2	C <sub>2</sub> H <sub>6</sub>	0.3
CFC11	0.15	C <sub>6</sub> H <sub>6</sub>	0.3
CFC12	0.05	C <sub>7</sub> H <sub>8</sub>	0.6
CFC13	2	GC-MD only*	
CFC113	0.2	CH <sub>4</sub>	0.05
CFC114	0.3	N <sub>2</sub> O	0.05
CFC115	0.8	CO	0.2
		H <sub>2</sub>	0.6

\*CO and H<sub>2</sub> are measured by GC-MD at Mace Head and Cape Grim only  
(ppt = parts per trillion, ppb = parts per billion)

To improve the quality of the ongoing ADS-GCMS measurements at Zeppelin Observatory, the two instruments (Medusa and ADS-GCMS) will be run in parallel for at least 6 months. Results from the comparison between the two will be used to improve the quality of the species measured with the ADS-GCMS so far.

#### Details about aerosol optical depth measurements

The amount of particles in the air is monitored by use of a Precision-Filter-Radiometer (PFR) sun photometer (NILU) in Ny-Ålesund and a Cimel instrument at Birkenes, see details below.

--	--

	
<p><b>AERONET - Cimel C-318</b></p> <ul style="list-style-type: none"> <li>• Sun (9 channels) and sky radiances</li> <li>• Wavelength range:: 340-1640 nm nm</li> <li>• 15 min sampling</li> <li>• No temperature stabilized</li> <li>• AOD uncertainty: 0.01-0.02</li> </ul>	<p><b>PFR-GAW - Precision Filter Radiometer</b></p> <ul style="list-style-type: none"> <li>• Direct sun measurements (4 channels)</li> <li>• Wavelength range: 368-862 nm</li> <li>• Continuous sampling (1 min)</li> <li>• Temperature stabilized</li> <li>• AOD uncertainty: 0.01</li> </ul>
<p><i>Figure 50: Photos and typical features of the standard instrument of the AERONET (left panel) and GAW PFR network instruments (right panel) (adapted from Toledano et al. (2010)).</i></p>	

Aerosol optical depth measurements started at the new Birkenes observatory in spring 2009, utilizing an automatic sun and sky radiometer (CIMEL type CE-318), with spectral interference filters centered at selected wavelengths: 340, 380, 440, 500, 675, 870, 1020, and 1640 nm. The measurement frequency is approximately 15 minutes (depends on the air-mass and time). Calibration was performed in Izaña in the period 13 May to 24 of July 2008 (RIMA-AERONET sub-network). Post-calibration and pre-calibration for the next measurement period were made between 11 December 2009 and 26 January 2010 at Autilla del Pino (Palencia, Spain), the operational calibration platform managed by GOA for RIMA-AERONET sun photometers.

The PFR measurements in Ny-Ålesund are part of the global network of aerosol optical depth (AOD) observations, which started in 1999 on behalf of the WMO GAW program. The instrument is located on the roof of the Sverdrup station, Ny-Ålesund, close to the EMEP station on the Zeppelin Mountain (78.9°N, 11.9°E, 474 m asl). The PFR has been in operation since May 2002. In Ny-Ålesund the polar night lasts from 26<sup>th</sup> October to 16<sup>th</sup> February, leading to short observational seasons. However during the summer it is possible to measure day and night if the weather conditions are satisfactory. The instrument measures direct solar radiation in four narrow spectral bands centred at 862, 501, 411, and 368 nm. Data quality control includes instrumental control like detector temperature and solar pointing control as well as objective cloud screening. [Measurements are taken every full minute for 1.25 second.](#) SCIAMACHY TOSOMI ozone columns and meteorological data from Ny-Ålesund were used in the retrieval of the aerosol optical depth.

### **Status and outlook on observations of aerosol properties at Birkenes in 2010 and 2011**

Up to 2009, the instrumentation for observing properties of atmospheric aerosol particles at Birkenes consisted of a Differential Mobility Particle Sizer (DMPS), a single-wavelength Particle Soot Absorption Photometer (PSAP), and a PM<sub>2.5</sub> and PM<sub>10</sub> filter samplers for collecting samples for chemical analysis. A DMPS measures the particles number size

distribution, usually in the range of about 0.02 – 0.8  $\mu\text{m}$  particle diameter. After putting the aerosol particle phase into a defined state of charge by exposing them to an ionised atmosphere in thermal equilibrium, the DMPS uses a cylindrical capacitor to select a narrow size fraction of the particle phase. The particle size in the selected size fraction is determined by the voltage applied to the capacitor. The particle number concentration in the selected size fraction is then counted by a Condensation Particle Counter (CPC). A mathematical inversion that considers charge probability, transfer function of the capacitor, and counting efficiency of the CPC is then used to calculate the particle number size distribution. A PSAP measures the aerosol absorption coefficient by measuring the decrease in optical transmissivity of a filter while the filter is loaded with the aerosol sample. The transmissivity time series is subsequently translated into a absorption coefficient time series by using Lambert-Beer's law, the same law also used in optical spectroscopy. The PM<sub>2.5</sub> and PM<sub>10</sub> filter samples of the aerosol particle phase are analysed by ion chromatography to reveal the chemical speciation.

From 2010, all instruments measuring aerosol properties in Birkenes listed in section 6.1 were in full operation. This now also includes a 3-wavelength integrating nephelometer and an Optical Particle Counter (OPC). The integrating nephelometer measures the aerosol scattering coefficient at three wavelength across the visible spectrum by illuminating an aerosol-filled confined volume with a Lambertian light source, and collecting the light scattered by the particles in the volume. This observation is complementary to the measurements of the aerosol absorption coefficient by PSAP, can be used to increase the accuracy of the PSAP measurements. The OPC measures the particle number size distribution in the size range of 0.25 – 10  $\mu\text{m}$  particle diameter, and is thus complementary to the DMPS measurements. Together, DMPS and OPC cover the full particle size range commonly considered by atmospheric aerosol observations. In the OPC, the particles in the sample pass through a laser beam. By correlating the amplitude of the peak of scattered light generated while passing the laser beam with particle size, the particle size distribution is measured.

Moreover, the measurement programme at Birkenes is due to be extended in 2011 with a multi-wavelength absorption photometer and a cloud condensation nucleus counter (CCNC). The absorption photometer will measure the aerosol absorption coefficient at three wavelength across the visible spectrum, and will, after an intercomparison period, replace the old single wavelength instrument used so far. The information on spectral particle absorption will allow conclusion about the nature of the absorber, and its distribution with particle size. The CCNC will measure the number of particles available for acting as cloud condensation nuclei as a function of particle size and water vapour supersaturation. The instrument achieves this by exposing the sample to an “artificial cloud” of defined user-selectable supersaturation. This will ultimately allow statements not only on the direct, but also the indirect aerosol climate effect.

This full picture will not only allow a better source apportionment of the aerosol observed. The full set of optical properties will also facilitate an estimate of local, instantaneous direct aerosol radiative forcing, and a comparison with the radiative forcing of greenhouse gases at the site.

**Model studies: calculation of trends**

To calculate the annual trends the observations have been fitted as described in Simmonds et al. (2006) by an empirical equation of Legendre polynomials and harmonic functions with linear, quadratic, and annual and semi-annual harmonic terms:

$$f(t) = a + b \left( \frac{N}{12} \right) \cdot P_1 \left( \frac{t}{N} - 1 \right) + \frac{1}{3} \cdot d \left( \frac{N}{12} \right)^2 \cdot P_2 \left( \frac{t}{N} - 1 \right) + c_1 \cdot \cos \left( \frac{2\pi t}{N} \right) + s_1 \sin \left( \frac{2\pi t}{N} \right) + c_2 \cdot \cos \left( \frac{4\pi t}{N} \right) + s_2 \sin \left( \frac{4\pi t}{N} \right)$$

The observed  $f$  can be expressed as functions of time measures from the 2N-months interval of interest. The coefficient  $a$  defines the average mole fraction,  $b$  defines the trend in the mole fraction and  $d$  defines the acceleration in the trend. The  $c$  and  $s$  define the annual and inter-annual cycles in mole fraction.  $N$  is the mid-point of the period of investigation.  $P_i$  are the Legendre polynomials of order  $i$ .

**Determination of background data**

Based on the daily mean concentrations an algorithm is selected to find the values assumed as clean background air. If at least 75% of the trajectories within +/- 12 hours of the sampling day are arriving from a so-called clean sector, defined below, one can assume the air for that specific day to be non-polluted. The remaining 25% of the trajectories from European, Russian or North-American sector are removed before calculating the background.



## **Appendix II: Acknowledgments and affiliations of external authors**

We gratefully acknowledge the work of the station personnel from the Norwegian Polar Institute for taking care of the observations in Ny-Ålesund. The authors acknowledge the NOAA Air Resources Laboratory (ARL) for the provision of the HYSPLIT transport and dispersion model and/or READY website ([arl.noaa.gov/ready.php](http://arl.noaa.gov/ready.php)). Analyses and visualization used in this report were produced with the Giovanni online data system, developed and maintained by the NASA GES DISC. We also acknowledge the MODIS mission scientists and associated NASA personnel for the production of the data used here. SCIAMACHY TOSOMI ozone overpass data were obtained from the TEMIS website ([temis.nl/protocols/o3field/overpass\\_scia.html](http://temis.nl/protocols/o3field/overpass_scia.html)), Meteorological data for Ny-Ålesund were received via eKlima ([www.eklima.no](http://www.eklima.no)), the web portal from the Norwegian Meteorological Institute. We greatly acknowledge the personnel for obtaining the data and making them publically available.

Christoph Wehrli and Carlos Toledano are included as co-authors due to their contributions with the aerosol observations, quality assurance and interpretations.

Christoph Wehrli  
WORCC, PMOD/WRC, Dorfstrasse 33, Davos Dorf  
CH-7260, Switzerland

Carlos Toledano  
Grupo de Óptica Atmosférica  
Universidad de Valladolid  
Prado de la Magdalena s/n  
47071 Valladolid, Spain



Utførende institusjon NILU – Norwegian Institute for Air Research NILU project no.: O-99093 NILU report no.: OR 33/2011	ISBN-nummer 978-82-425-2403-4 (trykt) 978-82-425-2404-1 (elektronisk)
--	--

Oppdragstakers prosjektansvarlig Cathrine Lund Myhre	Kontaktperson i Klif Harold Leffertstra	TA-nummer TA-2805/2011
		SPFO-nummer 1102/2011

	År 2011	Sidetall	Klifs kontraktnummer
--	------------	----------	----------------------

Utgiver NILU – Norsk institutt for luftforskning	Prosjektet er finansiert av Klima- og forurensningsdirektoratet (Klif) og NILU – Norsk institutt for luftforskning
---	---

Forfatter(e) C.L. Myhre, O. Hermansen, A.M. Fjæraa, C. Lunder, M. Fiebig, N. Schmidbauer, T. Krognæs, K. Stebel (all NILU), C. Toledano, (GOA), C. Wehrli (WORCC)
Tittel - norsk og engelsk  Overvåking av klimagasser og partikler på Svalbard og Birkenes: Årsrapport 2009  Monitoring of greenhouse gases and aerosols at Svalbard and Birkenes: Annual report 2009
Sammendrag – summary  Rapporten presenterer aktiviteter og måleresultater fra klimagassovertvåkingen ved Zeppelin observatoriet på Svalbard for årene 2001-2009 og klimagassmålinger og klimarelevant partikkelmålinger fra Birkenes for 2009.  Overvåkningsprogrammet utføres av NILU – Norsk institutt for luftforskning og er finansiert av Statens forurensningstilsyn (SFT) (nå Klima- og forurensningsdirektoratet (Klif)) og NILU – Norsk institutt for luftforskning.  The report summaries the activities and results of the greenhouse gas monitoring at the Zeppelin and observatory situated on Svalbard in Arctic Norway during the period 2001-2009 and the greenhouse gas monitoring and aerosol observations from Birkenes for 2009.  The monitoring programme is performed by the NILU – Norwegian Institute for Air Research and funded by the Norwegian Pollution Control Authority (SFT) (now Climate and Pollution Agency) and NILU – Norwegian Institute for Air Research.

4 emneord Drivhusgasser, partikler, Arktis, halokarboner	4 subject words Greenhouse gases, aerosols, Arctic, halocarbons
---	--



**Klima- og forurensningsdirektoratet**

Postboks 8100 Dep,  
0032 Oslo

Besøksadresse: Strømsveien 96

Telefon: 22 57 34 00

Telefaks: 22 67 67 06

E-post: [postmottak@klif.no](mailto:postmottak@klif.no)

[www.klif.no](http://www.klif.no)

## Om Statlig program for forurensningsovervåking

Statlig program for forurensningsovervåking omfatter overvåking av forurensningsforholdene i luft og nedbør, skog, vassdrag, fjorder og havområder. Overvåkingsprogrammet dekker langsiktige undersøkelser av:

- overgjødsling
- forsuring (sur nedbør)
- ozon (ved bakken og i stratosfæren)
- klimagasser
- miljøgifter

Overvåkingsprogrammet skal gi informasjon om tilstanden og utviklingen av forurensningssituasjonen, og påvise eventuell uheldig utvikling på et tidlig tidspunkt. Programmet skal dekke myndighetenes informasjonsbehov om forurensningsforholdene, registrere virkningen av iverksatte tiltak for å redusere forurensningen, og danne grunnlag for vurdering av nye tiltak. Klima- og forurensningsdirektoratet er ansvarlig for gjennomføringen av overvåkingsprogrammet.

SPFO-rapport 1102/2011

TA-2805/2011

ISBN 978-82-425-2403-4

ISBN 978-82-425-2404-1